

Designing Molecular Qubits: Computational Insights into First-Row and Group 6 Transition Metal Complexes

Supporting Information

Arturo Sauza-de la Vega[§],[†] Andrea Darù[§],[†] Stephanie Nofz,[‡] and Laura Gagliardi^{*,†,‡,¶}

†Department of Chemistry, Chicago Center for Theoretical Chemistry, University of Chicago, Illinois, 60637, USA.

[‡]Pritzker School of Molecular Engineering, University of Chicago, Illinois 60637, USA.

¶James Franck Institute, University of Chicago, Illinois 60637, USA.

E-mail: lgagliardi@uchicago.edu

Contents

[§] These authors contributed equally to this work.

2 Energy Gaps	S5
3 Zero-Field Splitting Background Theory	S9
4 Zero-Field Splitting Parameters	S11
5 Relative Electronic Energies	S14
5.1 Single State CASPT2	S14
5.2 Hybrid MC-PDFT (tPBE0)	S22
5.3 Relative Energies	S30
5.4 Absolute Energies	S39
5.5 Absolute Energies for Zero-Field Splitting Calculations	S47
6 Active Space Dependency	S53
6.1 Energy Gaps	S53
6.2 Zero-Field Splitting Parameters	S55
6.3 Absolute Electronic Energies	S58
6.3.1 Cr(<i>o-tol</i>) ₄ Complex	S58
6.3.2 Mo(<i>o-tol</i>) ₄ Complex	S61
6.3.3 W(<i>o-tol</i>) ₄ Complex	S64
6.3.4 V(<i>o-tol</i>) ₄ ⁻ Complex	S66
6.3.5 Ti(<i>o-tol</i>) ₄ ²⁻ Complex	S69
6.3.6 Fe(<i>o-tol</i>) ₄ ²⁻ Complex	S72
6.3.7 Co(<i>o-tol</i>) ₄ ²⁻ Complex	S78
6.3.8 Ni(<i>o-tol</i>) ₄ ²⁻ Complex	S81
7 Geometrical Distortions Following Lower Energetic Vibrational Modes	S84

1 Molecular Geometries

1.1 RMSD, Bond Length, and Angles Values of DFT Optimized Complexes

The geometrical features of all optimized metal complexes are reported in Table S1. Specifically, metal-ligand distance, and ligand-metal-ligand angles.

Table S1: Metal-ligand bond distances in Å and angles in degrees for the TPSSh-D3BJ/def2-TZVP optimized structures at the respective spin state reported per column. The metal name is used to refer to the full compound (i.e. Cr is Cr(*o*-tol)₄).

	Ti	V	Cr	Fe	Co	Ni	Mo	W	
Spin State									
		Triplet	Triplet	Triplet	Quintet	Quartet	Triplet	Triplet	Triplet
Bond length									
M–C(<i>o</i> -tol)		2.16	2.07	1.98	2.06	1.86	2.0	2.07	2.08
Angles									
C1–M–C2		106.0	105.2	104.9	105.3	98.2	100.6	105.3	105.1
C1–M–C3		111.2	111.7	111.8	111.6	115.4	107.0	111.6	111.7
C1–M–C4		110.2	111.7	111.8	111.6	115.5	133.2	111.6	111.7
C2–M–C3		111.2	111.7	111.8	111.6	115.3	106.5	111.6	111.7
C2–M–C4		110.2	111.7	111.8	111.6	115.4	106.9	111.6	111.7
C3–M–C4		106.0	105.2	104.9	105.4	98.1	100.6	105.3	105.1
Spin State									
		Singlet	Singlet	Singlet	Triplet	Doublet	Singlet	Singlet	Singlet
Bond length									
M–C(<i>o</i> -tol)		2.13	2.03	1.96	1.90	1.95	1.96	2.06	2.06
Angles									
C1–M–C2		102.8	105.1	97.2	94.8	93.6	93.6	105.5	107.7
C1–M–C3		112.9	111.7	115.9	128.1	144.5	89.2	113.8	113.4
C1–M–C4		112.9	111.7	115.9	117.3	91.6	176.7	114.4	111.4
C2–M–C3		112.9	111.7	115.9	113.3	90.4	176.7	103.5	103.0
C2–M–C4		112.9	111.7	115.9	109.1	162.4	89.2	113.8	113.5
C3–M–C4		102.8	105.1	97.2	94.3	95.0	88.2	105.5	107.7

Table S2: Root mean square deviation (RMSD) of the DFT optimized structures of all considered complexes. The triplet-singlet structures are used for all complexes beside the Fe and Co one where the quintet-triplet and the quartet-doublet are used respectively.

Complex	PBE	TPSSh	B3LYP	M06
$\text{Ti}(o\text{-tol})_4^{2-}$	0.44	0.39	0.39	0.32
$\text{Cr}(o\text{-tol})_4$	0.03	0.29	0.39	0.40
$\text{V}(o\text{-tol})_4^-$	0.26	0.18	0.19	0.20
$\text{Fe}(o\text{-tol})_4^{2-}$	1.53	1.39	1.43	2.00
$\text{Co}(o\text{-tol})_4^{2-}$	1.62	2.43	2.36	2.81
$\text{Ni}(o\text{-tol})_4^{2-}$	2.10	2.11	2.12	2.21
$\text{Mo}(o\text{-tol})_4$	0.20	0.22	0.21	0.26
$\text{W}(o\text{-tol})_4$	0.41	0.17	0.12	0.22

1.2 DFT Relative Stability Between Spin-States

Along group 6, the energy difference between the triplet and singlet optimized geometries decreases with increasing atomic number (Table S3). For $\text{Cr}(o\text{-tol})_4$, the energy gap is 1.55 eV and decreases to 1.07 eV for the complex $\text{Mo}(o\text{-tol})_4$, and continues decreasing the triplet-singlet gap to 0.91 for the $\text{W}(o\text{-tol})_4$ compound.

Table S3: Triplet-Singlet energy difference for the $\text{Cr}(o\text{-tol})_4$, $\text{Mo}(o\text{-tol})_4$, and $\text{W}(o\text{-tol})_4$ complexes computed with TPSSh-D3BJ/def2-TZVP. The energy differences were computed between the triplet and singlet-optimized geometries.

Metal	ΔE_{T-S} (eV)
$\text{Cr}(o\text{-tol})_4$	1.55
$\text{Mo}(o\text{-tol})_4$	1.07
$\text{W}(o\text{-tol})_4$	0.91

Similarly, along the first row, when the atomic number of the metal increases, the triplet-singlet gap increases (See Table S4). The energy gap for $\text{Ti}(o\text{-tol})_4^{2-}$ is 0.41 eV, and increases to 1.36 and 1.55 eV for $\text{V}(o\text{-tol})_4^-$, and $\text{Cr}(o\text{-tol})_4$ complexes, respectively. However, for $\text{Ni}(o\text{-tol})_4^{2-}$ complex, the optimized singlet molecule is lower in energy than the triplet-optimized structure. Even if the singlet is the ground state, we use the triplet-optimized molecular geometry for the multiconfigurational calculations to compare the same ligand field for all complexes and observe the net effect of the metal substitution.

Table S4: Triplet-Singlet energy differences for the $\text{Ti}(o\text{-tol})_4^{2-}$, $\text{V}(o\text{-tol})_4^-$, $\text{Cr}(o\text{-tol})_4$, and $\text{Ni}(o\text{-tol})_4^{2-}$ complexes computed with TPSSh-D3BJ/def2-TZVP. The energy differences were computed between the triplet and singlet-optimized geometries.

Molecule	$\Delta E_{\text{T-S}}$ (eV)
$\text{Ti}(o\text{-tol})_4^{2-}$	0.41
$\text{V}(o\text{-tol})_4^-$	1.36
$\text{Cr}(o\text{-tol})_4$	1.55
$\text{Ni}(o\text{-tol})_4^{2-}$	-1.00

The negative signs in Table S5 indicate that, in the case of $\text{Fe}(o\text{-tol})_4^{2-}$ ion, the triplet optimized structure is more stable than the singlet and quintet optimized geometries. However, the triplet geometry is not pseudo-tetrahedral. Therefore, for the purpose of this study, we used the quintet geometry for the multireference calculations. Similarly, for the $\text{Co}(o\text{-tol})_4^{2-}$ compound, the doublet geometry resulted to be lower in energy than the quartet structure, but only the quartet-optimized geometry displayed a pseudo-tetrahedral ligand field.

Table S5: Energy differences for the $\text{Fe}(o\text{-tol})_4^{2-}$ and $\text{Co}(o\text{-tol})_4^{2-}$ complexes computed with TPSSh-D3BJ/def2-TZVP. The energy differences were computed between the quintet, triplet, and singlet-optimized geometries of $\text{Fe}(o\text{-tol})_4^{2-}$ complex, and the quartet and doublet geometries of $\text{Co}(o\text{-tol})_4^{2-}$ complex.

Molecule	ΔE (eV)
$\text{Fe}(o\text{-tol})_4^{2-}$ (quintet-triplet)	-0.12
$\text{Fe}(o\text{-tol})_4^{2-}$ (quintet-singlet)	0.59
$\text{Co}(o\text{-tol})_4^{2-}$ (quartet-doublet)	-0.18

2 Energy Gaps

In Table S6 are shown the SA-CASSCF, CASPT2, tPBE, and tPBE0 calculated energy gaps when substituting the metal center down the group. For $\text{Cr}(o\text{-tol})_4$ complex, the experimental energy gap is 1.20 eV.¹ The SA-CASSCF method overestimates this reference by 0.48–0.70 eV, while CASPT2 computed values differ by $\pm \sim 0.20$ eV from the experiment. The tPBE method is, in all cases, underestimating the energy gap. The tPBE method underestimates the reference by 0.16 eV. However, tPBE0 shows an important agreement with

experimental reference.

The CASPT2 and tPBE0 methods provide energy values close to the experimental reference. Therefore, these two methods are the most reliable for predicting the $\Delta E_{\text{T-S}}$ gaps of the complexes studied herein. Figure S1 shows the CASPT2 and tPBE0 $\Delta E_{\text{T-S}}$ of $\text{Cr}(o\text{-tol})_4$, $\text{Mo}(o\text{-tol})_4$, and $\text{W}(o\text{-tol})_4$ complexes using (10,15) active space. Consistently, we observe a decrease in the $\Delta E_{\text{T-S}}$ when substituting the chromium center for the elements down the periodic table. For example, in Figure S1 (d), the CASPT2 energy gaps for $\text{Cr}(o\text{-tol})_4$, $\text{Mo}(o\text{-tol})_4$, and $\text{W}(o\text{-tol})_4$ complexes are 1.44, 0.82, and 0.65 eV, respectively. Similarly, the tPBE0 method shows a decrease in $\Delta E_{\text{T-S}}$, from 1.20 to 0.67 and 0.55 eV, respectively.

Table S6: Computed triplet-singlet gaps (ΔE_{TS}) for the $\text{Ti}(o\text{-tol})_4^{2-}$, $\text{V}(o\text{-tol})_4^-$, $\text{Cr}(o\text{-tol})_4$, $\text{Mo}(o\text{-tol})_4$, and $\text{W}(o\text{-tol})_4$ complexes using the triplet optimized geometries. The ΔE_{TS} were obtained with SA-CASSCF, CASPT2, tPBE, and tPBE0 methods using the (8,13) active space for $\text{V}(o\text{-tol})_4^-$, and (10,15) for the other molecules. The values reported are in eV.

Complex	SA-CASSCF	CASPT2	tPBE	tPBE0
$\text{Ti}(o\text{-tol})_4^{2-}$	0.73	0.56	0.49	0.55
$\text{V}(o\text{-tol})_4^-$	1.46	1.18	0.65	0.85
$\text{Cr}(o\text{-tol})_4$	1.69	1.44	1.04	1.20
$\text{Mo}(o\text{-tol})_4$	1.05	0.82	0.54	0.67
$\text{W}(o\text{-tol})_4$	0.90	0.65	0.43	0.55

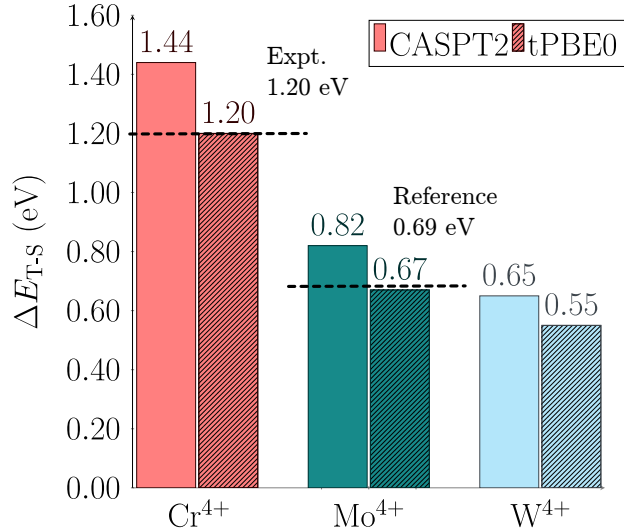


Figure S1: Calculated triplet-singlet gaps (ΔE_{T-S}) with the CASPT2 (solid bar) and tPBE0 (striped bar) methods for the $\text{Cr}(o\text{-tol})_4$ (red), $\text{Mo}(o\text{-tol})_4$ (green) and $\text{W}(o\text{-tol})_4$ (blue) complexes using (10,15) active space. Dashed lines correspond to reported data from references 1 and 2.

The SA-CASSCF values, like in the group analysis, display the largest values compared to the other methods. Also, the tPBE energy gaps are the smallest values for each complex and active space. This is consistent with what was observed previously for the group analysis.

Table S7: Computed triplet-singlet gaps (ΔE) for the $\text{Ni}(o\text{-tol})_4^{2-}$ complex, quintet-triplet for $\text{Fe}(o\text{-tol})_4^{2-}$ complex, and quartet-doublet for $\text{Co}(o\text{-tol})_4^{2-}$ molecule. The ΔE were obtained with SA-CASSCF, CASPT2, tPBE, and the tPBE0 methods. The $(n+6,13)$ active space was used, where $n = 6, 7$, and 8 for $\text{Fe}(o\text{-tol})_4^{2-}$, $\text{Co}(o\text{-tol})_4^{2-}$, and $\text{Ni}(o\text{-tol})_4^{2-}$, respectively. The values reported are in eV.

Complex	SA-CASSCF	CASPT2	tPBE	tPBE0
$\text{Fe}(o\text{-tol})_4^{2-}$	1.59	1.53	0.83	1.02
$\text{Co}(o\text{-tol})_4^{2-}$	1.99	1.71	1.38	1.53
$\text{Ni}(o\text{-tol})_4^{2-}$	1.64	1.10	0.67	0.91

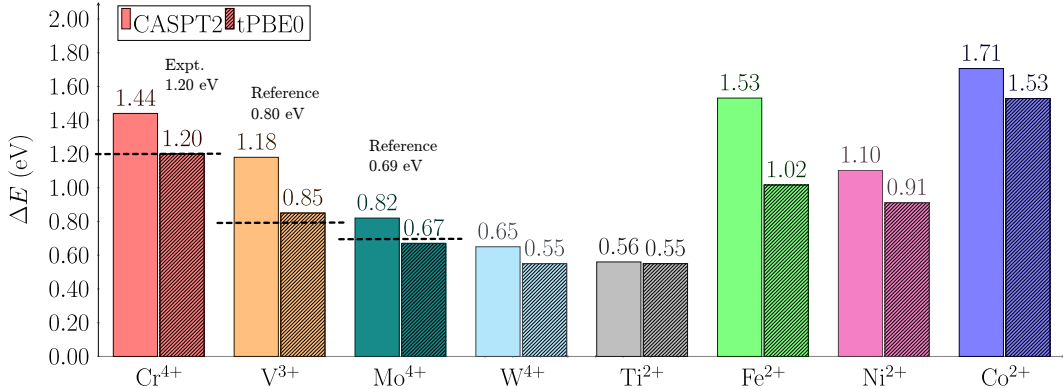


Figure S2: Calculated vertical triplet-singlet gaps for $\text{Cr}(o\text{-tol})_4$, $\text{Ti}(o\text{-tol})_4^{2-}$, $\text{Mo}(o\text{-tol})_4$, $\text{W}(o\text{-tol})_4$, and $\text{V}(o\text{-tol})_4^-$ complexes with $n = 2$, quintet-triplet gap for $\text{Fe}(o\text{-tol})_4^{2-}$ ($n = 6$), triplet-singlet for $\text{Ni}(o\text{-tol})_4^{2-}$ ($n = 8$), and quartet-doublet for $\text{Co}(o\text{-tol})_4^{2-}$ ($n = 7$). The complexes order is reported as discussed in the main text: d^2 triplet state complexes first followed by non- d^2 complexes. Energy gaps are computed with the CASPT2 (solid bar), and the tPBE0 (striped bar) methods. The red, orange, teal, cyan, gray, green, magenta, and blue colors are used for the $\text{Cr}(o\text{-tol})_4$, $\text{V}(o\text{-tol})_4^-$, $\text{Mo}(o\text{-tol})_4$, $\text{W}(o\text{-tol})_4$, $\text{Ti}(o\text{-tol})_4^{2-}$, $\text{Fe}(o\text{-tol})_4^{2-}$, $\text{Ni}(o\text{-tol})_4^{2-}$, and $\text{Co}(o\text{-tol})_4^{2-}$ complexes. For $\text{Cr}(o\text{-tol})_4$, $\text{Mo}(o\text{-tol})_4$, $\text{W}(o\text{-tol})_4$, and $\text{Ti}(o\text{-tol})_4^{2-}$ the $(10,15)$ active space was used, and for $\text{V}(o\text{-tol})_4^-$, $\text{Fe}(o\text{-tol})_4^{2-}$, and $\text{Co}(o\text{-tol})_4^{2-}$ compounds the $(n + 6,13)$ active spaces. Dashed lines correspond to experimental data from references 1 and 2.

The energy differences between the triplet ground state and the first singlet excited state ($\Delta E_{T_0-S_1}$), the triplet ground state and first triplet excited state ($\Delta E_{T_0-T_1}$), and between the triplet and singlet excited states ($(\Delta E_{S_1-T_1})$) are reported in Table S8.

Table S8: Energy differences in eV between ground state T_0 and first excited state S_1 , between the two triplet excited states T_0-T_1 , and between the singlet and triplet excited states S_1-T_1 .

Complex	$\Delta E_{T_0-S_1}$		$\Delta E_{T_0-T_1}$		$\Delta E_{S_1-T_1}$	
	CASPT2	tPBE0	CASPT2	tPBE0	CASPT2	tPBE0
$\text{Cr}(o\text{-tol})_4$	1.44	1.20	2.10	2.23	0.66	1.03
$\text{V}(o\text{-tol})_4^-$	1.18	0.85	1.30	1.30	0.12	0.45
$\text{Mo}(o\text{-tol})_4$	0.82	0.67	2.57	2.57	1.75	1.90
$\text{W}(o\text{-tol})_4^-$	0.65	0.55	2.31	2.21	1.66	1.66
$\text{Ti}(o\text{-tol})_4^{2-}$	0.56	0.55	0.61	0.65	0.05	0.10

3 Zero-Field Splitting Background Theory

The ZFS parameters are obtained by solving the Hamiltonian:

$$\hat{H}_{\text{ZFS}} = \hat{\mathbf{S}} \cdot \mathbf{D} \cdot \hat{\mathbf{S}} \quad (\text{S1})$$

where $\hat{\mathbf{S}}$ is the spin operator, and \mathbf{D} is a second rank tensor that describes the ZFS.³ By standard convention, the D-tensor is traceless and diagonalized, thus

$$D_{xx} + D_{yy} + D_{zz} = 0 \quad (\text{S2})$$

We define the axial (D) and rhombic (E) parameters as

$$D = \frac{3}{2}D_{zz}, \quad E = \frac{1}{2}(D_{xx} - D_{yy}) \quad (\text{S3})$$

When considering the relation between the total spin and the spatial coordinate components, $\hat{S}^2 = \hat{S}_x^2 + \hat{S}_y^2 + \hat{S}_z^2$, the spin Hamiltonian that describes the ZFS is given by

$$\hat{H}_{\text{ZFS}} = \frac{3}{2}D \left[\hat{S}_z^2 - \frac{1}{3}S(S+1) \right] + E \left(\hat{S}_x^2 - \hat{S}_y^2 \right) \quad (\text{S4})$$

Theoretical computation of the ZFS parameters can be performed using two methodolo-

gies. In the first approach, the second-order perturbation equation is employed:

$$D_{ij} = -\frac{\zeta^2}{4S^2} \sum_{p,q} \frac{\langle \Psi_p | \hat{\ell}_i | \Psi_q \rangle \langle \Psi_q | \hat{\ell}_j | \Psi_p \rangle}{\varepsilon_q - \varepsilon_p}, \quad (\text{S5})$$

where i and j represent the spatial components x , y , and z , and ζ , denotes the effective spin-orbit coupling constant of the metal ion. The wave functions Ψ_p and Ψ_q correspond to the ground-state p and excited states q , respectively, with energies ε_p and ε_q .^{4,5} This equation is applicable only within a single spin-state manifold. To account for other manifolds, additional spin-flip terms must be included.^{4,5}

In the second methodology, a pseudospin basis is constructed using selected spin states. The effective spin Hamiltonian is then used to diagonalize this basis, yielding the diagonal elements of the D -tensor. Detailed descriptions of this approach are provided in references 6–8.

It has previously been reported that density functional approximations are not the most accurate for computing zero-field splitting parameters in molecular spin qubits.⁹ Consequently, active space-based methods were employed to compute such parameters. The reference multiconfigurational wave functions were obtained through state-averaged complete active space self-consistent field (SA-CASSCF)¹⁰ calculations. The dynamic correlation was incorporated into the SA-CASSCF reference wave functions via post-CASSCF calculations. State-specific complete active space second-order perturbation theory (CASPT2),^{11,12} multiconfigurational pair-density functional theory (MC-PDFT),¹³ and hybrid MC-PDFT (HMC-PDFT)¹⁴ were employed, given their favorable performance for computing magnetic properties and their accuracy comparable to the CASPT2 method.^{9,15–18}

4 Zero-Field Splitting Parameters

We can compute the parameters with perturbation theory using the equation:

$$D_{ij} = -\frac{\zeta^2}{4S^2} \sum_{p,q} \frac{\langle \Psi_p | \hat{l}_i | \Psi_q \rangle \langle \Psi_q | \hat{l}_j | \Psi_p \rangle}{\epsilon_q - \epsilon_p}. \quad (\text{S6})$$

Figure S3 (a) shows the axial parameters of Cr(*o*-tol)₄, Mo(*o*-tol)₄, and W(*o*-tol)₄ complexes in cm⁻¹ units. It is observed that there is a significant trend of increasing the |*D*| parameter with the atomic number.

A close relationship exists between the axial parameter *D* and the spin-orbit coupling constant ζ as highlighted in red in equation S6. Also, it is known that the spin-orbit coupling constant increases with the atomic number as Z^4 .¹⁹

Figure S3 (a) shows the computed |*D*| values for the Cr(*o*-tol)₄, Mo(*o*-tol)₄, and W(*o*-tol)₄ complexes. The increasing trend with the metal substitution is similar to the increasing values of the atomic number as Z^4 (Figure S3 (b)). In the literature are reported the spin-orbit coupling constants for the ions Cr(*o*-tol)₄, Mo(*o*-tol)₄, and W(*o*-tol)₄ are 325, 950, and 2,300 cm⁻¹,²⁰ respectively. The squared of such constants (Figure S3 (c)) also present the same increasing trend as the computed |*D*| values. Therefore, we can conclude the observed trend is due to the increase in the relativistic effects when substituting the chromium center for heavier elements.

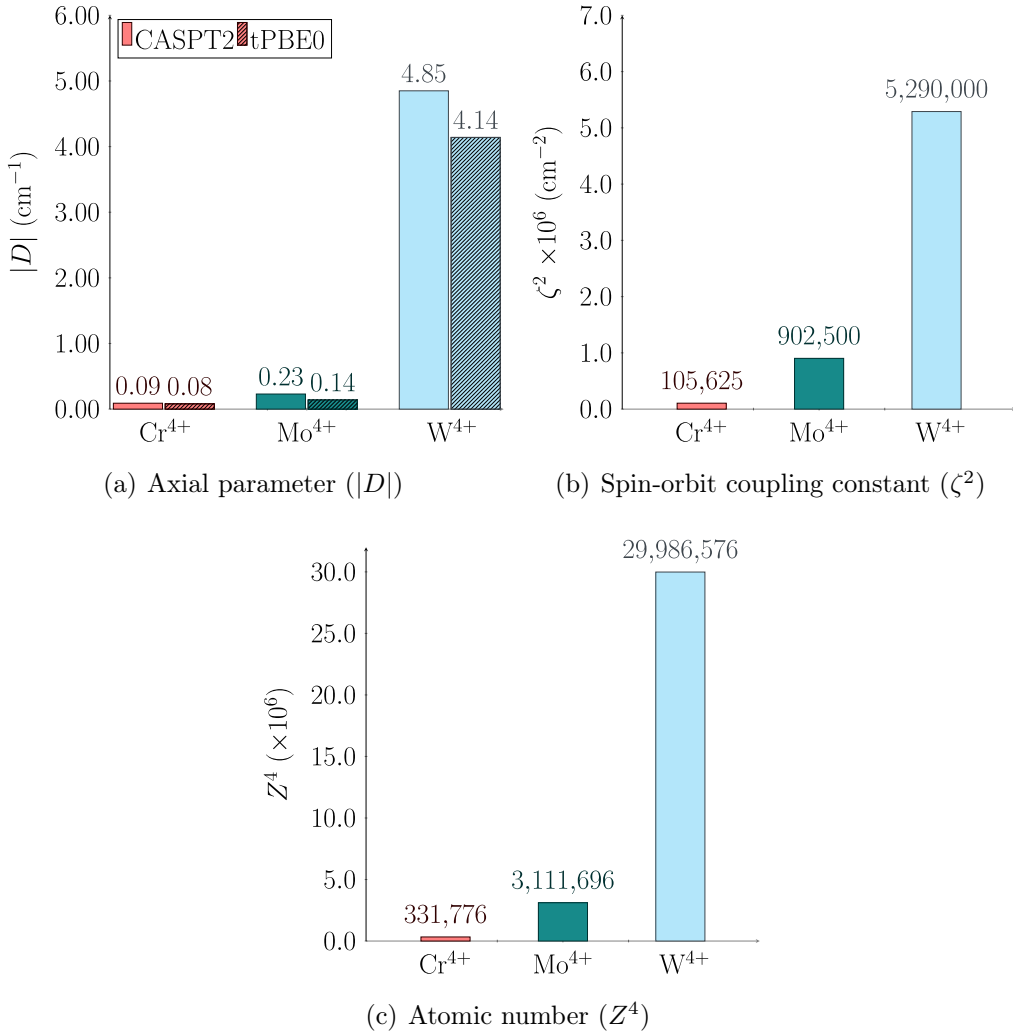


Figure S3: (a) The axial parameter $|D|$ computed using (10,15) active space, (b) Spin-orbit coupling constants squared, and (c) Increasing values for the atomic numbers as Z^4 . The ζ constants were obtained from reference 20.

To compute the ZFS parameters of the molecules across the period, we selected different numbers of spin-states to be included in the state-interaction step of each calculation. The description is given below.

When computing $|D|$ for the $\text{Cr}(o\text{-tol})_4$, $\text{Mo}(o\text{-tol})_4$, and $\text{W}(o\text{-tol})_4$ complexes, 7 triplets, and 9 singlets were mixed with spin-orbit coupling which are the state below the 3.5, eV cutoff. This cutoff was chosen *ad-hoc* following the natural energy gap found in the relative energies of the complexes studied. The 16 spin-orbit-free states are in a range of 0.0–3.5

eV (Figures S4–S6 and S12–S14); in the $\text{V}(o\text{-tol})_4^-$ complex, 7 triplets and 9 singlets below the 3.0 eV cutoff were used (Figures S8 and S16). Differently, for the $\text{Ti}(o\text{-tol})_4^{2-}$ complex, 10 triplets and 15 singlets were present below the ~ 2.5 eV cutoff, thus these ones were considered (Figure S7 and S15).

Increasing the number of triplets and singlets for the computation of the ZFS parameters leads to larger values, and in the case of $\text{Mo}(o\text{-tol})_4$ complex, the increasing trend for $|D|$ of $\text{Cr}(o\text{-tol})_4 < \text{V}(o\text{-tol})_4^- < \text{Mo}(o\text{-tol})_4$ is broken (See Table S9). The number of triplets (T) and singlets (S) were selected based on the relative energy plots shown in Figures S4–S8 and S12–S16.

Table S9: Computed ZFS axial parameters $|D|$ for the $\text{Ti}(o\text{-tol})_4^{2-}$, $\text{V}(o\text{-tol})_4^-$, $\text{Cr}(o\text{-tol})_4$, $\text{Mo}(o\text{-tol})_4$, and $\text{W}(o\text{-tol})_4$ complexes using the triplet optimized geometries. The $|D|$ parameters were obtained with SA-CASSCF, CASPT2, tPBE, and tPBE0 methods using the (10,15) active space for all complexes, except for $\text{V}(o\text{-tol})_4^-$, for which the (8,13) active space was used. The letters T and S stand for Triplets and Singlets, respectively. The values reported are in GHz.

Molecule	No. states	SA-CASSCF	CASPT2	tPBE	tPBE0
$\text{Ti}(o\text{-tol})_4^{2-}$	14T, 19S	17.28	16.15	13.15	14.49
$\text{V}(o\text{-tol})_4^-$	10T, 15S	6.98	5.96	4.07	5.56
$\text{Cr}(o\text{-tol})_4$	10T, 15S	4.98	3.99	2.76	3.66
$\text{Mo}(o\text{-tol})_4$	15T, 18S	3.65	4.90	7.76	4.26
$\text{W}(o\text{-tol})_4$	16T, 19S	817.08	946.23	816.29	823.98

Table S10: Computed rhombic parameters $|E|$ for the $\text{Ti}(o\text{-tol})_4^{2-}$, $\text{V}(o\text{-tol})_4^-$, $\text{Cr}(o\text{-tol})_4$, $\text{Mo}(o\text{-tol})_4$, and $\text{W}(o\text{-tol})_4$ complexes using the triplet optimized geometries. The $|E|$ parameters were obtained with SA-CASSCF, CASPT2, tPBE, and tPBE0 methods using the (10,15) active space for all complexes, except for $\text{V}(o\text{-tol})_4^-$, for which the (8,13) active space was used. The letters T and S stand for Triplets and Singlets, respectively. The values reported are in GHz.

Molecule	No. states	SA-CASSCF	CASPT2	tPBE	tPBE0
$\text{Ti}(o\text{-tol})_4^{2-}$	14T, 19S	0.01	0.01	0.01	0.01
$\text{V}(o\text{-tol})_4^-$	10T, 15S	0.00	0.00	0.00	0.00
$\text{Cr}(o\text{-tol})_4$	10T, 15S	0.00	0.00	0.00	0.00
$\text{Mo}(o\text{-tol})_4$	15T, 18S	0.10	0.58	2.19	2.10
$\text{W}(o\text{-tol})_4$	16T, 19S	147.16	181.54	159.38	155.98

5 Relative Electronic Energies

5.1 Single State CASPT2

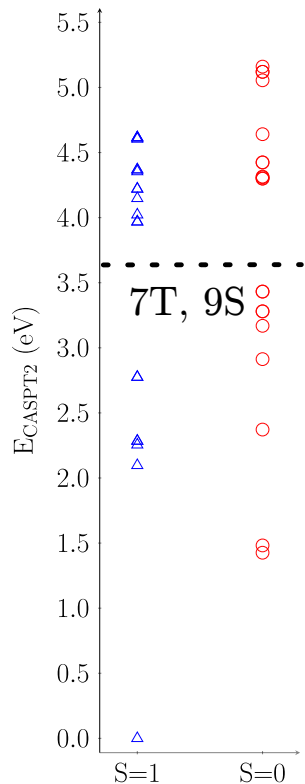


Figure S4: Relative energies of $\text{Cr}(o\text{-tol})_4$ molecule computed with the CASPT2 method for the (10,15) active space. The blue triangles correspond to triplet states and the red circles to singlet states.

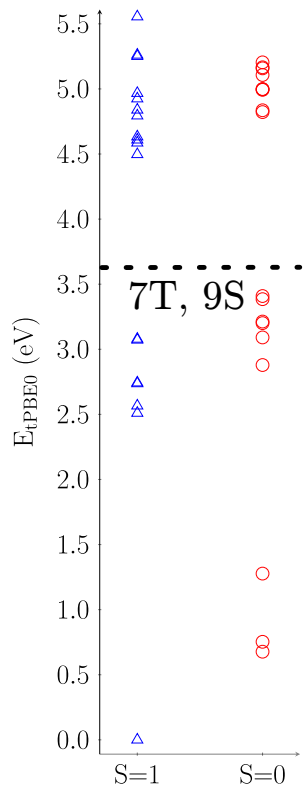


Figure S5: Relative energies of $\text{Mo}(o\text{-tol})_4$ molecule computed with the CASPT2 method for the (10,15) active space. The blue triangles correspond to triplet states and the red circles to singlet states.

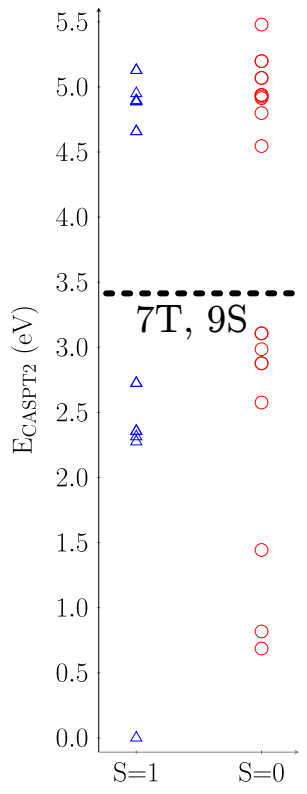


Figure S6: Relative energies of $\text{W}(o\text{-tol})_4$ molecule computed with the CASPT2 method for the (10,15) active space. The blue triangles correspond to triplet states and the red circles to singlet states.

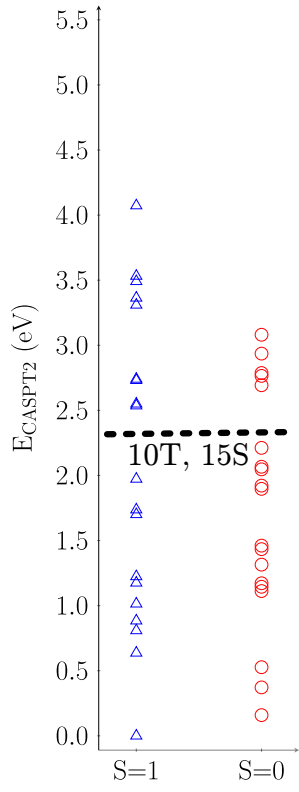


Figure S7: Relative energies of $\text{Ti}(o\text{-tol})_4^{2-}$ molecule computed with the CASPT2 method for the (10,15) active space. The blue triangles correspond to triplet states and the red circles to singlet states.

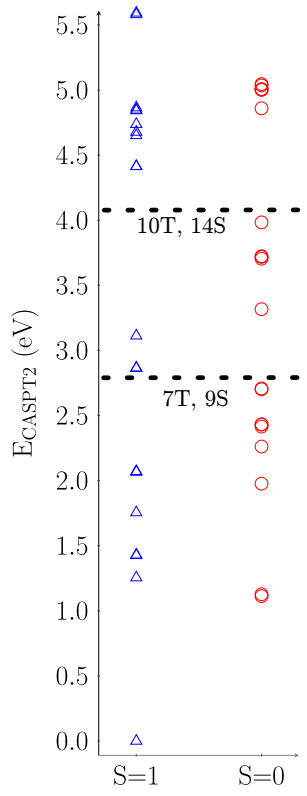


Figure S8: Relative energies of $\text{V}(o\text{-tol})_4^-$ molecule computed with the CASPT2 method for the (8,13) active space. The blue triangles correspond to triplet states and the red circles to singlet states.

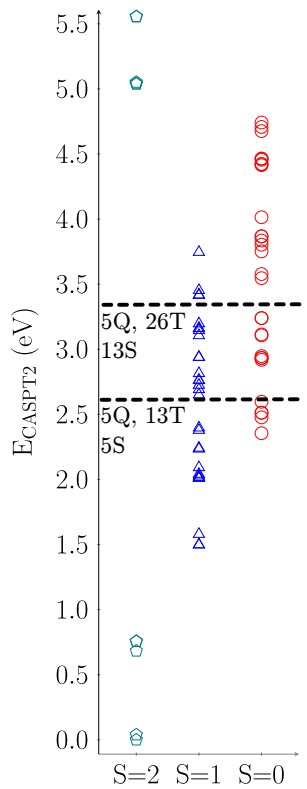


Figure S9: Relative energies of $\text{Fe}(o\text{-tol})_4^{2-}$ molecule computed with the CASPT2 method for the (12,13) active space. The green pentagons correspond to quintet states, the blue triangles to triplet states, and the red circles to singlet states.

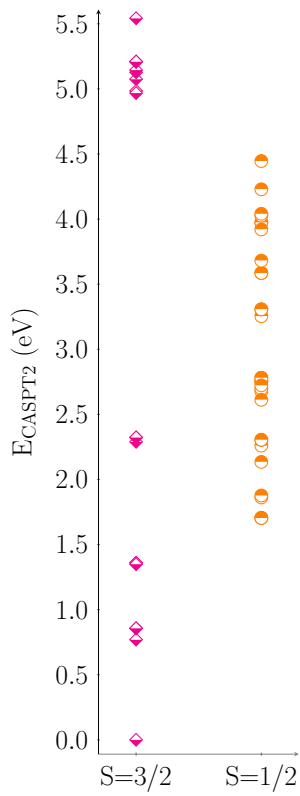


Figure S10: Relative energies of $\text{Co}(o\text{-tol})_4^{2-}$ molecule computed with the CASPT2 method for the (13,13) active space. The magenta half-filled rhombus corresponds to quartet states and the orange half-filled circles to doublet states.

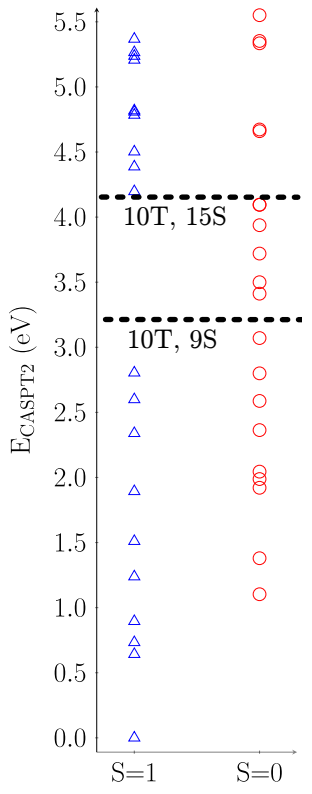


Figure S11: Relative energies of $\text{Ni}(o\text{-tol})_4^{2-}$ molecule computed with the CASPT2 method for the (14,13) active spaces. The blue triangles correspond to triplet states and the red circles to singlet states.

5.2 Hybrid MC-PDFT (tPBE0)

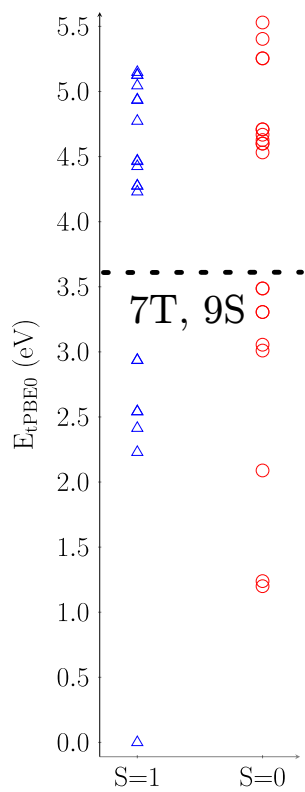


Figure S12: Relative energies of $\text{Cr}(o\text{-tol})_4$ molecule computed with the tPBE0 method for the (10,15) active spaces. The blue triangles correspond to triplet states and the red circles to singlet states.

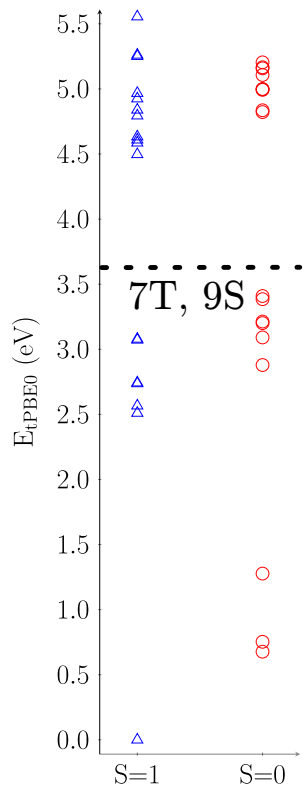


Figure S13: Relative energies of $\text{Mo}(o\text{-tol})_4$ molecule computed with the tPBE0 method for the (10,15) active spaces. The blue triangles correspond to triplet states and the red circles to singlet states.

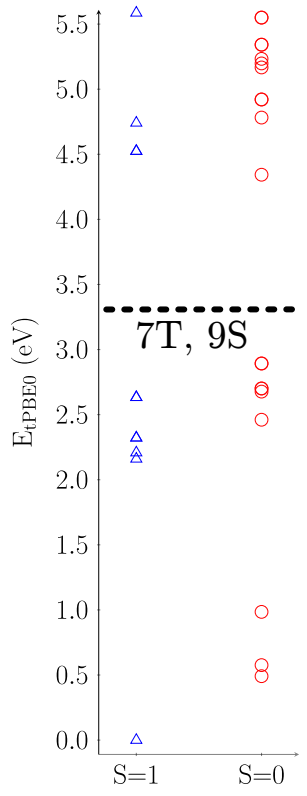


Figure S14: Relative energies of $\text{W}(o\text{-tol})_4$ molecule computed with the tPBE0 method for the (10,15) active spaces. The blue triangles correspond to triplet states and the red circles to singlet states.

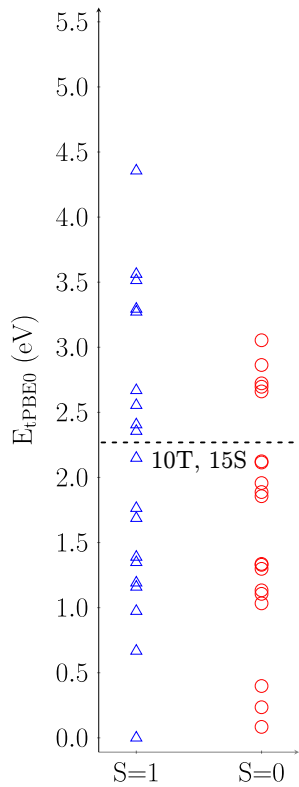


Figure S15: Relative energies of $\text{Ti}(o\text{-tol})_4^{2-}$ molecule computed with the tPBE0 method for the (10,15) active spaces. The blue triangles correspond to triplet states and the red circles to singlet states.

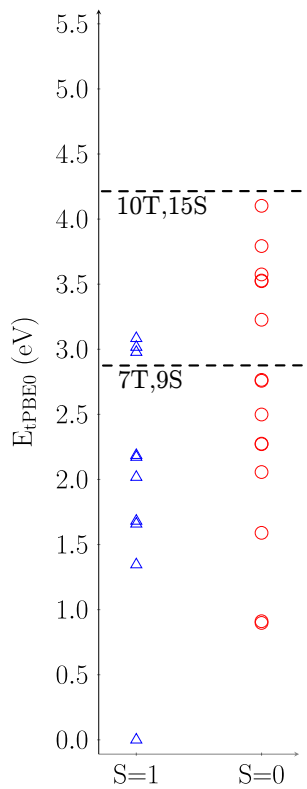


Figure S16: Relative energies of $\text{V}(o\text{-tol})_4^-$ molecule computed with the tPBE0 method for the (8,13) active spaces. The blue triangles correspond to triplet states and the red circles to singlet states.

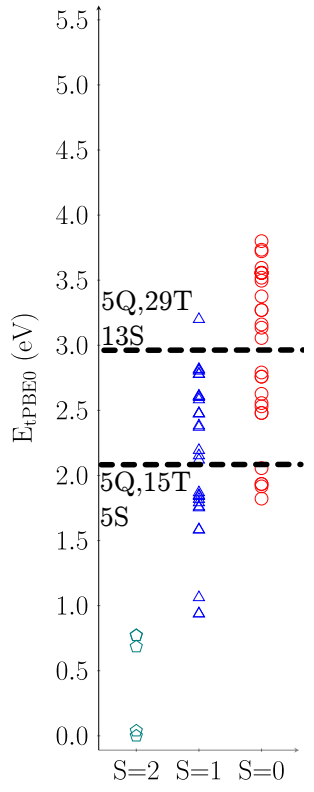


Figure S17: Relative energies of $\text{Fe}(o\text{-tol})_4^{2-}$ molecule computed with the tPBE0 method for the (12,13) active spaces. The green pentagons correspond to quintet states, the blue triangles to triplet states, and the red circles to singlet states.

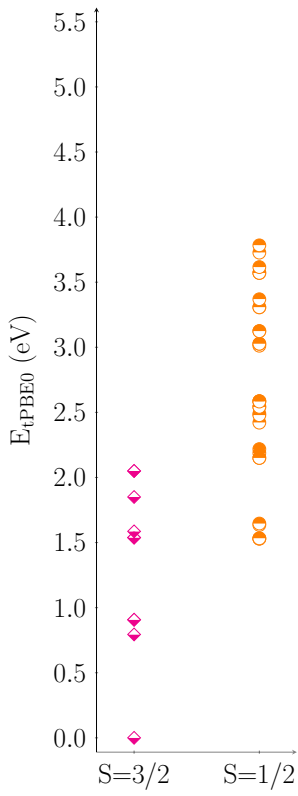


Figure S18: Relative energies of $\text{Co}(o\text{-tol})_4^{2-}$ molecule computed with the tPBE0 method for the (13,13) active spaces. The magenta half-filled rhombus corresponds to quartet states and the orange half-filled circles to doublet states.

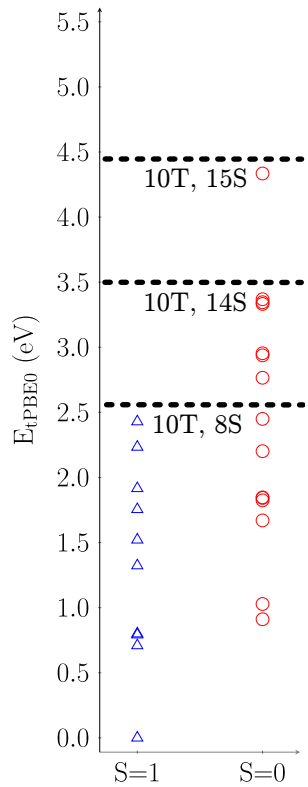


Figure S19: Relative energies of $\text{Ni}(o\text{-tol})_4^{2-}$ molecule computed with the tPBE0 method for the (14,13) active spaces. The blue triangles correspond to triplet states and the red circles to singlet states.

5.3 Relative Energies

Table S11: Computed relative energies with the SA-CASSCF, CASPT2, tPBE, and tPBE0 methods for the relative energies of Cr(*o*-tol)₄ molecule when using the (10,15) active space. The values reported are in eV.

No.	SA-CASSCF		CASPT2		tPBE		tPBE0	
	Triplet	Singlet	Triplet	Singlet	Triplet	Singlet	Triplet	Singlet
1	0.000	1.701	0.000	1.426	0.000	1.033	0.000	1.200
2	2.496	1.764	2.097	1.482	2.140	1.064	2.229	1.239
3	2.740	2.843	2.255	2.372	2.305	1.837	2.414	2.089
4	2.768	3.495	2.284	2.913	2.465	2.909	2.541	3.055
5	2.769	3.735	2.284	3.169	2.466	2.768	2.542	3.010
6	3.342	3.933	2.775	3.280	2.799	3.097	2.935	3.306
7	3.344	3.933	2.775	3.280	2.801	3.097	2.937	3.306
8	4.387	4.101	3.969	3.432	4.238	3.282	4.275	3.487
9	4.389	4.101	3.967	3.432	4.237	3.282	4.275	3.487
10	4.484	4.846	4.022	4.300	4.145	4.517	4.230	4.600
11	4.685	4.846	4.148	4.300	4.339	4.517	4.425	4.600
12	4.690	4.922	4.220	4.315	4.387	4.529	4.463	4.627
13	4.692	4.928	4.221	4.310	4.394	4.401	4.468	4.532
14	4.940	5.016	4.368	4.424	4.931	4.606	4.933	4.709
15	4.944	5.016	4.368	4.424	4.934	4.606	4.937	4.709
16	5.046	5.447	4.354	4.641	4.682	4.408	4.773	4.668
17	5.265	5.837	4.604	5.055	4.972	5.260	5.045	5.404
18	5.290	5.925	4.615	5.160	5.071	5.399	5.126	5.530
19	5.292	6.030	4.614	5.120	5.070	4.996	5.126	5.254
20	5.309	6.030	4.614	5.120	5.094	4.996	5.148	5.255

Table S12: Computed relative energies with the SA-CASSCF, CASPT2, tPBE, and tPBE0 methods for the relative energies of Mo(*o*-tol)₄ molecule when using the (10,15) active space. The values reported are in eV.

No.	SA-CASSCF		CASPT2		tPBE		tPBE0	
	Triplet	Singlet	Triplet	Singlet	Triplet	Singlet	Triplet	Singlet
1	0.000	1.033	0.000	0.816	0.000	0.558	0.000	0.677
2	2.852	1.154	2.571	0.938	2.471	0.620	2.566	0.753
3	2.876	1.998	2.499	1.629	2.388	1.037	2.510	1.277
4	2.982	3.345	2.638	2.813	2.655	2.724	2.737	2.879
5	2.988	3.761	2.637	3.262	2.661	2.868	2.743	3.091
6	3.446	3.769	3.042	3.181	2.947	3.011	3.072	3.201
7	3.449	3.782	3.040	3.180	2.955	3.023	3.079	3.213
8	4.897	4.014	4.149	3.410	4.512	3.176	4.609	3.385
9	4.961	4.024	4.088	3.419	4.342	3.204	4.497	3.409
10	4.962	5.287	4.142	4.410	4.524	4.686	4.633	4.836
11	5.060	5.371	4.179	4.539	4.428	4.866	4.586	4.993
12	5.247	5.376	4.397	4.538	4.643	4.871	4.794	4.997
13	5.312	5.412	4.444	4.451	4.796	4.626	4.925	4.822
14	5.361	5.522	4.444	4.636	4.665	5.037	4.839	5.158
15	5.540	5.529	4.583	4.636	4.776	5.045	4.967	5.166
16	5.843	5.631	5.179	4.636	5.053	4.788	5.251	4.999
17	5.854	5.843	5.182	5.049	5.064	4.861	5.261	5.107
18	6.194	5.921	5.505	4.873	5.342	4.965	5.555	5.204
19	6.471	6.393	5.424	5.547	5.816	5.404	5.979	5.651
20	6.580	6.541	5.621	5.690	6.160	5.385	6.265	5.674

Table S13: Computed relative energies with the SA-CASSCF, CASPT2, tPBE, and tPBE0 methods for the relative energies of $\text{W}(o\text{-tol})_4$ molecule when using the (10,15) active space. The values reported are in eV.

No.	SA-CASSCF		CASPT2		tPBE		tPBE0	
	Triplet	Singlet	Triplet	Singlet	Triplet	Singlet	Triplet	Singlet
1	0.000	0.966	0.000	0.686	0.000	0.332	0.000	0.491
2	2.493	1.099	2.314	0.817	2.112	0.401	2.208	0.576
3	2.545	1.851	2.275	1.443	2.032	0.696	2.160	0.985
4	2.576	3.100	2.356	2.576	2.237	2.248	2.322	2.461
5	2.577	3.440	2.356	2.877	2.237	2.455	2.322	2.701
6	3.025	3.440	2.724	2.877	2.503	2.455	2.633	2.701
7	3.025	3.522	2.725	2.985	2.503	2.395	2.633	2.677
8	5.108	3.718	4.658	3.107	4.330	2.617	4.524	2.893
9	5.108	3.718	4.658	3.107	4.330	2.617	4.524	2.893
10	5.388	5.230	4.896	4.546	4.525	4.047	4.741	4.343
11	6.083	5.660	4.891	4.926	5.524	4.490	5.664	4.782
12	6.083	5.877	4.891	4.799	5.524	4.931	5.664	5.167
13	6.160	5.947	4.886	4.938	5.395	5.140	5.586	5.342
14	6.229	5.947	4.950	4.938	5.429	5.140	5.629	5.342
15	6.437	6.029	5.128	5.198	5.611	4.552	5.818	4.921
16	6.437	6.029	5.128	5.198	5.611	4.552	5.818	4.921
17	7.126	6.068	5.819	4.914	6.441	4.954	6.613	5.233
18	7.294	6.162	5.968	5.069	6.589	5.346	6.765	5.550
19	7.591	6.162	6.295	5.069	6.851	5.346	7.036	5.550
20	7.591	6.335	6.295	5.479	6.851	4.820	7.036	5.198

Table S14: Computed relative energies with the SA-CASSCF, CASPT2, tPBE, and tPBE0 methods for the relative energies of $\text{Ti}(o\text{-tol})_4^{2-}$ molecule when using the (10,15) active space. The values reported are in eV.

No.	SA-CASSCF		CASPT2		tPBE		tPBE0	
	Triplet	Singlet	Triplet	Singlet	Triplet	Singlet	Triplet	Singlet
1	0.000	0.721	0.000	0.570	0.000	0.495	0.000	0.552
2	0.657	0.959	0.605	0.712	0.641	0.500	0.645	0.615
3	1.130	1.426	0.929	0.990	1.013	0.761	1.042	0.927
4	1.131	1.752	0.928	1.399	1.013	1.169	1.042	1.315
5	1.426	2.114	0.972	1.599	1.028	1.567	1.128	1.703
6	1.560	2.185	1.152	1.635	1.347	1.638	1.400	1.775
7	1.561	2.185	1.153	1.635	1.347	1.638	1.401	1.775
8	2.167	2.419	1.694	1.800	1.623	1.636	1.759	1.832
9	2.168	2.419	1.694	1.800	1.624	1.636	1.760	1.832
10	2.306	2.699	1.852	2.199	1.804	2.095	1.930	2.246
11	5.247	2.997	4.109	2.322	4.182	2.201	4.448	2.400
12	5.292	3.165	4.184	2.475	4.379	2.249	4.607	2.478
13	5.977	3.165	4.268	2.475	5.054	2.249	5.285	2.478
14	6.549	3.464	4.993	2.741	5.169	2.492	5.514	2.735
15	6.615	4.658	4.378	3.342	5.489	2.604	5.771	3.118
16	6.628	5.347	4.377	4.120	5.500	4.465	5.782	4.686
17	6.670	6.716	4.464	5.088	5.260	5.514	5.612	5.814
18	6.747	6.735	4.950	4.476	5.281	5.608	5.647	5.889
19	6.748	6.736	4.949	4.476	5.281	5.608	5.648	5.890
20	7.050	7.161	4.669	4.754	5.618	5.695	5.976	6.061

Table S15: Computed relative energies with the SA-CASSCF, CASPT2, tPBE, and tPBE0 methods for the relative energies of $\text{V}(o\text{-tol})_4^-$ molecule when using the (8,13) active space. The values reported are in eV.

No.	SA-CASSCF		CASPT2		tPBE		tPBE0	
	Triplet	Singlet	Triplet	Singlet	Triplet	Singlet	Triplet	Singlet
1	0.000	1.417	0.000	1.185	0.000	0.695	0.000	0.876
2	1.313	1.444	1.302	1.212	1.298	0.710	1.302	0.894
3	1.491	2.413	1.479	1.994	1.519	1.215	1.512	1.515
4	1.496	2.629	1.483	2.362	1.524	1.803	1.517	2.010
5	2.009	2.742	1.783	2.403	1.901	2.271	1.928	2.389
6	2.227	2.800	2.045	2.543	2.072	2.043	2.110	2.232
7	2.232	2.803	2.051	2.547	2.077	2.046	2.116	2.236
8	3.259	3.044	2.897	2.665	2.468	2.487	2.666	2.626
9	3.262	3.049	2.903	2.671	2.475	2.494	2.672	2.633
10	3.426	3.695	3.182	3.320	2.847	2.900	2.992	3.099
11	6.378	4.032	4.699	3.675	5.908	3.238	6.026	3.436
12	6.382	4.117	4.699	3.777	5.908	3.199	6.026	3.429
13	6.464	4.121	4.745	3.782	5.535	3.204	5.767	3.433
14	6.506	4.369	4.758	4.047	5.509	3.472	5.758	3.696
15	6.519	5.731	4.812	4.698	5.592	3.579	5.824	4.117
16	6.720	6.742	4.870	4.971	5.508	5.725	5.811	5.979
17	6.722	6.746	4.956	4.974	5.560	5.729	5.851	5.983
18	6.725	6.889	4.948	5.092	5.534	5.850	5.832	6.110
19	6.755	6.892	4.971	5.094	5.606	5.851	5.893	6.112
20	6.759	6.906	4.976	4.977	5.600	5.378	5.890	5.760

S35

Table S16: Computed relative energies with the SA-CASSCF, CASPT2, tPBE, and tPBE0 methods for the relative energies of Fe(*o*-tol)₄²⁻ molecule when using the (12,13) active space. The values reported are in eV.

No.	SA-CASSCF			CASPT2			tPBE			tPBE0		
	Quintet	Triplet	Singlet	Quintet	Triplet	Singlet	Quintet	Triplet	Singlet	Quintet	Triplet	Singlet
1	0.000	1.446	2.567	0.000	1.499	2.355	0.000	0.770	1.574	0.000	0.939	1.822
2	0.033	1.447	2.662	0.039	1.499	2.477	0.041	0.768	1.667	0.039	0.938	1.916
3	0.679	1.532	2.672	0.683	1.580	2.513	0.687	0.906	1.688	0.685	1.063	1.934
4	0.751	2.029	2.674	0.756	2.010	2.512	0.778	1.433	1.689	0.771	1.582	1.935
5	0.751	2.032	2.742	0.757	2.016	2.597	0.779	1.437	1.828	0.772	1.585	2.056
6	7.599	2.080	3.151	5.039	2.012	2.933	6.275	1.760	2.256	6.606	1.840	2.480
7	7.600	2.091	3.151	5.040	2.028	2.934	6.276	1.767	2.256	6.607	1.848	2.480
8	7.674	2.093	3.168	5.052	2.092	2.919	5.641	1.726	2.352	6.149	1.818	2.556
9	8.099	2.150	3.242	5.555	2.041	2.948	6.702	1.673	2.294	7.052	1.792	2.531
10	8.100	2.226	3.283	5.556	2.235	3.107	6.703	1.595	2.409	7.053	1.753	2.627
11	8.186	2.231	3.373	5.634	2.242	3.114	6.342	1.605	2.597	6.803	1.761	2.791
12	8.199	2.537	3.422	5.675	2.379	3.239	6.482	1.981	2.537	6.911	2.120	2.759
13	8.247	2.590	3.422	5.810	2.397	3.240	6.338	1.628	2.538	6.815	1.869	2.759
14	8.311	2.742	3.872	5.681	2.692	3.578	6.226	2.263	2.890	6.747	2.383	3.135
15	8.316	2.815	3.881	5.695	2.761	3.752	6.198	2.361	2.920	6.728	2.475	3.160
16	8.316	2.817	3.919	5.695	2.764	3.546	6.197	2.363	2.768	6.726	2.476	3.056
17	8.410	2.833	3.973	5.857	2.651	3.867	6.463	1.926	3.036	6.950	2.153	3.270
18	8.445	2.859	3.974	5.863	2.815	3.868	6.429	2.514	3.037	6.933	2.600	3.271
19	8.548	2.896	4.150	6.056	2.725	3.835	6.555	1.959	3.309	7.053	2.194	3.519
20	8.565	2.944	4.170	5.977	2.938	3.803	6.702	2.496	3.112	7.168	2.608	3.376
21	8.566	2.947	4.308	5.978	2.940	4.014	6.702	2.499	3.305	7.168	2.611	3.556
22	9.030	3.125	4.578	6.306	3.145	4.422	6.585	2.402	3.214	7.197	2.583	3.555
23	9.097	3.200	4.578	6.331	3.160	4.423	6.631	2.635	3.215	7.247	2.777	3.556
24	9.107	3.202	4.635	6.308	3.162	4.456	6.673	2.639	3.249	7.281	2.780	3.595
25	9.173	3.541	4.933	6.398	3.106	4.414	6.767	1.982	3.016	7.368	2.372	3.496
26	9.173	3.549	4.989	6.399	3.415	4.464	6.768	2.566	3.079	7.369	2.812	3.556
27	9.877	3.552	4.991	6.863	3.419	4.465	6.612	2.571	3.081	7.428	2.816	3.558
28	9.934	3.564	5.156	6.853	3.453	4.742	7.046	2.550	3.260	7.768	2.803	3.734
29	9.935	3.615	5.221	6.853	3.197	4.676	7.045	2.096	3.222	7.768	2.476	3.722
30	9.951	3.664	5.253	6.842	3.746	4.708	6.613	3.046	3.315	7.447	3.200	3.800

Table S17: Computed relative energies with the SA-CASSCF, CASPT2, tPBE, and tPBE0 methods for the relative energies of $\text{Co}(o\text{-tol})_4^{2-}$ molecule when using the (13,13) active space. The values reported are in eV.

No.	SA-CASSCF		CASPT2		tPBE		tPBE0	
	Quartet	Doublet	Quartet	Doublet	Quartet	Doublet	Quartet	Doublet
1	0.000	1.991	0.000	1.706	0.000	1.376	0.000	1.529
2	0.759	1.994	0.770	1.704	0.806	1.378	0.794	1.532
3	0.835	1.994	0.857	1.704	0.931	1.378	0.907	1.532
4	0.835	2.091	0.857	1.862	0.931	1.483	0.907	1.635
5	1.379	2.105	1.360	1.877	1.591	1.492	1.538	1.646
6	1.379	2.380	1.360	2.135	1.591	2.164	1.538	2.218
7	1.395	2.616	1.349	2.260	1.649	2.045	1.586	2.188
8	2.735	2.650	2.289	2.304	1.555	1.984	1.850	2.150
9	2.745	2.650	2.323	2.305	1.819	1.984	2.050	2.150
10	2.745	2.879	2.323	2.678	1.819	2.359	2.050	2.489
11	7.670	2.937	5.075	2.752	6.044	2.469	6.451	2.586
12	7.674	2.937	4.985	2.753	5.967	2.469	6.394	2.586
13	7.674	2.959	4.968	2.697	5.991	2.242	6.412	2.421
14	7.691	3.005	5.128	2.612	6.041	2.303	6.454	2.478
15	7.701	3.035	5.145	2.781	6.032	2.378	6.450	2.542
16	7.917	3.035	5.208	2.781	6.054	2.378	6.519	2.542
17	7.947	3.106	5.210	2.723	6.009	2.409	6.493	2.583
18	7.947	3.560	5.210	3.254	6.009	2.829	6.493	3.012
19	8.217	3.571	5.543	3.307	6.397	2.846	6.852	3.027
20	8.286	3.571	5.622	3.307	6.394	2.846	6.867	3.027
21	8.416	3.766	5.699	3.586	6.336	3.154	6.856	3.307
22	8.545	3.766	5.902	3.586	6.354	3.154	6.902	3.307
23	8.615	3.831	5.924	3.681	6.453	3.215	6.994	3.369
24	8.615	4.073	5.924	3.974	6.453	3.403	6.994	3.571
25	8.676	4.074	5.935	3.974	6.444	3.403	7.002	3.571
26	8.746	4.102	5.871	4.026	6.279	3.453	6.896	3.616
27	8.771	4.513	6.046	4.229	6.614	3.464	7.153	3.727
28	8.771	4.537	6.047	4.446	6.614	3.532	7.153	3.783
29	8.985	4.606	6.310	3.921	6.853	2.631	7.386	3.125
30	8.985	4.870	6.310	4.041	6.852	2.540	7.386	3.123

Table S18: Computed relative energies with the SA-CASSCF, CASPT2, tPBE, and tPBE0 methods for the relative energies of $\text{Ni}(o\text{-tol})_4^{2-}$ molecule when using the (14,13) active space. The values reported are in eV.

No.	SA-CASSCF		CASPT2		tPBE		tPBE0	
	Triplet	Singlet	Triplet	Singlet	Triplet	Singlet	Triplet	Singlet
1	0.000	1.500	0.000	1.034	0.000	0.597	0.000	0.823
2	0.630	1.782	0.691	1.372	0.819	0.667	0.772	0.946
3	0.694	2.319	0.768	1.981	0.889	1.406	0.840	1.635
4	0.836	2.404	0.951	1.991	0.941	1.504	0.915	1.729
5	1.194	2.414	1.287	2.078	1.543	1.598	1.456	1.802
6	1.424	2.943	1.572	2.396	1.779	1.430	1.690	1.809
7	1.799	3.076	1.965	2.637	1.979	2.209	1.934	2.426
8	2.747	3.226	2.397	2.836	1.791	1.837	2.030	2.185
9	2.983	3.478	2.626	3.083	2.093	2.736	2.316	2.922
10	3.144	3.776	2.809	3.543	2.312	2.603	2.520	2.896
11	7.500	3.787	4.555	3.555	6.189	2.603	6.517	2.899
12	7.527	4.000	4.491	3.779	5.778	3.140	6.216	3.355
13	7.648	4.255	4.619	4.257	6.349	3.217	6.674	3.476
14	8.046	4.284	5.056	4.249	6.171	3.167	6.640	3.446
15	8.120	6.830	4.960	5.501	6.008	3.627	6.536	4.428
16	8.156	7.469	4.978	4.243	6.098	5.827	6.613	6.237
17	8.356	8.118	5.331	4.854	6.303	6.096	6.816	6.602
18	8.420	8.242	5.328	4.870	6.458	6.377	6.948	6.843
19	8.548	8.756	5.535	5.733	6.693	6.196	7.156	6.836
20	8.686	8.774	5.590	5.669	6.457	6.182	7.014	6.830

5.4 Absolute Energies

Table S19: Computed absolute energies with the SA-CASSCF, CASPT2, tPBE, and tPBE0 methods for the relative energies in Figures S4 and S12 of Cr(*o-tol*)₄ molecule when using the (10,15) active space.

No.	SA-CASSCF			CASPT2			tPBE			tPBE0		
	Triplet	Singlet	Triplet	Singlet	Triplet	Singlet	Triplet	Singlet	Triplet	Singlet	Triplet	Singlet
1	-2126.47618830	-2126.41356374	-2129.40563868	-2129.35271166	-2133.28573804	-2133.24721356	-2131.58335061	-2131.53880111				
2	-2126.38844137	-2126.41186793	-2129.32870869	-2129.35105113	-2133.20851813	-2133.24636305	-2131.50349894	-2131.53773927				
3	-2126.37985386	-2126.37138764	-2129.32357574	-2129.31780887	-2133.19893847	-2133.21789096	-2131.49416732	-2131.50626513				
4	-2126.37985244	-2126.34718574	-2129.32357631	-2129.29849510	-2133.19893792	-2133.17773266	-2131.49416655	-2131.47009593				
5	-2126.37737144	-2126.33987031	-2129.32184779	-2129.29063913	-2133.20136262	-2133.18460486	-2131.49536483	-2131.47342122				
6	-2126.35914341	-2126.33521348	-2129.30557911	-2129.28699005	-2133.1864301	-2133.17508987	-2131.47961811	-2131.46512077				
7	-2126.35914250	-2126.33521330	-2129.30557905	-2129.28698995	-2133.18644173	-2133.17508967	-2131.47961692	-2131.46512058				
8	-2126.30885914	-2126.32992037	-2129.25806800	-2129.28327992	-2133.12474874	-2133.16516573	-2131.42077634	-2131.45635439				
9	-2126.30885700	-2126.32992011	-2129.25807101	-2129.28327955	-2133.12475187	-2133.16516512	-2131.42077815	-2131.45635387				
10	-2126.30473836	-2126.29574305	-2129.25620875	-2129.24880493	-2133.12734398	-2133.12104870	-2131.42169258	-2131.41472229				
11	-2126.29893248	-2126.29574304	-2129.25008163	-2129.24880485	-2133.12015229	-2133.12104862	-2131.41484734	-2131.41472223				
12	-2126.29893054	-2126.29247010	-2129.25008121	-2129.24723648	-2133.12014448	-2133.12075467	-2131.41484100	-2131.41368353				
13	-2126.29592867	-2126.29074238	-2129.24854909	-2129.24391650	-2133.11780763	-2133.11627091	-2131.41233789	-2131.40988878				
14	-2126.2930141	-2126.29074228	-2129.24538615	-2129.24391636	-2133.10105876	-2133.11627045	-2131.39904442	-2131.40988841				
15	-2126.29299749	-2126.29055431	-2129.24538610	-2129.24451464	-2133.10105421	-2133.11422472	-2131.39904003	-2131.40830712				
16	-2126.28671722	-2126.27636513	-2129.24430592	-2129.23695798	-2133.10852511	-2133.12412141	-2131.40307314	-2131.41218234				
17	-2126.2857367	-2126.25937556	-2129.24273209	-2129.22435950	-2133.12331582	-2133.08951273	-2131.41393028	-2131.38197844				
18	-2126.2857173	-2126.25746186	-2129.24273153	-2129.21984837	-2133.10419175	-2131.41392909	-2131.39250928					
19	-2126.28224922	-2126.25746162	-2129.23841297	-2129.21984808	-2133.09864713	-2133.10419158	-2131.39454765	-2131.39250909				
20	-2126.28177455	-2126.25707948	-2129.23806713	-2129.22099506	-2133.10126953	-2133.10526669	-2131.39639579	-2131.39321989				

Table S20: Computed absolute energies with the SA-CASSCF, CASPT2, tPBE, and tPBE0 methods for the relative energies in Figures S5 and S13 of Mo(*o*-tol)₄ molecule when using the (10,15) active space.

No.	SA-CASSCF			CASPT2			tPBE			tPBE0		
	Triplet	Singlet	Triplet	Singlet	Triplet	Singlet	Triplet	Singlet	Triplet	Singlet	Triplet	Singlet
1	-5122.57076289	-5122.53210926	-5125.47422173	-5125.44351824	-5130.30002591	-5130.27914473	-5128.36771016	-5128.34238586	-5128.27119684	-5128.33992926	-5128.27191267	-5128.32064192
2	-5122.46343769	-5122.52836194	-5125.37718974	-5125.43975048	-5130.20711656	-5130.27711836	-5128.27119684	-5128.33992926	-5128.27191267	-5128.32064192	-5128.27191267	-5128.32064192
3	-5122.46110829	-5122.49682362	-5125.37849058	-5125.41393963	-5130.2084746	-5130.26191469	-5128.27191267	-5128.32064192	-5128.27191267	-5128.32064192	-5128.27191267	-5128.32064192
4	-5122.46086774	-5122.44373694	-5125.37693655	-5125.36675695	-5130.20244798	-5130.19651515	-5128.26705292	-5128.25832060	-5128.26681247	-5128.24996527	-5128.26681247	-5128.24996527
5	-5122.46063466	-5122.43169598	-5125.37693649	-5125.35688377	-5130.20220507	-5130.18938837	-5128.26681247	-5128.24996527	-5128.26681247	-5128.24996527	-5128.26681247	-5128.24996527
6	-5122.44448387	-5122.43131110	-5125.36285203	-5125.35696322	-5130.19260459	-5130.18898167	-5128.25557441	-5128.24956403	-5128.25557441	-5128.24956403	-5128.25557441	-5128.24956403
7	-5122.44434501	-5122.42948579	-5125.36289290	-5125.35142474	-5130.19226851	-5130.19232468	-5128.25528764	-5128.25161496	-5128.25528764	-5128.25161496	-5128.25528764	-5128.25161496
8	-5122.39165678	-5122.42326739	-5125.32262592	-5125.34900389	-5130.13531485	-5130.18446805	-5128.19940033	-5128.24416789	-5128.19940033	-5128.24416789	-5128.19940033	-5128.24416789
9	-5122.38938431	-5122.42298464	-5125.322294649	-5125.34874110	-5130.13508463	-5130.18348868	-5128.19865955	-5128.24336267	-5128.19865955	-5128.24336267	-5128.19865955	-5128.24336267
10	-5122.38907082	-5122.37671881	-5125.32430843	-5125.31221457	-5130.14086848	-5130.12808800	-5128.20291907	-5128.19024570	-5128.20291907	-5128.19024570	-5128.20291907	-5128.19024570
11	-5122.38494837	-5122.37431640	-5125.32058843	-5125.30817713	-5130.13736510	-5130.12196221	-5128.19926092	-5128.18505076	-5128.19926092	-5128.18505076	-5128.19926092	-5128.18505076
12	-5122.37909415	-5122.37412925	-5125.31370286	-5125.30820795	-5130.13085866	-5130.12179999	-5128.19291753	-5128.18488231	-5128.19291753	-5128.18488231	-5128.19291753	-5128.18488231
13	-5122.37678767	-5122.37269095	-5125.31202470	-5125.31115507	-5130.12516064	-5130.13066363	-5128.18806740	-5128.19117046	-5128.18806740	-5128.19117046	-5128.18806740	-5128.19117046
14	-5122.37451738	-5122.36912189	-5125.31164430	-5125.30480292	-5130.12937367	-5130.11597039	-5128.17925827	-5128.17207925	-5128.17925827	-5128.17207925	-5128.17925827	-5128.17925827
15	-5122.36853566	-5122.36884837	-5125.30694314	-5125.30480461	-5130.12569016	-5130.11561700	-5128.18640154	-5128.17892484	-5128.18640154	-5128.17892484	-5128.18640154	-5128.17892484
16	-5122.35327080	-5122.36434593	-5125.28094000	-5125.30411283	-5130.11222569	-5130.12464516	-5128.17248697	-5128.18457035	-5128.17248697	-5128.18457035	-5128.17248697	-5128.18457035
17	-5122.35283766	-5122.35522096	-5125.28078532	-5125.29654202	-5130.11182644	-5130.11928385	-5128.17207925	-5128.17826813	-5128.17207925	-5128.17826813	-5128.17207925	-5128.17826813
18	-5122.34351639	-5122.35058729	-5125.27205506	-5125.28229481	-5130.10478870	-5130.11673353	-5128.16447062	-5128.17519697	-5128.16447062	-5128.17519697	-5128.16447062	-5128.17519697
19	-5122.33229885	-5122.33609025	-5125.27369191	-5125.27023645	-5130.08501474	-5130.10224960	-5128.14683577	-5128.16070976	-5128.14683577	-5128.16070976	-5128.14683577	-5128.16070976
20	-5122.32744796	-5122.32741735	-5125.26600346	-5125.26200585	-5130.07260451	-5130.09993434	-5128.13631537	-5128.15680509	-5128.13631537	-5128.15680509	-5128.13631537	-5128.15680509

Table S21: Computed absolute energies with the SA-CASSCF, CASPT2, tPBE, and tPBE0 methods for the relative energies in Figures S6 and S14 of W(*o*-tol)₄ molecule when using the (10,15) active space.

No.	SA-CASSCF			CASPT2			tPBE			tPBE0		
	Triplet	Singlet	Triplet	Singlet	Triplet	Singlet	Triplet	Singlet	Triplet	Singlet	Triplet	Singlet
1	-17204.3008392	-17204.26866065	-17207.19989114	-17207.17294089	-17215.61304871	-17215.59622405	-17212.78500751	-17212.76433320	-17212.78500751	-17212.76433320	-17212.76172718	-17212.74721333
2	-17204.21364958	-17204.26430606	-17207.11374566	-17207.16881359	-17215.53548029	-17215.59420088	-17212.70502261	-17212.76172718	-17212.70502261	-17212.76172718	-17212.74721333	-17212.74721333
3	-17204.21353512	-17204.23732965	-17207.11501596	-17207.14514343	-17215.53433839	-17215.58384122	-17212.70413757	-17212.74721333	-17212.70413757	-17212.74721333	-17212.74721333	-17212.74721333
4	-17204.21346835	-17204.19459055	-17207.11503187	-17207.10228776	-17215.53430277	-17215.52455553	-17212.70409417	-17212.69206429	-17212.70409417	-17212.69206429	-17212.69206429	-17212.69206429
5	-17204.21076954	-17204.18506371	-17207.11613637	-17207.09474342	-17215.53881852	-17215.52072046	-17212.70680628	-17212.68680627	-17212.70680628	-17212.68680627	-17212.68680627	-17212.68680627
6	-17204.19613594	-17204.18498499	-17207.10187860	-17207.09470994	-17215.52471914	-17215.52073321	-17212.69257334	-17212.68679616	-17212.69257334	-17212.68679616	-17212.68679616	-17212.68679616
7	-17204.19610145	-17204.18034268	-17207.10185327	-17207.08772683	-17215.52478786	-17215.52008027	-17212.69261626	-17212.68514587	-17212.69261626	-17212.68514587	-17212.68514587	-17212.68514587
8	-17204.12348610	-17204.17654511	-17207.02929311	-17207.08578866	-17215.45715511	-17215.51443880	-17212.62373786	-17212.67996538	-17212.62373786	-17212.67996538	-17212.67996538	-17212.67996538
9	-17204.12343171	-17204.176477825	-17207.02928811	-17207.08575534	-17215.45713891	-17215.51422850	-17212.62371211	-17212.67979094	-17212.62371211	-17212.67979094	-17212.67979094	-17212.67979094
10	-17204.11674097	-17204.11966351	-17207.02320608	-17207.02918922	-17215.45247158	-17215.45813132	-17212.61853893	-17212.62351437	-17212.61853893	-17212.62351437	-17212.62351437	-17212.62351437
11	-17204.09730144	-17204.10956386	-17207.03512082	-17207.01969439	-17215.42858242	-17215.44696701	-17212.59576218	-17212.61261622	-17212.59576218	-17212.61261622	-17212.61261622	-17212.61261622
12	-17204.09146068	-17204.09342890	-17207.03709824	-17207.00664829	-17215.433341892	-17215.44115199	-17212.59792936	-17212.60422122	-17212.59792936	-17212.60422122	-17212.60422122	-17212.60422122
13	-17204.08729694	-17204.09329109	-17207.03418622	-17207.00652624	-17215.43234242	-17215.44095423	-17212.59608105	-17212.60403845	-17212.59608105	-17212.60403845	-17212.60403845	-17212.60403845
14	-17204.08397213	-17204.08444955	-17207.03014949	-17206.99849457	-17215.42912738	-17215.43521048	-17212.59283857	-17212.59752025	-17212.59752025	-17212.59752025	-17212.59752025	-17212.59752025
15	-17204.07935767	-17204.08179197	-17207.02501305	-17207.02160853	-17215.42066072	-17215.41237493	-17212.58533496	-17212.57972919	-17212.58533496	-17212.57972919	-17212.57972919	-17212.57972919
16	-17204.07621026	-17204.07426325	-17207.02320797	-17207.01978768	-17215.41561177	-17215.41356116	-17212.58076139	-17212.57783668	-17212.58076139	-17212.57783668	-17212.57783668	-17212.57783668
17	-17204.07478982	-17204.07212258	-17207.01286620	-17207.01328291	-17215.42773040	-17215.42288217	-17212.58949526	-17212.58519227	-17212.58519227	-17212.58519227	-17212.58519227	-17212.58519227
18	-17204.05660618	-17204.07188866	-17206.99642981	-17207.01997236	-17215.40941578	-17215.41122426	-17212.57121338	-17212.57639036	-17212.57639036	-17212.57639036	-17212.57639036	-17212.57639036
19	-17204.05375623	-17204.07076673	-17207.00002886	-17207.02004677	-17215.39505086	-17215.41367094	-17212.55972720	-17212.57794489	-17212.55972720	-17212.57794489	-17212.57794489	-17212.57794489
20	-17204.04749954	-17204.06596411	-17206.99415183	-17206.98771797	-17215.38955392	-17215.43057034	-17212.55404033	-17212.58941878	-17212.55404033	-17212.58941878	-17212.58941878	-17212.58941878

Table S22: Computed absolute energies with the SA-CASSCF, CASPT2, tPBE, and tPBE0 methods for the relative energies in Figures S7 and S15 of $\text{Ti}(o\text{-tol})_4^{2-}$ molecule when using the (10,15) active space.

No.	SA-CASSCF			CASPT2			tPBE			tPBE0		
	Triplet	Singlet	Triplet	Singlet	Triplet	Singlet	Triplet	Singlet	Triplet	Singlet	Triplet	Singlet
1	-1929.56112982	-1929.53464811	-1932.38605538	-1932.36510569	-1936.26308029	-1936.24487492	-1934.58759267	-1934.56731822				
2	-1929.53697293	-1929.52589171	-1932.36381450	-1932.35987600	-1936.23953148	-1936.24470474	-1934.56389184	-1934.56500148				
3	-1929.51960472	-1929.50870890	-1932.35193110	-1932.34965843	-1936.22584283	-1936.23512528	-1934.54928330	-1934.55352119				
4	-1929.51957750	-1929.49675110	-1932.35195099	-1932.33465072	-1936.22586204	-1936.22010511	-1934.54929091	-1934.53926661				
5	-1929.50872030	-1929.48346010	-1932.35033910	-1932.32730178	-1936.22529815	-1936.20550045	-1934.54615369	-1934.52499036				
6	-1929.50380912	-1929.48082208	-1932.34370507	-1932.32598100	-1936.21359065	-1936.20286899	-1934.53614527	-1934.52235726				
7	-1929.50377894	-1929.48082135	-1932.34369587	-1932.32598113	-1936.21357097	-1936.20286835	-1934.53612296	-1934.52235660				
8	-1929.48149118	-1929.47223213	-1932.32380707	-1932.31989720	-1936.20344495	-1936.20297044	-1934.52295651	-1934.52028586				
9	-1929.48146038	-1929.47223169	-1932.32378377	-1932.31989762	-1936.20339655	-1936.20297109	-1934.52291251	-1934.52028624				
10	-1929.47638415	-1929.46195008	-1932.31800663	-1932.30523415	-1936.19677999	-1936.18609340	-1934.51668103	-1934.50505757				
11	-1929.36831968	-1929.45098772	-1932.23504435	-1932.30072129	-1936.10940352	-1936.18218060	-1934.42413256	-1934.49938238				
12	-1929.36665352	-1929.44480404	-1932.23230500	-1932.29508490	-1936.10215310	-1936.18041432	-1934.41827821	-1934.49651175				
13	-1929.34148216	-1929.44480377	-1932.22920718	-1932.29508412	-1936.07733611	-1936.18041566	-1934.39337262	-1934.49651269				
14	-1929.32046783	-1929.43383217	-1932.20256012	-1932.28532798	-1936.07313653	-1936.17151905	-1934.38496936	-1934.48709733				
15	-1929.31803658	-1929.38993502	-1932.22516586	-1932.26323510	-1936.06135554	-1936.16738309	-1934.37552580	-1934.47302107				
16	-1929.31754532	-1929.36462225	-1932.22521031	-1932.23465436	-1936.06097709	-1936.09898674	-1934.37511915	-1934.41539562				
17	-1929.31600851	-1929.31430716	-1932.22200024	-1932.19906273	-1936.06979051	-1936.06045511	-1934.38134501	-1934.37391812				
18	-1929.31319042	-1929.31361451	-1932.20415746	-1932.22155196	-1936.06902411	-1936.05700761	-1934.38006569	-1934.37115934				
19	-1929.31314297	-1929.31360474	-1932.20419646	-1932.22155436	-1936.06900524	-1936.05699960	-1934.38003967	-1934.37115089				
20	-1929.30204140	-1929.29798478	-1932.21446019	-1932.21133777	-1936.05663611	-1936.05380743	-1934.36798743	-1934.36485177				

Table S23: Computed absolute energies with the SA-CASSCF, CASPT2, tPBE, and tPBE0 methods for the relative energies in Figures S8 and S16 of $\text{V}(o\text{-tol})_4^-$ molecule when using the (8,13) active space.

No.	SA-CASSCF			CASPT2			tPBE			tPBE0		
	Triplet	Singlet	Triplet	Singlet	Triplet	Singlet	Triplet	Singlet	Triplet	Singlet	Triplet	Singlet
1	-2025.05164243	-2024.99796795	-2027.94286453	-2027.89856034	-2031.82275164	-2031.79731936	-2030.12997434	-2030.09748151				
2	-2025.00399064	-2024.99703302	-2027.89523609	-2027.89758846	-2031.77595598	-2031.79683609	-2030.08296465	-2030.09688532				
3	-2024.99862166	-2024.96103323	-2027.89066537	-2027.86857128	-2031.76833393	-2031.77823360	-2030.07590586	-2030.07393351				
4	-2024.99861744	-2024.95355120	-2027.89065870	-2027.85504006	-2031.76833149	-2031.75669304	-2030.07590298	-2030.05590758				
5	-2024.97828660	-2024.94860533	-2027.87733696	-2027.85295156	-2031.75308376	-2031.73857075	-2030.05938447	-2030.04107940				
6	-2024.97139227	-2024.94853896	-2027.86950908	-2027.85157426	-2031.74451050	-2031.74642336	-2030.05123094	-2030.04695226				
7	-2024.97138784	-2024.94853828	-2027.86950692	-2027.85156489	-2031.74450607	-2031.74642286	-2030.05122651	-2030.04695172				
8	-2024.93336872	-2024.93882666	-2027.83619126	-2027.84462330	-2031.72685464	-2031.73117995	-2030.02848316	-2030.03309163				
9	-2024.93336680	-2024.93882365	-2027.83618801	-2027.84461877	-2031.72685324	-2031.73117259	-2030.02848163	-2030.03308536				
10	-2024.92850517	-2024.91438090	-2027.82887337	-2027.81967596	-2031.72339266	-2031.71684034	-2030.02467079	-2030.01622548				
11	-2024.80274933	-2024.90399882	-2027.77161509	-2027.80899817	-2031.59152007	-2031.70676777	-2029.89432739	-2030.00607553				
12	-2024.80271363	-2024.89981022	-2027.77162146	-2027.80433002	-2031.59151154	-2031.70503802	-2029.89431206	-2030.00373107				
13	-2024.80044114	-2024.89980927	-2027.77289371	-2027.80432969	-2031.60969416	-2031.70503747	-2029.90738091	-2030.00373042				
14	-2024.79913864	-2024.89194892	-2027.77067673	-2027.79603682	-2031.6095644	-2031.69869482	-2029.90702699	-2029.99700835				
15	-2024.79880771	-2024.83839995	-2027.77058247	-2027.76895903	-2031.60805457	-2031.69520167	-2029.90574286	-2029.98100124				
16	-2024.79267958	-2024.79368743	-2027.76706903	-2027.76001840	-2031.61034777	-2031.60286842	-2029.90593072	-2029.90057317				
17	-2024.79169763	-2024.79368306	-2027.76261075	-2027.76001509	-2031.60956521	-2031.60286604	-2029.90509832	-2029.90057030				
18	-2024.79169350	-2024.78901780	-2027.76260504	-2027.75883522	-2031.60956172	-2031.61660942	-2029.90509467	-2029.90971152				
19	-2024.78865833	-2024.78901482	-2027.75799905	-2027.75883697	-2031.60248493	-2031.61660472	-2029.89902828	-2029.90970725				
20	-2024.78862283	-2024.78889670	-2027.75802810	-2027.75960405	-2031.60266081	-2031.61886229	-2029.89915132	-2029.91137089				

Table S24: Computed absolute energies with the SA-CASSCF, CASPT2, tPBE, and tPBE0 methods for the relative energies in Figures S9 and S17 of $\text{Fe}(o\text{-tol})_4^{2-}$ molecule when using the (12,13) active space.

No.	SA-CASSCF						CASPT2						tPBE						
	Quintet	Singlet	Triplet	Quintet	Singlet	Triplet	Quintet	Singlet	Triplet	Quintet	Singlet	Triplet	Quintet	Singlet	Triplet	Quintet	Singlet	Triplet	
1	-2348.1112424	-2348.0550983	-2348.0168974	-2351.1050636	-2351.0496631	-2351.0185024	-2355.0305745	-2355.0022956	-2355.3007415	-2354.9727318	-2354.9685455	-2353.262463	-2353.3303461	-2353.2296695	-2353.2262795	-2353.2251687	-2353.2251293	-2353.2251657	-2353.224787
2	-2348.1100255	-2348.0508676	-2348.0134111	-2351.1032675	-2351.0496674	-2351.0140527	-2355.0290796	-2355.0023501	-2355.3007415	-2354.9683244	-2354.9685455	-2353.262463	-2353.3303461	-2353.2296695	-2353.2262795	-2353.2251687	-2353.2251293	-2353.2251657	-2353.224787
3	-2348.0862805	-2348.059480	-2348.0130416	-2351.0469981	-2351.0127263	-2350.9976557	-2355.0053400	-2355.0053400	-2355.3007415	-2354.9726887	-2354.9685455	-2353.262463	-2353.3303461	-2353.2296695	-2353.2262795	-2353.2251687	-2353.2251293	-2353.2251657	-2353.224787
4	-2348.0863625	-2348.0365696	-2348.0104640	-2351.0772556	-2351.0311835	-2351.0172459	-2355.0011980	-2355.0011980	-2355.3007415	-2354.9778118	-2354.9684913	-2353.262463	-2353.3303461	-2353.2296695	-2353.2262795	-2353.2251687	-2353.2251293	-2353.2251657	-2353.224787
5	-2348.08636347	-2348.0365696	-2348.0104640	-2351.0772556	-2351.0311835	-2351.0172459	-2355.0011980	-2355.0011980	-2355.3007415	-2354.9778118	-2354.9684913	-2353.262463	-2353.3303461	-2353.2296695	-2353.2262795	-2353.2251687	-2353.2251293	-2353.2251657	-2353.224787
6	-2347.8219916	-2348.0348038	-2347.9954566	-2350.9198791	-2351.0311064	-2350.9972891	-2355.00119630	-2355.00119630	-2355.3007415	-2354.9659042	-2354.9476553	-2353.262463	-2353.3303461	-2353.2296695	-2353.2262795	-2353.2251687	-2353.2251293	-2353.2251657	-2353.224787
7	-2347.8219503	-2348.0348928	-2347.9954517	-2350.9198791	-2351.0305416	-2350.9972428	-2355.00119630	-2355.00119630	-2355.3007415	-2354.9656256	-2354.9476732	-2353.262463	-2353.3303461	-2353.2296695	-2353.2262795	-2353.2251687	-2353.2251293	-2353.2251657	-2353.224787
8	-2347.8292441	-2348.0343277	-2347.9948096	-2350.9194188	-2351.0307660	-2350.9978117	-2355.00119630	-2355.00119630	-2355.3007415	-2354.9441490	-2354.9441490	-2353.262463	-2353.3303461	-2353.2296695	-2353.2262795	-2353.2251687	-2353.2251293	-2353.2251657	-2353.224787
9	-2347.8136171	-2348.0322448	-2347.9921125	-2350.9093306	-2351.0307660	-2350.9967219	-2355.00119630	-2355.00119630	-2355.3007415	-2354.9462618	-2354.9462618	-2353.262463	-2353.3303461	-2353.2296695	-2353.2262795	-2353.2251687	-2353.2251293	-2353.2251657	-2353.224787
10	-2347.810715	-2348.0294353	-2347.9896060	-2350.9908854	-2351.0293322	-2350.9908850	-2355.00119630	-2355.00119630	-2355.3007415	-2354.9422995	-2354.9422995	-2353.262463	-2353.3303461	-2353.2296695	-2353.2262795	-2353.2251687	-2353.2251293	-2353.2251657	-2353.224787
11	-2347.8104081	-2348.0292843	-2347.9878243	-2350.890234	-2351.0265444	-2350.8902344	-2355.00119630	-2355.00119630	-2355.3007415	-2354.951257	-2354.951257	-2353.262463	-2353.3303461	-2353.2296695	-2353.2262795	-2353.2251687	-2353.2251293	-2353.2251657	-2353.224787
12	-2347.8093245	-2348.0179952	-2347.9854962	-2350.8965022	-2351.0176515	-2350.9860227	-2355.00119630	-2355.00119630	-2355.3007415	-2354.977885	-2354.977885	-2353.262463	-2353.3303461	-2353.2296695	-2353.2262795	-2353.2251687	-2353.2251293	-2353.2251657	-2353.224787
13	-2347.80160530	-2348.0178457	-2347.9854784	-2350.8915382	-2351.0169628	-2350.9860115	-2355.00119630	-2355.00119630	-2355.3007415	-2354.976633	-2354.976633	-2353.262463	-2353.3303461	-2353.2296695	-2353.2262795	-2353.2251687	-2353.2251293	-2353.2251657	-2353.224787
14	-2347.80581188	-2348.0104733	-2347.9854784	-2350.8963051	-2351.0015285	-2350.9735890	-2355.00119630	-2355.00119630	-2355.3007415	-2354.9741741	-2354.9741741	-2353.262463	-2353.3303461	-2353.2296695	-2353.2262795	-2353.2251687	-2353.2251293	-2353.2251657	-2353.224787
15	-2347.8036454	-2348.0077850	-2347.9863437	-2350.8957907	-2351.0035835	-2350.9671661	-2355.00119630	-2355.00119630	-2355.3007415	-2354.982836	-2354.982836	-2353.262463	-2353.3303461	-2353.2296695	-2353.2262795	-2353.2251687	-2353.2251293	-2353.2251657	-2353.224787
16	-2347.8056387	-2348.0071358	-2347.9877187	-2350.8957959	-2351.0034753	-2350.9794753	-2355.00119630	-2355.00119630	-2355.3007415	-2354.9828342	-2354.9828342	-2353.262463	-2353.3303461	-2353.2296695	-2353.2262795	-2353.2251687	-2353.2251293	-2353.2251657	-2353.224787
17	-2347.801850	-2348.0061703	-2347.9873244	-2350.8898170	-2351.006454	-2350.9860227	-2355.00119630	-2355.00119630	-2355.3007415	-2354.9919795	-2354.9919795	-2353.262463	-2353.3303461	-2353.2296695	-2353.2262795	-2353.2251687	-2353.2251293	-2353.2251657	-2353.224787
18	-2347.8008877	-2348.0061703	-2347.9873244	-2350.8896177	-2351.0061211	-2350.9862929	-2355.00119630	-2355.00119630	-2355.3007415	-2354.9819206	-2354.9819206	-2353.262463	-2353.3303461	-2353.2296695	-2353.2262795	-2353.2251687	-2353.2251293	-2353.2251657	-2353.224787
19	-2347.7971080	-2348.0048160	-2347.9873282	-2350.8824985	-2351.0049327	-2350.98614306	-2355.00119630	-2355.00119630	-2355.3007415	-2354.9867442	-2354.9867442	-2353.262463	-2353.3303461	-2353.2296695	-2353.2262795	-2353.2251687	-2353.2251293	-2353.2251657	-2353.224787
20	-2347.7964931	-2348.0030396	-2347.9873294	-2350.8854032	-2351.0039094	-2350.9790994	-2355.00119630	-2355.00119630	-2355.3007415	-2354.9882440	-2354.9882440	-2353.262463	-2353.3303461	-2353.2296695	-2353.2262795	-2353.2251687	-2353.2251293	-2353.2251657	-2353.224787
21	-2347.7964645	-2348.0029584	-2347.9873294	-2350.8853588	-2351.0039094	-2350.9792993	-2355.00119630	-2355.00119630	-2355.3007415	-2354.9882440	-2354.9882440	-2353.262463	-2353.3303461	-2353.2296695	-2353.2262795	-2353.2251687	-2353.2251293	-2353.2251657	-2353.224787
22	-2347.7973870	-2348.0029584	-2347.9873294	-2350.8853588	-2351.0039094	-2350.9792993	-2355.00119630	-2355.00119630	-2355.3007415	-2354.9884774	-2354.9884774	-2353.262463	-2353.3303461	-2353.2296695	-2353.2262795	-2353.2251687	-2353.2251293	-2353.2251657	-2353.224787
23	-2347.7769333	-2347.801850	-2347.9873244	-2350.8898471	-2351.0041313	-2350.9860227	-2355.00119630	-2355.00119630	-2355.3007415	-2354.9884774	-2354.9884774	-2353.262463	-2353.3303461	-2353.2296695	-2353.2262795	-2353.2251687	-2353.2251293	-2353.2251657	-2353.224787
24	-2347.7765656	-2347.9935255	-2347.9873244	-2350.8984711	-2351.0041313	-2350.9860227	-2355.00119630	-2355.00119630	-2355.3007415	-2354.9884774	-2354.9884774	-2353.262463	-2353.3303461	-2353.2296695	-2353.2262795	-2353.2251687	-2353.2251293	-2353.2251657	-2353.224787
25	-2347.7741591	-2347.99299439	-2347.9873244	-2350.8699375	-2351.0049325	-2350.9909363	-2355.00119630	-2355.00119630	-2355.3007415	-2354.9756677	-2354.9756677	-2353.262463	-2353.3303461	-2353.2296695	-2353.2262795	-2353.2251687	-2353.2251293	-2353.2251657	-2353.224787
26	-2347.7741282	-2347.9927883	-2347.9873244	-2350.8699101	-2351.004904861	-2350.9756677	-2355.00119630	-2355.00119630	-2355.3007415	-2354.9756677	-2354.9756677	-2353.262463	-2353.3303461	-2353.2296695	-2353.2262795	-2353.2251687	-2353.2251293	-2353.2251657	-2353.224787
27	-2347.77482840	-2347.9927883	-2347.9873244	-2350.8699101	-2351.004904861	-2350.9756677	-2355.00119630	-2355.00119630	-2355.3007415	-2354.9756677	-2354.9756677	-2353.262463	-2353.3303461	-2353.2296695	-2353.2262795	-2353.2251687	-2353.2251293	-2353.2251657	-2353.224787
28	-2347.7741674	-2347.9928183	-2347.9873244	-2350.8699101	-2351.004904861	-2350.9756677	-2355.00119630	-2355.00119630	-2355.3007415	-2354.9756677	-2354.9756677	-2353.262463	-2353.3303461	-2353.2296695	-2353.2262795	-2353.2251687	-2353.2251293	-2353.2251657	-2353.224787
29	-2347.7741295	-2347.9927883	-2347.9873244	-2350.8699101	-2351.004904861	-2350.9756677	-2355.00119630	-2355.00119630	-2355.3007415	-2354.9756677	-2354.9756677	-2353.262463	-2353.3303461	-2353.2296695	-2353.2262795	-2353.2251687	-2353.2251293	-2353.2251657	-2353.224787
30	-2347.7741765	-2347.9927883	-2347.9873244	-2350.8699101	-2351.004904861	-2350.9756677	-2355.00119630	-2355.00119630	-2355.3007415	-2354.9756677	-2354.9756677	-2353.262463	-2353.3303461	-2353.2296695	-2353.2262795	-2353.2251687	-2353.2251293	-2353.2251657	-2353.224787

Table S25: Computed absolute energies with the SA-CASSCF, CASPT2, tPBE, and tPBE0 methods for the relative energies in Figures S10 and S18 of $\text{Co}(o\text{-tol})_4^{2-}$ molecule when using the (13,13) active space.

No.	SA-CASSCF			CASPT2			tPBE			tPBE0	
	Quartet	Doublet	Quartet	Doublet	Quartet	Doublet	Quartet	Doublet	Quartet	Doublet	Quartet
1	-2468.67917357	-2468.60596668	-2471.67914107	-2471.61646211	-2475.66229034	-2475.61173898	-2473.91651115	-2473.86030341	-2473.86020889	-2473.88319211	-2473.85641944
2	-2468.65128763	-2468.60587897	-2471.65085325	-2471.61652917	-2475.63267012	-2475.61165219	-2473.883192450	-2473.86020788	-2473.88319211	-2473.86020788	-2473.88318962
3	-2468.64850296	-2468.60587748	-2471.64765744	-2471.61652738	-2475.62808849	-2475.61165134	-2473.88319211	-2473.86020788	-2473.88318962	-2473.85641944	-2473.85999407
4	-2468.64850035	-2468.60231760	-2471.64765497	-2471.61073218	-2475.62808604	-2475.60778672	-2473.88318962	-2473.86020788	-2473.88318962	-2473.85641944	-2473.85603299
5	-2468.62848521	-2468.60180491	-2471.62916605	-2471.61014797	-2475.60383035	-2475.60744235	-2473.85999407	-2473.86020788	-2473.88318962	-2473.85641944	-2473.85603299
6	-2468.62848379	-2468.59169234	-2471.62916462	-2471.60067112	-2475.60382955	-2475.58275382	-2473.85999311	-2473.86020788	-2473.88318962	-2473.85641944	-2473.83498845
7	-2468.62789027	-2468.58301965	-2471.62957586	-2471.59610565	-2475.60168720	-2475.58715379	-2473.85823797	-2473.8612026	-2473.88318962	-2473.85641944	-2473.83612026
8	-2468.57865370	-2468.58180094	-2471.59502065	-2471.59445450	-2475.60513306	-2475.58939468	-2473.84851322	-2473.83749625	-2473.88318962	-2473.85641944	-2473.83749625
9	-2468.577830324	-2468.58179842	-2471.59378685	-2471.59445137	-2475.59545084	-2475.58939337	-2473.84116394	-2473.83749463	-2473.88318962	-2473.85641944	-2473.83749463
10	-2468.577830030	-2468.57335570	-2471.59378415	-2471.58072342	-2475.5954529	-2475.57559048	-2473.84115904	-2473.82503179	-2473.88318962	-2473.85641944	-2473.83749625
11	-2468.39730326	-2468.57123724	-2471.49263478	-2471.57779146	-2475.44017739	-2475.57155998	-2473.67945886	-2473.82147930	-2473.88318962	-2473.85641944	-2473.83749625
12	-2468.39714496	-2468.57123450	-2471.49593832	-2471.577798845	-2475.44301328	-2475.57155644	-2473.68154620	-2473.82147596	-2473.88318962	-2473.85641944	-2473.83749625
13	-2468.39714211	-2468.57044505	-2471.49658503	-2471.58001575	-2475.44213912	-2475.57990614	-2473.68088987	-2473.82754087	-2473.88318962	-2473.85641944	-2473.83749625
14	-2468.39651989	-2468.56875867	-2471.49070500	-2471.58315585	-2475.44027502	-2475.577767494	-2473.67933624	-2473.82147930	-2473.88318962	-2473.85641944	-2473.83749625
15	-2468.39616126	-2468.56763271	-2471.49005554	-2471.57695097	-2475.44060220	-2475.57490614	-2473.67949197	-2473.82147596	-2473.88318962	-2473.85641944	-2473.83749625
16	-2468.38823630	-2468.56762968	-2471.48776263	-2471.57694792	-2475.43982393	-2475.57490324	-2473.67692702	-2473.82308778	-2473.88318962	-2473.85641944	-2473.83749625
17	-2468.38713937	-2468.56502496	-2471.48769377	-2471.57906601	-2475.44146568	-2475.57375923	-2473.67788410	-2473.82157566	-2473.88318962	-2473.85641944	-2473.83749625
18	-2468.38713766	-2468.54833200	-2471.48769184	-2471.55955415	-2475.44146419	-2475.55833470	-2473.67788256	-2473.82308778	-2473.88318962	-2473.85641944	-2473.83749625
19	-2468.37721418	-2468.54793522	-2471.47542350	-2471.55762554	-2475.42720423	-2475.55770259	-2473.66470672	-2473.80526075	-2473.88318962	-2473.85641944	-2473.83749625
20	-2468.37468537	-2468.54793398	-2471.47254729	-2471.55762518	-2475.42731923	-2475.55770105	-2473.66416077	-2473.80525928	-2473.88318962	-2473.85641944	-2473.83749625
21	-2468.36987613	-2468.54078396	-2471.46970738	-2471.54736020	-2475.42943069	-2475.54637291	-2473.66454205	-2473.79497567	-2473.88318962	-2473.85641944	-2473.83749625
22	-2468.36515365	-2468.54078172	-2471.46225300	-2471.54735634	-2475.42877096	-2475.54636784	-2473.66286663	-2473.79497131	-2473.88318962	-2473.85641944	-2473.83749625
23	-2468.36257505	-2468.53837888	-2471.46142118	-2471.54386800	-2475.42514451	-2475.54412413	-2473.65950215	-2473.79268782	-2473.88318962	-2473.85641944	-2473.83749625
24	-2468.36257440	-2468.52947536	-2471.46142720	-2471.53310183	-2475.42514273	-2475.53722468	-2473.65950065	-2473.78528735	-2473.88318962	-2473.85641944	-2473.83749625
25	-2468.36033701	-2468.52947275	-2471.46104647	-2471.53309853	-2475.42549328	-2475.53722225	-2473.65920421	-2473.78528488	-2473.88318962	-2473.85641944	-2473.83749625
26	-2468.35775008	-2468.52841158	-2471.46338298	-2471.53120200	-2475.43153822	-2475.53538253	-2473.66309119	-2473.78363979	-2473.88318962	-2473.85641944	-2473.83749625
27	-2468.35685719	-2468.51333048	-2471.45695847	-2471.52371399	-2475.41923068	-2475.53497374	-2473.65363731	-2473.77956293	-2473.88318962	-2473.85641944	-2473.83749625
28	-2468.35685454	-2468.51242425	-2471.45693082	-2471.51575458	-2475.41922866	-2475.53248995	-2473.65363513	-2473.77747353	-2473.88318962	-2473.85641944	-2473.83749625
29	-2468.34899255	-2468.50990074	-2471.44726911	-2471.53504932	-2475.41044492	-2475.56559396	-2473.64508183	-2473.80167066	-2473.88318962	-2473.85641944	-2473.83749625
30	-2468.34898914	-2468.50021261	-2471.44727065	-2471.53064503	-2475.41046598	-2475.56892936	-2473.64509677	-2473.80175017	-2473.88318962	-2473.85641944	-2473.83749625

Table S26: Computed absolute energies with the SA-CASSCF, CASPT2, tPBE, and tPBE0 methods for the relative energies in Figures S11 and S19 of $\text{Ni}(o\text{-tol})_4^{2-}$ molecule when using the (14,13) active space.

No.	SA-CASSCF			CASPT2			tPBE			tPBE0		
	Triplet	Singlet	Triplet	Singlet	Triplet	Singlet	Triplet	Singlet	Triplet	Singlet	Triplet	Singlet
1	-2595.90860311	-2595.85346906	-2598.97746637	-2598.93946168	-2602.94031575	-2602.91836788	-2601.18238759	-2601.15214318				
2	-2595.88543343	-2595.84310586	-2598.95208014	-2598.92703257	-2602.91023545	-2602.91581356	-2601.15403495	-2601.14763664				
3	-2595.88311501	-2595.82336403	-2598.94925318	-2598.90468013	-2602.90764227	-2602.88863888	-2601.15151046	-2601.12232017				
4	-2595.87787624	-2595.82024141	-2598.94252221	-2598.90428476	-2602.90573732	-2602.88505620	-2601.14877220	-2601.11885250				
5	-2595.86473408	-2595.81990678	-2598.93018752	-2598.90109732	-2602.88360080	-2602.88159083	-2601.12888412	-2601.11616982				
6	-2595.85627311	-2595.80043907	-2598.91970254	-2598.88941210	-2602.87493434	-2602.88775208	-2601.12026903	-2601.11592383				
7	-2595.84248994	-2595.79554470	-2598.90524643	-2598.88057510	-2602.86760038	-2602.85914575	-2601.11132277	-2601.09324549				
8	-2595.80764482	-2595.79004252	-2598.88936057	-2598.87322790	-2602.87448371	-2602.87279393	-2601.10777399	-2601.10210608				
9	-2595.79898935	-2595.78078744	-2598.88097566	-2598.86415473	-2602.86339026	-2602.83976701	-2601.09729003	-2601.07502212				
10	-2595.79305487	-2595.76983141	-2598.87423122	-2598.84726541	-2602.85535233	-2602.84465403	-2601.08977797	-2601.07594838				
11	-2595.63299400	-2595.76944428	-2598.81007390	-2598.84682342	-2602.71287123	-2602.84464088	-2600.94290192	-2601.07584173				
12	-2595.63197335	-2595.76162378	-2598.81241925	-2598.83857732	-2602.72796093	-2602.82492747	-2600.95396404	-2601.05910155				
13	-2595.62753205	-2595.75225219	-2598.80771420	-2598.82102062	-2602.70706065	-2602.82210778	-2600.93713755	-2601.05464388				
14	-2595.61293606	-2595.75115464	-2598.79166782	-2598.82130285	-2602.71353333	-2602.82392662	-2600.93838401	-2601.05573363				
15	-2595.61021022	-2595.65758732	-2598.79519406	-2598.77530076	-2602.71953864	-2602.80704270	-2600.94220654	-2601.01967886				
16	-2595.60887550	-2595.63412107	-2598.79452740	-2598.82155166	-2602.71621460	-2602.72619010	-2600.93937983	-2600.95317284				
17	-2595.60151620	-2595.61028034	-2598.78156690	-2598.79909148	-2602.70868981	-2602.71628632	-2600.93189641	-2600.93978483				
18	-2595.59919075	-2595.60571583	-2598.7816268	-2598.79850183	-2602.70300572	-2602.70595510	-2600.92705198	-2600.93089528				
19	-2595.59446052	-2595.58683855	-2598.77407719	-2598.76677988	-2602.69436923	-2602.71260791	-2600.91939205	-2600.93116557				
20	-2595.58938057	-2595.58618228	-2598.77202108	-2598.76914631	-2602.70304327	-2602.71313475	-2600.92462760	-2600.93139663				

5.5 Absolute Energies for Zero-Field Splitting Calculations

The following tables include the energies obtained after the multireference calculations performed for the computation of ZFS parameters.

Summary of spin-states used for the computation of $|D|$:

- $\text{Ti}(o\text{-tol})_4^{2-}$ (10,15): 10 triplets and 15 singlets
- $\text{V}(o\text{-tol})_4^-$ (8,13): 7 triplets and 9 singlets
- $\text{Cr}(o\text{-tol})_4$ (10,15): 7 triplets and 9 singlets
- $\text{Mo}(o\text{-tol})_4$ (10,15): 7 triplets and 9 singlets
- $\text{W}(o\text{-tol})_4$ (10,15): 7 triplets and 9 singlets

Table S27: Computed absolute energies with the SA-CASSCF, CASPT2, tPBE, and tPBE0 methods of Cr(*o*-tol)₄ molecule when using the (10,15) active space to obtain the ZFS.

No.	SA-CASSCF			CASPT2			tPBE			tPBE0		
	Triplet	Singlet	Triplet	Singlet	Triplet	Singlet	Triplet	Singlet	Triplet	Singlet	Triplet	Singlet
1	-2126.47551516	-2126.41345938	-2129.40514835	-2129.35234568	-2129.4190	-2133.24672773	-2131.58258522	-2131.53841064				
2	-2126.38914476	-2126.41175298	-2129.32794308	-2129.35069372	-2133.20786826	-2133.24589269	-2131.50318739	-2131.53735776				
3	-2126.38075988	-2126.37129253	-2129.32278386	-2129.31746819	-2133.19815642	-2133.21740519	-2131.49380729	-2131.50587703				
4	-2126.38075970	-2126.34734606	-2129.32278372	-2129.29802713	-2133.19815625	-2133.17720456	-2131.49380711	-2131.46973994				
5	-2126.37798317	-2126.34001935	-2129.32103216	-2129.29020764	-2133.20048660	-2133.18415866	-2131.49486074	-2131.47312383				
6	-2126.35992718	-2126.33549251	-2129.30499517	-2129.28647136	-2133.18649032	-2133.17473772	-2131.47984954	-2131.46492642				
7	-2126.35992686	-2126.33549232	-2129.30499482	-2129.28647125	-2133.18648993	-2133.17473753	-2131.47984916	-2131.46492623				
8		-2126.33011658	-2129.28274231		-2133.16461980		-2131.45599400					
9		-2126.33011632	-2129.28274196		-2133.16461918		-2131.45599347					

Table S28: Computed absolute energies with the SA-CASSCF, CASPT2, tPBE, and tPBE0 methods of Mo(*o*-tol)₄ molecule when using the (10,15) active space to obtain the ZFS.

No.	SA-CASSCF			CASPT2			tPBE			tPBE0		
	Triplet	Singlet	Triplet	Singlet	Triplet	Singlet	Triplet	Singlet	Triplet	Singlet	Triplet	Singlet
1	-5122.57232500	-5122.53364475	-5125.47208168	-5125.44193198	-5130.29700364	-5130.27705127	-5128.36583398	-5128.34119964				
2	-5122.46799929	-5122.52981070	-5125.37456213	-5125.43805069	-5130.20486252	-5130.27493877	-5128.27064671	-5128.33865675				
3	-5122.46531335	-5122.49772244	-5125.37560031	-5125.41181070	-5130.20258851	-5130.25973453	-5128.26826972	-5128.31923151				
4	-5122.46530941	-5122.44663801	-5125.37559770	-5125.36571622	-5130.20258716	-5130.19600770	-5128.26826772	-5128.25866528				
5	-5122.46474139	-5122.43510870	-5125.37641914	-5125.35472987	-5130.20727361	-5130.18676997	-5128.27164056	-5128.24885465				
6	-5122.44868565	-5122.43510456	-5125.36060539	-5125.35472603	-5130.19108799	-5130.18676926	-5128.25548741	-5128.24885309				
7	-5122.44868130	-5122.43267228	-5125.36060119	-5125.35005424	-5130.19108358	-5130.19154195	-5128.25548301	-5128.25182453				
8		-5122.42707509	-5125.34755451	-5130.18348066	-5130.18347927	-5128.24437927	-5128.24437617					
9		-5122.42707286	-5125.34755130	-5130.18347727								

Table S29: Computed absolute energies with the SA-CASSCF, CASPT2, tPBE, and tPBE0 methods of W(*o-tol*)₄ molecule when using the (10,15) active space to obtain the ZFS.

No.	SA-CASSCF			CASPT2			tPBE			tPBE0		
	Triplet	Singlet	Triplet	Singlet	Triplet	Singlet	Triplet	Singlet	Triplet	Singlet	Singlet	
1	-17204.30179508	-17204.26932854	-17207.19880830	-17207.17232645	-17215.60945088	-17215.59430235	-17212.78253693	-17212.76305890				
2	-17204.21498800	-17204.26489458	-17207.11448438	-17207.16812124	-17215.53010149	-17215.59226278	-17212.70132312	-17212.76042073				
3	-17204.21489737	-17204.23773251	-17207.11447723	-17207.14443487	-17215.53006733	-17215.58172665	-17212.70127484	-17212.74572812				
4	-17204.21465639	-17204.19497693	-17207.11303172	-17207.10147742	-17215.53141264	-17215.52255934	-17212.70222358	-17212.69066374				
5	-17204.21197286	-17204.18529444	-17207.11542909	-17207.09290100	-17215.53502442	-17215.51506983	-17212.70426153	-17212.68262598				
6	-17204.19709499	-17204.18525849	-17207.10099989	-17207.09296056	-17215.52042655	-17215.51512515	-17212.68959366	-17212.68265849				
7	-17204.19706572	-17204.18037866	-17207.10103167	-17207.08675123	-17215.52045991	-17215.51775984	-17212.68961136	-17212.68341455				
8		-17204.17674489		-17207.08377144		-17215.51156463		-17212.677785970				
9		-17204.17667574		-17207.08379289		-17215.51157476		-17212.677785001				

Table S30: Computed absolute energies with the SA-CASSCF, CASPT2, tPBE, and tPBE0 methods of $\text{Ti}(o\text{-tol})_4^{2-}$ molecule when using the (10,15) active space to obtain the ZFS.

No.	SA-CASSCF			CASPT2			tPBE			tPBE0		
	Triplet	Singlet	Triplet	Singlet	Triplet	Singlet	Triplet	Singlet	Triplet	Singlet	Triplet	Singlet
1	-1929.56107248	-1929.53422236	-1932.38520810	-1932.36454340	-1936.26200191	-1936.24403485	-1934.58676955	-1934.56658173				
2	-1929.53735394	-1929.52549097	-1932.36273281	-1932.35939393	-1936.23852696	-1936.24388016	-1934.56323371	-1934.56428286				
3	-1929.52019277	-1929.50825080	-1932.35082107	-1932.34905714	-1936.22485065	-1936.23415098	-1934.54868618	-1934.55267594				
4	-1929.52019271	-1929.49682023	-1932.35082093	-1932.33392515	-1936.22485046	-1936.21935933	-1934.54868602	-1934.53872456				
5	-1929.50904801	-1929.48348570	-1932.34930727	-1932.32661958	-1936.22386989	-1936.20457429	-1934.54516442	-1934.52430214				
6	-1929.50435387	-1929.48093581	-1932.34255449	-1932.32574379	-1936.21196383	-1936.20305215	-1934.53506134	-1934.52252307				
7	-1929.50435383	-1929.48093572	-1932.34255456	-1932.32574366	-1936.21196346	-1936.20305204	-1934.53506105	-1934.52252296				
8	-1929.48212891	-1929.47241397	-1932.32278093	-1932.31938699	-1936.20275347	-1936.20112668	-1934.52259733	-1934.51894850				
9	-1929.48212884	-1929.47241389	-1932.32278080	-1932.31938687	-1936.20275345	-1936.20112628	-1934.52259730	-1934.51894818				
10	-1929.47716644	-1929.46256743	-1932.31699463	-1932.30444599	-1936.19619992	-1936.18558980	-1934.51644155	-1934.50483421				
11		-1929.45159284		-1932.29996563		-1936.18156759		-1934.49907390				
12		-1929.44534064		-1932.29449528		-1936.18155552		-1934.49750180				
13		-1929.44534056		-1932.29449494		-1936.18155543		-1934.49750171				
14		-1929.43447537		-1932.28452777		-1936.17093477		-1934.48681992				
15		-1929.39042708		-1932.26249793		-1936.16687645		-1934.47276411				

Table S31: Computed absolute energies with the SA-CASSCF, CASPT2, tPBE, and tPBE0 methods of $\text{V}(o\text{-tol})_4^-$ molecule when using the (8,13) active space to obtain the ZFS.

No.	SA-CASSCF			CASPT2			tPBE			tPBE0		
	Triplet	Singlet	Triplet	Singlet	Triplet	Singlet	Triplet	Singlet	Triplet	Singlet	Triplet	Singlet
1	-2025.05200481	-2024.99823961	-2027.94025349	-2027.89707284	-2031.81888592	-2031.79496485	-2030.12716564	-2030.09578354				
2	-2025.00579861	-2024.99728412	-2027.89287475	-2027.89606643	-2031.77288973	-2031.79448166	-2030.08111695	-2030.09518228				
3	-2025.00063901	-2024.96130532	-2027.88754099	-2027.86721940	-2031.76718562	-2031.77601271	-2030.07554897	-2030.07233586				
4	-2025.00063573	-2024.95382997	-2027.88753749	-2027.85362702	-2031.76718307	-2031.75451552	-2030.07554624	-2030.05434413				
5	-2024.98035598	-2024.94896023	-2027.87488149	-2027.85058297	-2031.74965942	-2031.74310576	-2030.05733356	-2030.04456938				
6	-2024.97367743	-2024.94895970	-2027.86715898	-2027.85058333	-2031.74030518	-2031.74310514	-2030.04864824	-2030.04456878				
7	-2024.97367382	-2024.94890915	-2027.86715640	-2027.85152663	-2031.74029982	-2031.73635417	-2030.04864332	-2030.03949292				
8		-2024.93909397		-2027.84318909		-2031.72906957		-2030.03157567				
9		-2024.93909137		-2027.84318455		-2031.72906277		-2030.03156992				

6 Active Space Dependency

6.1 Energy Gaps

Table S32: Computed triplet-singlet gaps for the Cr(*o*-tol)₄ complex. The energy values were obtained with SA-CASSCF, CASPT2, tPBE, and tPBE0 methods. The values reported are in eV. Percentage of the dominant configurations for the triplet ground state (T_0) and the lowest singlet state (S_1).

Active Space	SA-CASSCF	CASPT2	tPBE	tPBE0	T_0 (%)	S_1 (%)
(2,5)	1.91	0.98	0.48	0.84	83.42	70.41
(2,10)	1.84	1.02	0.52	0.85	84.10	61.26
(8,8)	1.90	1.32	0.82	1.09	88.99	57.56
(10,15)	1.69	1.44	1.04	1.20	84.17	50.83

Table S33: Computed triplet-singlet gaps for the Mo(*o*-tol)₄ complex. The energy values were obtained with SA-CASSCF, CASPT2, tPBE, and tPBE0 methods. The values reported are in eV. Percentage of the dominant configurations for the triplet ground state (T_0) and the lowest singlet state (S_1).

Active Space	SA-CASSCF	CASPT2	tPBE	tPBE0	T_0 (%)	S_1 (%)
(2,5)	1.19	0.73	0.28	0.50	63.89	40.61
(2,10)	1.15	0.68	0.30	0.51	92.84	37.88
(8,8)	1.15	0.76	0.42	0.60	96.78	63.60
(10,15)	1.05	0.82	0.54	0.67	90.89	52.95

Table S34: Computed triplet-singlet gaps for the W(*o*-tol)₄ complex. The energy values were obtained with SA-CASSCF, CASPT2, tPBE, and tPBE0 methods. The values reported are in eV. Percentage of the dominant configurations for the triplet ground state (T_0) and the lowest singlet state (S_1).

Active Space	SA-CASSCF	CASPT2	tPBE	tPBE0	T_0 (%)	S_1 (%)
(2,5)	1.04	0.64	0.23	0.43	56.13	30.71
(2,10)	1.01	0.60	0.24	0.43	94.74	38.74
(8,8)	1.00	0.69	0.36	0.52	97.90	61.82
(10,15)	0.88	0.72	0.41	0.55	95.76	54.32

Table S35: Computed triplet-singlet gaps for the $\text{Ti}(o\text{-tol})_4^{2-}$ complex. The energy values were obtained with SA-CASSCF, CASPT2, tPBE, and tPBE0 methods. The values reported are in eV. Percentage of the dominant configurations for the triplet ground state (T_0) and the lowest singlet state (S_1).

Active Space	SA-CASSCF	CASPT2	tPBE	tPBE0	T_0 (%)	S_1 (%)
(2,5)	1.12	0.51	0.13	0.38	26.04	71.88
(2,10)	0.87	0.41	0.03	0.24	74.38	63.65
(8,8)	1.17	0.80	0.55	0.70	96.49	56.98
(10,15)	0.73	0.56	0.49	0.55	67.72	71.45

Table S36: Computed triplet-singlet gaps for the $\text{V}(o\text{-tol})_4^-$ complex. The energy values were obtained with SA-CASSCF, CASPT2, tPBE, and tPBE0 methods. The values reported are in eV. Percentage of the dominant configurations for the triplet ground state (T_0) and the lowest singlet state (S_1).

Active Space	SA-CASSCF	CASPT2	tPBE	tPBE0	T_0 (%)	S_1 (%)
(2,5)	1.70	1.06	0.47	0.78	57.25	20.38
(2,10)	1.62	1.07	0.48	0.76	74.79	41.16
(8,8)	1.64	1.17	0.63	0.89	97.86	55.56
(8,13)	1.46	1.18	0.65	0.85	96.28	51.86

Table S37: Computed quintet-triplet (ΔE_{Q-T}) and quintet-triplet (ΔE_{Q-S}) gaps for the $\text{Fe}(o\text{-tol})_4^{2-}$ complex. The energy values were obtained with SA-CASSCF, CASPT2, tPBE, and tPBE0 methods. The values reported are in eV.

Active Space	SA-CASSCF		CASPT2		tPBE		tPBE0	
	ΔE_{Q-T}	ΔE_{Q-S}						
(6,5)	2.12	3.40	1.73	2.41	1.02	1.72	1.29	2.14
(6,10)	2.01	3.22	1.73	2.55	1.01	1.82	1.26	2.17
(12,8)	2.06	3.36	2.00	3.06	1.29	2.38	1.48	2.62
(12,13)	1.59	2.70	1.53	2.41	0.83	1.67	1.02	1.93

Table S38: Computed quartet-doublet gaps for the $\text{Co}(o\text{-tol})_4^{2-}$ complex. The energy values were obtained with SA-CASSCF, CASPT2, tPBE, and tPBE0 methods. The values reported are in eV.

Active Space	SA-CASSCF	CASPT2	tPBE	tPBE0
(7,5)	2.41	1.85	1.53	1.75
(7,10)	2.34	1.95	1.60	1.79
(13,8)	1.95	2.03	1.34	1.49
(13,13)	1.99	1.71	1.38	1.53

Table S39: Computed triplet-singlet gaps for the $\text{Ni}(o\text{-tol})_4^{2-}$ complex. The energy values were obtained with SA-CASSCF, CASPT2, tPBE, and tPBE0 methods. The values reported are in eV.

Active Space	SA-CASSCF	CASPT2	tPBE	tPBE0
(8,5)	1.95	1.17	0.61	0.95
(8,10)	1.89	1.41	0.84	1.10
(14,8)	1.96	1.46	0.85	1.12
(14,13)	1.64	1.10	0.67	0.91

6.2 Zero-Field Splitting Parameters

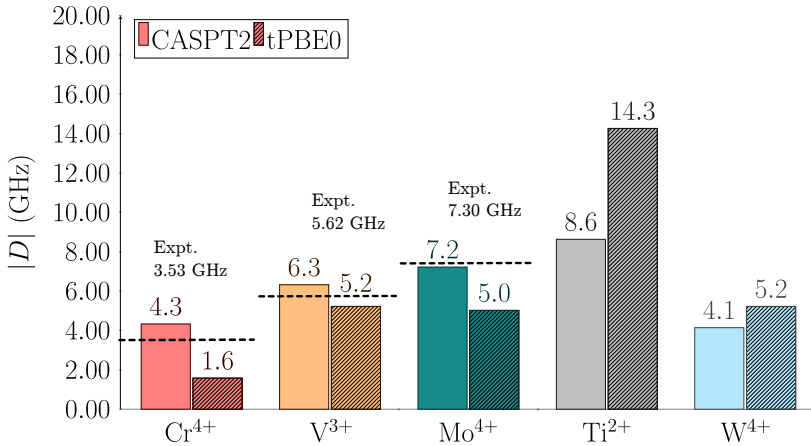


Figure S20: Calculated axial parameter ($|D|$) with the CASPT2 (solid bar) and tPBE0 (striped bar) methods for the $\text{Cr}(o\text{-tol})_4$ (red), $\text{V}(o\text{-tol})_4^-$ (orange), $\text{Mo}(o\text{-tol})_4$ (teal), $\text{Ti}(o\text{-tol})_4^{2-}$ (gray), and $\text{W}(o\text{-tol})_4$ (cyan) complexes using (2,5) active space. The values are in GHz. Dashed lines correspond to experimental data from references 1 and 2.

Table S40: Computed axial parameter ($|D|$) using the (2,5) active space for $\text{Cr}(o\text{-tol})_4$, $\text{V}(o\text{-tol})_4^-$, $\text{Mo}(o\text{-tol})_4$, $\text{Ti}(o\text{-tol})_4^{2-}$, and $\text{W}(o\text{-tol})_4$ complexes. The energy values were obtained with SA-CASSCF, CASPT2, tPBE, and tPBE0 methods. The values reported are in GHz.

Complex	SA-CASSCF	CASPT2	tPBE	tPBE0
$\text{Cr}(o\text{-tol})_4$	10.05	4.33	1.26	1.58
$\text{V}(o\text{-tol})_4^-$	8.11	6.32	2.95	5.22
$\text{Mo}(o\text{-tol})_4$	10.72	7.22	12.74	5.02
$\text{Ti}(o\text{-tol})_4^{2-}$	8.98	8.63	11.90	14.26
$\text{W}(o\text{-tol})_4$	169.21	4.14	120.73	5.22

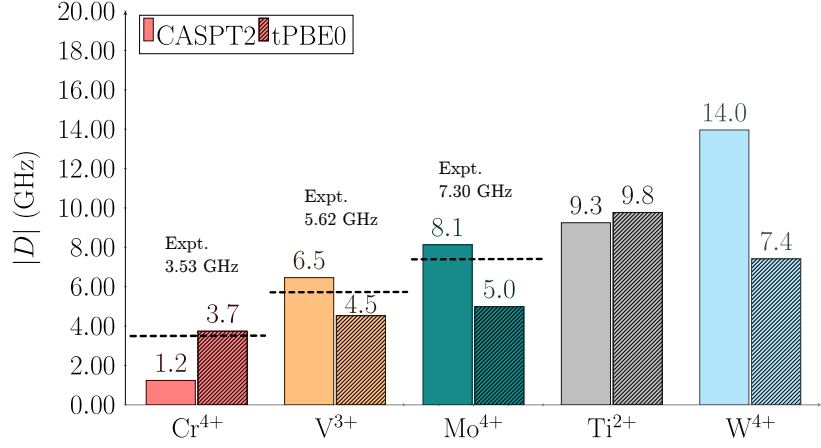


Figure S21: Calculated axial parameter ($|D|$) with the CASPT2 (solid bar) and tPBE0 (striped bar) methods for the $\text{Cr}(o\text{-tol})_4$ (red), $\text{V}(o\text{-tol})_4^-$ (orange), $\text{Mo}(o\text{-tol})_4$ (teal), $\text{Ti}(o\text{-tol})_4^{2-}$ (gray), and $\text{W}(o\text{-tol})_4$ (cyan) complexes using (2,10) active space. The values are in GHz. Dashed lines correspond to experimental data from references 1 and 2.

Table S41: Computed axial parameter ($|D|$) using the (2,10) active space for $\text{Cr}(o\text{-tol})_4$, $\text{V}(o\text{-tol})_4^-$, $\text{Mo}(o\text{-tol})_4$, $\text{Ti}(o\text{-tol})_4^{2-}$, and $\text{W}(o\text{-tol})_4$ complexes. The energy values were obtained with SA-CASSCF, CASPT2, tPBE, and tPBE0 methods. The values reported are in GHz.

Complex	SA-CASSCF	CASPT2	tPBE	tPBE0
$\text{Cr}(o\text{-tol})_4$	9.23	1.24	1.43	3.74
$\text{V}(o\text{-tol})_4^-$	7.90	6.46	2.59	4.53
$\text{Mo}(o\text{-tol})_4$	10.82	8.13	11.93	4.99
$\text{Ti}(o\text{-tol})_4^{2-}$	10.63	9.25	5.83	9.77
$\text{W}(o\text{-tol})_4$	201.07	13.96	95.64	7.42

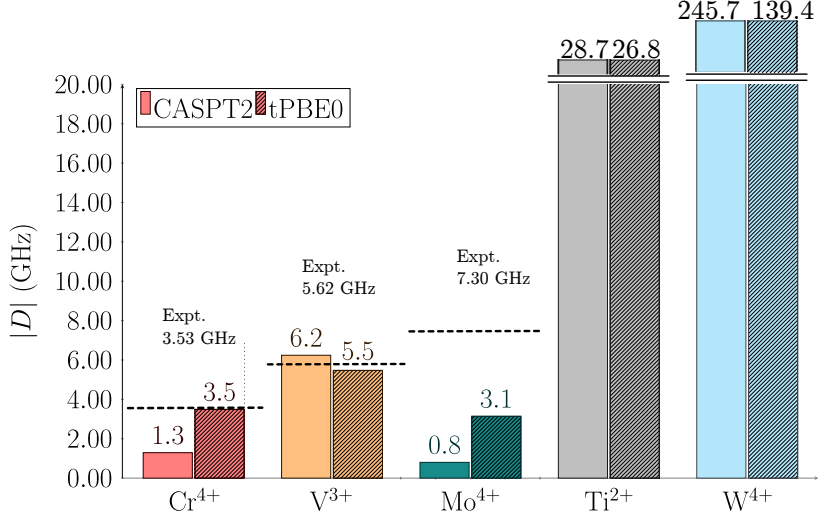


Figure S22: Calculated axial parameter ($|D|$) with the CASPT2 (solid bar) and tPBE0 (striped bar) methods for the $\text{Cr}(o\text{-tol})_4$ (red), $\text{V}(o\text{-tol})_4^-$ (orange), $\text{Mo}(o\text{-tol})_4$ (teal), $\text{Ti}(o\text{-tol})_4^{2-}$ (gray), and $\text{W}(o\text{-tol})_4$ (cyan) complexes using (8,8) active space. The values are in GHz. Dashed lines correspond to experimental data from references 1 and 2.

Table S42: Computed axial parameter ($|D|$) using the (8,8) active space for $\text{Cr}(o\text{-tol})_4$, $\text{V}(o\text{-tol})_4^-$, $\text{Mo}(o\text{-tol})_4$, $\text{Ti}(o\text{-tol})_4^{2-}$, and $\text{W}(o\text{-tol})_4$ complexes. The energy values were obtained with SA-CASSCF, CASPT2, tPBE, and tPBE0 methods. The values reported are in GHz.

Complex	SA-CASSCF	CASPT2	tPBE	tPBE0
$\text{Cr}(o\text{-tol})_4$	5.94	1.29	1.49	3.49
$\text{V}(o\text{-tol})_4^-$	7.63	6.24	3.23	5.47
$\text{Mo}(o\text{-tol})_4$	8.03	0.80	11.32	3.14
$\text{Ti}(o\text{-tol})_4^{2-}$	4.32	28.72	37.54	26.77
$\text{W}(o\text{-tol})_4$	201.36	185.62	12.29	102.96

Table S43: Computed axial parameter ($|D|$) using the (8,13) active space for $\text{V}(o\text{-tol})_4^-$ and (10,15) active space for $\text{Cr}(o\text{-tol})_4$, $\text{Mo}(o\text{-tol})_4$, $\text{Ti}(o\text{-tol})_4^{2-}$, and $\text{W}(o\text{-tol})_4$ complexes. The energy values were obtained with SA-CASSCF, CASPT2, tPBE, and tPBE0 methods. The values reported are in GHz.

Complex	SA-CASSCF	CASPT2	tPBE	tPBE0
$\text{Cr}(o\text{-tol})_4$	4.06	2.72	1.35	2.39
$\text{V}(o\text{-tol})_4^-$	6.96	6.87	0.34	2.95
$\text{Mo}(o\text{-tol})_4$	14.01	6.82	1.21	4.09
$\text{Ti}(o\text{-tol})_4^{2-}$	17.21	15.11	12.21	13.82
$\text{W}(o\text{-tol})_4$	219.85	145.50	68.10	124.04

6.3 Absolute Electronic Energies

6.3.1 Cr(*o-tol*)₄ Complex

Table S44: Computed absolute energies with the SA-CASSCF, CASPT2, tPBE, and tPBE0 methods for the Cr(*o-tol*)₄ complex when using the (2,5) active space.

No.	SA-CASSCF			CASPT2			tPBE			tPBE0		
	Triplet	Singlet	Triplet	Singlet	Triplet	Singlet	Triplet	Singlet	Triplet	Singlet	Triplet	Singlet
1	-2126.30624935	-2126.23614609	-2129.41767400	-2129.38157702	-2133.29414582	-2133.27635417	-2131.54717170	-2131.51630215				
2	-2126.24391589	-2126.23480260	-2129.32575277	-2129.37993967	-2133.20650494	-2133.27707479	-2131.46585768	-2131.51650674				
3	-2126.23827510	-2126.18619333	-2129.31814130	-2129.30027388	-2133.19944397	-2133.18454955	-2131.45915175	-2131.43496050				
4	-2126.23827495	-2126.18607161	-2129.31814068	-2129.29578829	-2133.19944335	-2133.19589975	-2131.45915125	-2131.44344272				
5	-2126.21845775	-2126.18441698	-2129.31059048	-2129.33659313	-2133.18614053	-2133.24727830	-2131.44421984	-2131.48156297				
6	-2126.20091935	-2126.18187156	-2129.28355144	-2129.29073043	-2133.16431175	-2133.18462200	-2131.42346365	-2131.43393439				
7	-2126.20091891	-2126.18187144	-2129.28354961	-2129.29072897	-2133.16430994	-2133.18462043	-2131.42346218	-2131.43393318				
8	-2126.15193413	-2126.16489564	-2129.21796830	-2129.27412270	-2133.10475889	-2133.16260354	-2131.36655270	-2131.41317657				
9	-2126.15193383	-2126.16489526	-2129.21796711	-2129.27412061	-2133.10475757	-2133.16260136	-2131.36655164	-2131.41317484				
10	-2126.1398435	-2126.13439739	-2129.19667564	-2129.21544694	-2133.08854322	-2133.11027670	-2131.35137850	-2131.36630687				
11		-2126.11458258	-2129.18927648		-2133.08099412		-2131.33939124					
12		-2126.10913139	-2129.19617145		-2133.08987593		-2131.34468980					
13		-2126.10913042	-2129.19617378		-2133.08987368		-2131.34468787					
14		-2126.09316917	-2129.18010502		-2133.07566352		-2131.33003993					
15		-2126.02876163	-2129.16257970		-2133.10295594		-2131.33440736					

Table S45: Computed absolute energies with the SA-CASSCF, CASPT2, tPBE, and tPBE0 methods for the Cr(*o*-tol)₄ complex when using the (2,10) active space.

No.	SA-CASSCF			CASPT2			tPBE			tPBE0		
	Triplet	Singlet	Triplet	Singlet	Triplet	Singlet	Triplet	Singlet	Triplet	Singlet	Triplet	Singlet
1	-2126.31047778	-2126.24297430	-2129.41808546	-2129.38045551	-2133.29316590	-2133.27408198	-2131.54749387	-2131.51630506				
2	-2126.24752839	-2126.24156349	-2129.32437172	-2129.37794840	-2133.20497655	-2133.27367894	-2131.46561451	-2131.51565008				
3	-2126.24189988	-2126.19409480	-2129.32093170	-2129.33588959	-2133.19322891	-2133.24209559	-2131.45539665	-2131.48009539				
4	-2126.24189964	-2126.19344450	-2129.32093159	-2129.30266740	-2133.19322861	-2133.18850714	-2131.45539637	-2131.43974148				
5	-2126.22382039	-2126.19249984	-2129.31098551	-2129.29330827	-2133.18478333	-2133.19348590	-2131.44454260	-2131.44323939				
6	-2126.20560174	-2126.18859698	-2129.28172786	-2129.28918377	-2133.16316725	-2133.18122479	-2131.42377587	-2131.43306784				
7	-2126.20560130	-2126.18859677	-2129.28172697	-2129.28918212	-2133.16316693	-2133.18122429	-2131.42377552	-2131.43306741				
8	-2126.15619785	-2126.17210725	-2129.21840991	-2129.27265856	-2133.10799913	-2133.15998060	-2131.37004881	-2131.41301226				
9	-2126.15619772	-2126.17210688	-2129.21840976	-2129.27265761	-2133.10799878	-2133.15997920	-2131.37004852	-2131.41301112				
10	-2126.14375943	-2126.13991628	-2129.19499208	-2129.21311510	-2133.08534118	-2133.10664531	-2131.34994799	-2131.36496305				
11		-2126.11946414	-2129.18701579	-2129.18701579	-2133.07865934	-2131.33886054	-2131.34642620					
12		-2126.11519283	-2129.19413148	-2129.19413148	-2133.09017065	-2131.34642620						
13		-2126.11519224	-2129.19413060	-2129.19413060	-2133.09016943	-2131.34642513						
14		-2126.09909505	-2129.17794082	-2129.17794082	-2133.07280097	-2131.32937449						
15		-2126.04396023	-2129.15669759	-2129.15669759	-2133.08690018	-2131.32616519						

Table S46: Computed absolute energies with the SA-CASSCF, CASPT2, tPBE, and tPBE0 methods for the Cr(*o*-tol)₄ complex when using the (8,8) active space.

No.	SA-CASSCF			CASPT2			tPBE			tPBE0		
	Triplet	Singlet	Triplet	Singlet	Triplet	Singlet	Triplet	Singlet	Triplet	Singlet	Triplet	Singlet
1	-2126.39283017	-2126.32312728	-2129.40002333	-2129.35163756	-2133.29073235	-2133.26069317	-2131.56625681	-2131.52630170				
2	-2126.31226633	-2126.32180143	-2129.31996490	-2129.34971401	-2133.21279139	-2133.26111149	-2131.48766013	-2131.52628398				
3	-2126.30524081	-2126.27560169	-2129.31725876	-2129.30948942	-2133.20273259	-2133.22958347	-2131.47835965	-2131.49108803				
4	-2126.30524062	-2126.25793795	-2129.31725868	-2129.29067318	-2133.20273247	-2133.18592383	-2131.47835951	-2131.45392736				
5	-2126.29487008	-2126.25447415	-2129.31163303	-2129.28522386	-2133.20250257	-2133.19711103	-2131.47559445	-2131.46145181				
6	-2126.27551209	-2126.24903450	-2129.29347114	-2129.28128005	-2133.18768219	-2133.18644678	-2131.45963967	-2131.45209371				
7	-2126.27551195	-2126.24903413	-2129.29347107	-2129.28127966	-2133.18768213	-2133.18644630	-2131.45963959	-2131.45209326				
8		-2126.23869904	-2129.27294908	-2129.27294908	-2133.17071092	-2133.17071092	-2131.43770795	-2131.43770726				
9		-2126.23869853	-2129.27294845	-2129.27294845	-2133.17071017	-2133.17071017	-2131.43770726	-2131.43770726				

6.3.2 Mo(*o*-tol)₄ Complex

Table S47: Computed absolute energies with the SA-CASSCF, CASPT2, tPBE, and tPBE0 methods for the Mo(*o*-tol)₄ complex when using the (2,5) active space.

No.	SA-CASSCF			CASPT2			tPBE			tPBE0		
	Triplet	Singlet	Triplet	Singlet	Triplet	Singlet	Triplet	Singlet	Triplet	Singlet	Triplet	Singlet
1	-5122.47095431	-5122.42719758	-5125.48079269	-5125.45384713	-5130.31301118	-5130.30290423	-5128.35249696	-5128.33397757				
2	-5122.38010025	-5122.42375388	-5125.37679076	-5125.45035629	-5130.21341881	-5130.30194237	-5128.25508917	-5128.33239525				
3	-5122.38009503	-5122.38678537	-5125.37679412	-5125.41835129	-5130.21341467	-5130.28765131	-5128.25508476	-5128.31243483				
4	-5122.37996090	-5122.35315874	-5125.37228680	-5125.365550296	-5130.21512704	-5130.21010975	-5128.25633551	-5128.24587200				
5	-5122.37192381	-5122.34322961	-5125.37202310	-5125.35608043	-5130.21430296	-5130.20670511	-5128.25370817	-5128.24083624				
6	-5122.35368005	-5122.34322423	-5125.35224673	-5125.35607654	-5130.19617664	-5130.20670346	-5128.23555249	-5128.24083365				
7	-5122.35367399	-5122.34143394	-5125.35223925	-5125.35219376	-5130.19616891	-5130.20914552	-5128.23554518	-5128.24221763				
8	-5122.28427546	-5122.33382533	-5125.26755218	-5125.34481709	-5130.11188844	-5130.19114248	-5128.15498520	-5128.22681319				
9	-5122.28426643	-5122.33381911	-5125.26755313	-5125.34480453	-5130.11188115	-5130.19113596	-5128.15497747	-5128.22680675				
10	-5122.27436034	-5122.27674343	-5125.25918189	-5125.27034009	-5130.10627447	-5130.12116640	-5128.14829594	-5128.16006066				
11	-5122.26285903	-5125.25810123	-5125.25810123	-5130.10757939	-5130.10757939	-5128.14639930	-5128.14639930					
12	-5122.24678080	-5125.25175329	-5125.25175329	-5130.10759554	-5130.10759554	-5128.14239186	-5128.14239186					
13	-5122.24677453	-5125.25199221	-5125.25199221	-5130.10758978	-5130.10758978	-5128.14238597	-5128.14238597					
14	-5122.23632315	-5125.24118825	-5125.24118825	-5130.10130151	-5130.10130151	-5128.13505692	-5128.13505692					
15	-5122.20387534	-5125.22869522	-5125.22869522	-5130.11075929	-5130.11075929	-5128.13403830	-5128.13403830					

Table S48: Computed absolute energies with the SA-CASSCF, CASPT2, tPBE, and tPBE0 methods for the Mo(*o*-tol)₄ complex when using the (2,10) active space.

No.	SA-CASSCF			CASPT2			tPBE			tPBE0		
	Triplet	Singlet	Triplet	Singlet	Triplet	Singlet	Triplet	Singlet	Triplet	Singlet	Triplet	Singlet
1	-5122.47315347	-5122.43075908	-5125.47959477	-5125.45467733	-5130.3135106	-5130.30269889	-5128.35345166	-5128.33471394				
2	-5122.38197876	-5122.42740667	-5125.37853012	-5125.45029085	-5130.21318928	-5130.30136041	-5128.25538665	-5128.33287198				
3	-5122.38197405	-5122.3934413	-5125.37852706	-5125.4198095	-5130.21318562	-5130.28680994	-5128.25538273	-5128.31346849				
4	-5122.38184027	-5122.35761822	-5125.37280977	-5125.36767141	-5130.21448182	-5130.21120113	-5128.25632143	-5128.24780540				
5	-5122.37504959	-5122.34758549	-5125.37395132	-5125.35720767	-5130.21496522	-5130.20654628	-5128.25498631	-5128.24180608				
6	-5122.35665116	-5122.34758016	-5125.35349929	-5125.35720537	-5130.19529058	-5130.20654566	-5128.23563073	-5128.24180429				
7	-5122.35664590	-5122.34552988	-5125.35349149	-5125.35111081	-5130.19528299	-5130.20772810	-5128.23562372	-5128.24217855				
8	-5122.28623907	-5122.33821435	-5125.26791181	-5125.34473521	-5130.11068996	-5130.19065479	-5128.15457724	-5128.22754468				
9	-5122.28623059	-5122.33820811	-5125.26790820	-5125.34472587	-5130.11068328	-5130.19064949	-5128.15457011	-5128.22753915				
10	-5122.27638412	-5122.27909025	-5125.25827457	-5125.27071734	-5130.10497898	-5130.12064225	-5128.14783027	-5128.16025425				
11		-5122.26511470		-5125.25864036		-5130.10689049		-5128.14644654				
12		-5122.25117065		-5125.25073943		-5130.10552276		-5128.14193473				
13		-5122.25116475		-5125.25074869		-5130.10551510		-5128.14192751				
14		-5122.24080049		-5125.24008267		-5130.09917043		-5128.13457795				
15		-5122.21455873		-5125.22661173		-5130.10239682		-5128.13043730				

Table S49: Computed absolute energies with the SA-CASSCF, CASPT2, tPBE, and tPBE0 methods for the Mo(*o*-tol)₄ complex when using the (8,8) active space.

No.	SA-CASSCF			CASPT2			tPBE			tPBE0		
	Triplet	Singlet	Triplet	Singlet	Triplet	Singlet	Triplet	Singlet	Triplet	Singlet	Triplet	Singlet
1	-5122.49778580	-5122.45535200	-5125.46883993	-5125.44080257	-5130.30694133	-5130.29149614	-5128.35465245	-5128.33246011				
2	-5122.39866650	-5122.45131556	-5125.37447894	-5125.43700025	-5130.21331829	-5130.29131078	-5128.25965534	-5128.33131198				
3	-5122.39866080	-5122.41640010	-5125.37447552	-5125.40789913	-5130.21331561	-5130.27431796	-5128.25965191	-5128.30983850				
4	-5122.39839483	-5122.37223423	-5125.37254160	-5125.36389670	-5130.21651185	-5130.20874868	-5128.26198260	-5128.24962007				
5	-5122.39309032	-5122.36165061	-5125.37349103	-5125.35453364	-5130.21670266	-5130.20584479	-5128.26079958	-5128.24479625				
6	-5122.37520644	-5122.36164494	-5125.35750984	-5125.35453209	-5130.20192130	-5130.20584524	-5128.24524259	-5128.24479517				
7	-5122.37520060	-5122.35998562	-5125.35750455	-5125.35172728	-5130.20191522	-5130.20952825	-5128.24523657	-5128.24714259				
8		-5122.35320047		-5125.34748262		-5130.19482424		-5128.23441830				
9		-5122.35319450		-5125.34747884		-5130.19481895		-5128.23441284				

6.3.3 W(*o-tol*)₄ Complex

Table S50: Computed absolute energies with the SA-CASSCF, CASPT2, tPBE, and tPBE0 methods for the W(*o-tol*)₄ complex when using the (2,5) active space.

No.	SA-CASSCF			CASPT2			tPBE			tPBE0		
	Triplet	Singlet	Triplet	Singlet	Triplet	Singlet	Triplet	Singlet	Triplet	Singlet	Triplet	Singlet
1	-17204.25781351	-17204.21904708	-17207.20022358	-17207.17567348	-17215.61416345	-17215.60569174	-17212.77507597	-17212.75590358				
2	-17204.17331501	-17204.21447094	-17207.10851957	-17207.17134643	-17215.52766349	-17215.60444291	-17212.68907637	-17212.75694992				
3	-17204.17329369	-17204.18233924	-17207.10851801	-17207.14303111	-17215.52765241	-17215.59337429	-17212.68906273	-17212.74061553				
4	-17204.17202038	-17204.14805246	-17207.10503791	-17207.09660081	-17215.52964719	-17215.52526033	-17212.69024049	-17212.68095836				
5	-17204.16577870	-17204.13820272	-17207.10460776	-17207.0886212	-17215.53003307	-17215.52230215	-17212.68896948	-17212.67627729				
6	-17204.14881368	-17204.13817721	-17207.08753360	-17207.08885350	-17215.51355487	-17215.52230866	-17212.67236957	-17212.67627580				
7	-17204.14879518	-17204.13371282	-17207.08753295	-17207.08358149	-17215.51353793	-17215.52435048	-17212.67235224	-17212.67669107				
8	-17204.08555784	-17204.12951412	-17207.01436138	-17207.07957260	-17215.44178143	-17215.51261618	-17212.60272553	-17212.66684067				
9	-17204.08551618	-17204.12950694	-17207.01432674	-17207.07955458	-17215.44176189	-17215.51258346	-17212.60270046	-17212.66681433				
10	-17204.07719765	-17204.07836099	-17207.00767911	-17207.01663409	-17215.43765060	-17215.45075459	-17212.59753736	-17212.60765597				
11		-17204.06693316		-17207.00647808		-17215.43957052		-17212.59641118				
12		-17204.04631977		-17206.99489516		-17215.43873947		-17212.59063455				
13		-17204.04630607		-17206.99494617		-17215.43873907		-17212.59063082				
14		-17204.03725542		-17206.98556800		-17215.43231715		-17212.58355172				
15		-17204.00660636		-17206.97208534		-17215.44097668		-17212.58224760				

Table S51: Computed absolute energies with the SA-CASSCF, CASPT2, tPBE, and tPBE0 methods for the W(*o*-tol)₄ complex when using the (2,10) active space.

No.	SA-CASSCF			CASPT2			tPBE			tPBE0		
	Triplet	Singlet	Triplet	Singlet	Triplet	Singlet	Triplet	Singlet	Triplet	Singlet	Triplet	Singlet
1	-17204.25967576	-17204.222225549	-17207.19923325	-17207.1760909	-17215.61548421	-17215.60648230	-17212.77653210	-17212.76042560				
2	-17204.17495059	-17204.21801930	-17207.10983175	-17207.17113379	-17215.522801035	-17215.60524989	-17212.68974541	-17212.75844224				
3	-17204.17492905	-17204.18883727	-17207.10982216	-17207.14425749	-17215.52800036	-17215.59449329	-17212.68973253	-17212.74307929				
4	-17204.17370638	-17204.15245747	-17207.10500074	-17207.09875202	-17215.52897412	-17215.52736390	-17212.69015719	-17212.68363729				
5	-17204.16885565	-17204.14256759	-17207.10672822	-17207.09008830	-17215.53203130	-17215.52283969	-17212.69123739	-17212.67777167				
6	-17204.15171008	-17204.14254224	-17207.08814750	-17207.09007943	-17215.51331350	-17215.52284922	-17212.67291265	-17212.67777248				
7	-17204.15169179	-17204.13793927	-17207.08813763	-17207.08218347	-17215.51329612	-17215.522444818	-17212.67289504	-17212.676732095				
8	-17204.08760244	-17204.13384859	-17207.01442911	-17207.07938227	-17215.44025318	-17215.51140431	-17212.60209050	-17212.666701538				
9	-17204.08756001	-17204.13383936	-17207.01439642	-17207.07936510	-17215.44023463	-17215.51137543	-17212.60206598	-17212.66699141				
10	-17204.07933028	-17204.08054211	-17207.00670555	-17207.01722393	-17215.43596914	-17215.45035417	-17212.59680943	-17212.60790116				
11		-17204.06912822		-17207.00703657		-17215.43877366		-17212.59636230				
12		-17204.05095540		-17206.99333038		-17215.43543249		-17212.58931322				
13		-17204.05094326		-17206.99334615		-17215.43544111		-17212.58931665				
14		-17204.04183774		-17206.98435369		-17215.42949008		-17212.58257694				
15		-17204.01657563		-17206.96975081		-17215.43340608		-17212.57919847				

Table S52: Computed absolute energies with the SA-CASSCF, CASPT2, tPBE, and tPBE0 methods for the W(*o*-tol)₄ complex when using the (8,8) active space.

No.	SA-CASSCF			CASPT2			tPBE			tPBE0		
	Triplet	Singlet	Triplet	Singlet	Triplet	Singlet	Triplet	Singlet	Triplet	Singlet	Triplet	Singlet
1	-17204.27601110	-17204.23883388	-17207.18442988	-17207.15853693	-17215.60777713	-17215.59440294	-17212.77483562	-17212.75551068				
2	-17204.18532289	-17204.23334516	-17207.09737108	-17207.15427607	-17215.522282197	-17215.59421946	-17212.68844720	-17212.75400089				
3	-17204.18530068	-17204.20186107	-17207.09734763	-17207.12813104	-17215.522280853	-17215.58098399	-17212.68843157	-17212.73620326				
4	-17204.18423429	-17204.15990286	-17207.09720086	-17207.08395008	-17215.52763978	-17215.51697471	-17212.69178441	-17212.67770675				
5	-17204.17892788	-17204.14974634	-17207.09610635	-17207.07525712	-17215.52609599	-17215.51413859	-17212.68930396	-17212.67304053				
6	-17204.16233739	-17204.14972708	-17207.08290156	-17207.07522683	-17215.51326072	-17215.51411115	-17212.67552989	-17212.67301513				
7	-17204.16232073	-17204.14643344	-17207.08288835	-17207.07403657	-17215.51324672	-17215.51995254	-17212.67657277	-17212.67301522				
8		-17204.14173161		-17207.07067605		-17215.50652858		-17212.66532934				
9		-17204.14169613		-17207.07063471		-17215.50645359		-17212.66526423				

6.3.4 $V(o\text{-tol})_4^-$ Complex

Table S53: Computed absolute energies with the SA-CASSCF, CASPT2, tPBE, and tPBE0 methods for the $V(o\text{-tol})_4^-$ complex when using the (2,5) active space.

No.	SA-CASSCF			CASPT2			tPBE			tPBE0		
	Triplet	Singlet										
1	-2025.01428063	-2024.95196111	-2027.93360146	-2027.89447567	-2031.81621252	-2031.79878126	-2030.11572955	-2030.08707622	-2030.11572955	-2030.08707622	-2030.06745335	-2030.08771706
2	-2024.97109524	-2024.95071759	-2027.88502307	-2027.89454200	-2031.76624205	-2031.80005021	-2030.06745335	-2030.08771706	-2030.06148850	-2030.04206034	-2030.06148829	-2030.06163190
3	-2024.96683916	-2024.91199892	-2027.87966467	-2027.84885058	-2031.75970495	-2031.75208081	-2030.06148850	-2030.04206034	-2031.77880275	-2031.75970473	-2030.06148829	-2030.06163190
4	-2024.96683897	-2024.91011933	-2027.87966449	-2027.86032646	-2031.75970473	-2031.77880275	-2030.06148829	-2030.06163190	-2031.73506875	-2031.74439795	-2030.03724966	-2030.03547704
5	-2024.94379239	-2024.90871430	-2027.86407360	-2027.84405327	-2031.73506875	-2031.74439795	-2030.03724966	-2030.03547704	-2027.85298510	-2027.84405329	-2031.73127542	-2030.03319687
6	-2024.93896122	-2024.90871416	-2024.90871416	-2027.85298510	-2027.84405329	-2031.73127542	-2030.03319687	-2030.03547688	-2027.83986827	-2027.83986827	-2031.73127525	-2030.03319670
7	-2024.93896105	-2024.90397114	-2024.90397114	-2027.85298487	-2027.83986827	-2031.73127525	-2030.03319670	-2030.02267499	-2027.81920382	-2027.82919528	-2031.71555429	-2030.01064152
8	-2024.89590319	-2024.89250341	-2024.89250341	-2027.81920382	-2027.82919528	-2031.71555429	-2030.01064152	-2030.01277686	-2027.81920374	-2027.82919498	-2031.71555417	-2030.01064142
9	-2024.89590318	-2024.89250320	-2024.89250320	-2027.81920374	-2027.82919498	-2031.71555417	-2030.01064142	-2030.01277660	-2027.80245823	-2027.80245823	-2031.71283056	-2030.00820033
10	-2024.89430963	-2024.87378941	-2027.81316951	-2027.81316951	-2031.71283056	-2031.70357311	-2029.99612719	-2029.99612719	-2027.78924052	-2027.78924052	-2031.68922973	-2029.98280806
11		-2024.86354306							-2027.78938476	-2027.78938476	-2031.69431462	-2029.98526909
12		-2024.85813251							-2027.78939980	-2027.78939980	-2031.69431439	-2029.98526888
13		-2024.85813233							-2027.78020542	-2027.78020542	-2031.68516860	-2029.97643503
14		-2024.85023432							-2027.73599903	-2027.73599903	-2031.70091911	-2029.96767097
15		-2024.76792655										

Table S54: Computed absolute energies with the SA-CASSCF, CASPT2, tPBE, and tPBE0 methods for the $\text{V}(o\text{-tol})_4^-$ complex when using the (2,10) active space.

No.	SA-CASSCF			CASPT2			tPBE			tPBE0		
	Triplet	Singlet	Triplet	Singlet	Triplet	Singlet	Triplet	Singlet	Triplet	Singlet	Singlet	
1	-2025.01826830	-2024.95890167	-2027.93295644	-2027.89371807	-2031.81434295	-2031.79686236	-2030.11532429	-2030.08737219				
2	-2024.97503115	-2024.95778032	-2027.88403168	-2027.89306344	-2031.76417295	-2031.79693151	-2030.06688750	-2030.08714371				
3	-2024.97070638	-2024.91944228	-2027.87844130	-2027.86060075	-2031.75851183	-2031.7755173	-2030.06156047	-2030.06167437				
4	-2024.97070624	-2024.91932728	-2027.87844078	-2027.84688369	-2031.75851142	-2031.74875190	-2030.06156013	-2030.04139575				
5	-2024.94884364	-2024.91583298	-2027.865523388	-2027.84214457	-2031.73319074	-2031.74220032	-2030.03710397	-2030.03560849				
6	-2024.94346681	-2024.91583283	-2027.85284382	-2027.84214682	-2031.72963986	-2031.74220012	-2030.03309660	-2030.03560830				
7	-2024.94346630	-2024.91207891	-2027.85284316	-2027.84047153	-2031.72963938	-2031.72665602	-2030.03309611	-2030.02301174				
8	-2024.90179058	-2024.90072972	-2027.81752947	-2027.82975829	-2031.70596585	-2031.71744634	-2030.0049203	-2030.01326719				
9	-2024.90178994	-2024.90072947	-2027.81752833	-2027.82975907	-2031.70596459	-2031.71744627	-2030.00492093	-2030.01326707				
10	-2024.89962134	-2024.88083138	-2027.81387778	-2027.80274678	-2031.70854428	-2031.70026057	-2030.00631355	-2029.99540327				
11	-2024.87028137		-2027.78955576		-2031.68649422		-2029.98244101					
12	-2024.86602314		-2027.78858223		-2031.69174867		-2029.98531729					
13	-2024.86602285		-2027.78858236		-2031.69174848		-2029.98531707					
14	-2024.85809008		-2027.77922232		-2031.68138994		-2029.97556498					
15	-2024.78873256		-2027.73546176		-2031.68464802		-2029.96066916					

Table S55: Computed absolute energies with the SA-CASSCF, CASPT2, tPBE, and tPBE0 methods for the $\text{V}(o\text{-tol})_4^-$ complex when using the (8,8) active space.

No.	SA-CASSCF			CASPT2			tPBE			tPBE0		
	Triplet	Singlet	Triplet	Singlet	Triplet	Singlet	Triplet	Singlet	Triplet	Singlet	Triplet	Singlet
1	-2025.03011643	-2024.96977105	-2027.93571277	-2027.89264443	-2031.82240985	-2031.79911074	-2030.12433650	-2030.09177582				
2	-2024.98358708	-2024.96870007	-2027.88903782	-2027.89198584	-2031.80006985	-2031.80006985	-2030.07743540	-2030.09222741				
3	-2024.97872334	-2024.92932564	-2027.88444910	-2027.86070400	-2031.76867497	-2031.77959686	-2030.07118706	-2030.06702906				
4	-2024.97872314	-2024.92468303	-2027.88444895	-2027.85047724	-2031.76867479	-2031.75871977	-2030.07118688	-2030.05021059				
5	-2024.95667829	-2024.92078733	-2027.87070060	-2027.84665198	-2031.74976624	-2031.74989477	-2030.05149425	-2030.04261791				
6	-2024.94996404	-2024.92078702	-2027.86164026	-2027.84665180	-2031.74448456	-2031.74989501	-2030.04585443	-2030.04261801				
7	-2024.94996386	-2024.91883692	-2027.86164003	-2027.84454696	-2031.74448438	-2031.73759605	-2030.04585425	-2030.03290627				
8		-2024.90751580	-2027.83783413	-2027.83950682	-2031.73950682	-2030.03150907	-2030.03150768					
9		-2024.90751506	-2027.83783296	-2027.83783296	-2031.73950522	-2030.03150768						

6.3.5 $\text{Ti}(o\text{-tol})_4^{2-}$ Complex

Table S56: Computed absolute energies with the SA-CASSCF, CASPT2, tPBE, and tPBE0 methods for the $\text{Ti}(o\text{-tol})_4^{2-}$ complex when using the (2,5) active space.

No.	SA-CASSCF			CASPT2			tPBE			tPBE0		
	Triplet	Singlet	Triplet	Singlet	Triplet	Singlet	Triplet	Singlet	Triplet	Singlet	Triplet	Singlet
1	-1929.50041525	-1929.45750872	-1932.37205812	-1932.35194936	-1936.25242554	-1936.24507187	-1934.56442297	-1934.54818108	-1936.24261968	-1934.54096084	-1934.54567302	
2	-1929.47389194	-1929.45483303	-1932.34883341	-1932.34994960	-1936.22998380	-1936.22888741	-1934.52556423	-1934.52882990	-1936.21185476	-1936.21185470	-1934.52556418	-1934.52347054
3	-1929.46669264	-1929.42865738	-1932.34200050	-1932.32898484	-1936.21185472	-1936.21185470	-1936.22241669	-1934.52556418	-1936.20092865	-1936.20811950	-1934.51309813	-1934.51097670
4	-1929.46669261	-1929.42663210	-1932.34200049	-1932.32649672	-1936.21185472	-1936.21185470	-1936.22241669	-1934.52556418	-1936.20811950	-1934.51309813	-1934.51097670	
5	-1929.44960655	-1929.41954829	-1932.33010639	-1932.31890264	-1936.21185472	-1936.21185470	-1936.22241669	-1934.52556418	-1936.20811950	-1934.51309813	-1934.51097670	
6	-1929.44791290	-1929.41954825	-1932.32703718	-1932.31893242	-1936.20227073	-1936.20811945	-1934.51368127	-1934.51097665	-1936.20227068	-1936.19680688	-1934.51368122	-1934.50213461
7	-1929.44791285	-1929.41811778	-1932.32697384	-1932.31305517	-1936.20227068	-1936.20811945	-1934.51368127	-1934.51097665	-1936.19147904	-1936.19376377	-1934.49881047	-1934.49914201
8	-1929.42080477	-1929.41527673	-1932.30329727	-1932.31080853	-1936.20227068	-1936.20811945	-1934.51368127	-1934.51097665	-1936.19147900	-1936.19376380	-1934.49881044	-1934.49914203
9	-1929.42080475	-1929.41527671	-1932.30329726	-1932.31107223	-1936.20227068	-1936.20811945	-1934.51368127	-1934.51097665	-1936.19188158	-1936.19178391	-1934.49869973	-1934.49522958
10	-1929.41915417	-1929.40556658	-1932.299926996	-1932.29941199	-1936.20227068	-1936.20811945	-1934.51368127	-1934.51097665	-1936.18081937	-1936.18081937	-1934.48480692	
11	-1929.39676958		-1932.28959680		-1936.19147900	-1936.19376380	-1934.49881044	-1934.49914203	-1936.18029388	-1936.18029388	-1934.48185072	
12		-1929.38652123		-1932.28670229		-1936.18029388		-1936.18029385		-1936.18029385	-1934.48185069	
13		-1929.38652121		-1932.28670216		-1936.17420661		-1936.17420661		-1936.17420661	-1934.47566128	
14		-1929.38002529		-1932.27630422		-1936.18351581		-1936.18351581		-1936.18351581	-1934.46717662	
15		-1929.31815906										

Table S57: Computed absolute energies with the SA-CASSCF, CASPT2, tPBE, and tPBE0 methods for the $\text{Ti}(o\text{-tol})_4^{2-}$ complex when using the (2,10) active space.

No.	SA-CASSCF			CASPT2			tPBE			tPBE0		
	Triplet	Singlet	Triplet	Singlet	Triplet	Singlet	Triplet	Singlet	Triplet	Singlet	Triplet	Singlet
1	-1929.50718353	-1929.47203876	-1932.37226889	-1932.35409808	-1936.25425309	-1936.25017876	-1934.56748570	-1934.55564376				
2	-1929.48164926	-1929.46866455	-1932.34794901	-1932.35103638	-1936.23038736	-1936.24873470	-1934.54320284	-1934.55371716				
3	-1929.47336851	-1929.4510045	-1932.34013201	-1932.33580331	-1936.21599607	-1936.23522937	-1934.53033918	-1934.53917214				
4	-1929.47336846	-1929.44361514	-1932.34013190	-1932.32508417	-1936.21599598	-1936.22401847	-1934.53033910	-1934.52891764				
5	-1929.45976635	-1929.43587165	-1932.33168666	-1932.31687054	-1936.20393467	-1936.20711002	-1934.51789259	-1934.51430043				
6	-1929.45722759	-1929.43587156	-1932.32664694	-1932.31687038	-1936.20222790	-1936.20710986	-1934.51597782	-1934.51430029				
7	-1929.45722754	-1929.43329357	-1932.32664692	-1932.31578248	-1936.20222787	-1936.20068632	-1934.51597779	-1934.50883813				
8	-1929.43348598	-1929.43288063	-1932.30666136	-1932.31445111	-1936.19026431	-1936.20441896	-1934.50106973	-1934.51153438				
9	-1929.43348596	-1929.43288058	-1932.30666128	-1932.31444702	-1936.19026426	-1936.20441898	-1934.50106969	-1934.51153438				
10	-1929.43060094	-1929.42113297	-1932.30284174	-1932.30388304	-1936.18950279	-1936.19381058	-1934.4997733	-1934.50064118				
11	-1929.41249097		-1932.29305383		-1936.18322266		-1934.49053974					
12	-1929.40590685		-1932.28797009		-1936.18416110		-1934.48959754					
13	-1929.40590680		-1932.28796581		-1936.18416103		-1934.48959747					
14	-1929.39821964		-1932.27920000		-1936.17616447		-1934.48167826					
15	-1929.36585472		-1932.25727086		-1936.16767249		-1934.46721805					

Table S58: Computed absolute energies with the SA-CASSCF, CASPT2, tPBE, and tPBE0 methods for the $\text{Ti}(o\text{-tol})_4^{2-}$ complex when using the (8,8) active space.

No.	SA-CASSCF			CASPT2			tPBE			tPBE0		
	Triplet	Singlet	Triplet	Singlet	Triplet	Singlet	Triplet	Singlet	Triplet	Singlet	Singlet	
1	-1929.49649523	-1929.45419262	-1932.38163742	-1932.36471766	-1936.26639420	-1936.25914637	-1934.57391946	-1934.55790793				
2	-1929.46755567	-1929.45417048	-1932.36643590	-1932.35500206	-1936.25345462	-1936.24782881	-1934.55697988	-1934.54941423				
3	-1929.46433900	-1929.43271052	-1932.34963064	-1932.34337446	-1936.22640157	-1936.24127643	-1934.5358593	-1934.53913495				
4	-1929.46433895	-1929.41903132	-1932.34963056	-1932.34515551	-1936.22640144	-1936.23964274	-1934.53588582	-1934.53448989				
5	-1929.44922483	-1929.41750841	-1932.34315537	-1932.32792064	-1936.22229535	-1936.21211520	-1934.52902772	-1934.51346350				
6	-1929.44320367	-1929.41750837	-1932.34229447	-1932.32792223	-1936.22223741	-1936.21211559	-1934.52747898	-1934.51346379				
7	-1929.44320356	-1929.41553396	-1932.34229441	-1932.31843737	-1936.22223738	-1936.20491676	-1934.52747893	-1934.50757106				
8	-1929.42306574	-1929.41553393	-1932.32207584	-1932.31843763	-1936.21652129	-1936.20491716	-1934.51815740	-1934.50757135				
9	-1929.42306570	-1929.41264912	-1932.32207586	-1932.31761473	-1936.21652136	-1936.20158228	-1934.51815745	-1934.50434899				
10	-1929.42193916	-1929.40483064	-1932.31278757	-1932.3212912	-1936.20495242	-1936.21230804	-1934.50919911	-1934.51043869				
11		-1929.39826176		-1932.29805684		-1936.18903744		-1934.49134352				
12		-1929.38605796		-1932.29851077		-1936.19413927		-1934.49211894				
13		-1929.38605787		-1932.29850920		-1936.19413942		-1934.49211903				
14		-1929.38187269		-1932.28274549		-1936.17974842		-1934.48027949				
15		-1929.32285776		-1932.26424568		-1936.19292734		-1934.47540995				

6.3.6 Fe(*o*-tol)₄²⁻ Complex

Table S59: Computed absolute energies with the SA-CASSCF, CASPT2, and tPBE methods for the Fe(*o*-tol)₄²⁻ complex when using the (6,5) active space.

No.	SA-CASSCF					CASPT2					tPBE				
	Quintet	Triplet	Singlet	Quintet	Triplet	Singlet	Quintet	Triplet	Singlet	Quintet	Triplet	Singlet	Quintet	Triplet	Singlet
1	-2348.03353430	-2347.95545424	-2347.90868802	-2351.12740928	-2351.06384979	-2351.03897428	-2355.05414078	-2355.01671931	-2354.99094483	-2351.03416064	-2355.05396763	-2354.99279581	-2351.03397334	-2355.03155777	-2355.01168657
2	-2348.03341646	-2347.95544011	-2347.908625456	-2351.12698950	-2351.06383449	-2351.03897428	-2355.05414078	-2355.01671931	-2354.99094483	-2351.03416064	-2355.05396763	-2354.99279581	-2351.03397334	-2355.03155777	-2355.01168657
3	-2348.01312218	-2347.95305898	-2347.90623454	-2351.10327757	-2351.06190568	-2351.03897428	-2355.05414078	-2355.01671931	-2354.99094483	-2351.03416064	-2355.05396763	-2354.99279581	-2351.03397334	-2355.03155777	-2355.01168657
4	-2348.01063671	-2347.93818660	-2347.90619589	-2351.10029320	-2351.05054689	-2351.03522716	-2355.028833566	-2355.028831963	-2354.98767838	-2354.98580524	-2355.028831963	-2354.98767838	-2355.028831963	-2354.98767838	-2355.028831963
5	-2348.01062167	-2347.93803178	-2347.90423677	-2351.10027635	-2351.05065474	-2351.035273758	-2355.028831963	-2354.98767838	-2354.98580524	-2355.028831963	-2354.98767838	-2355.028831963	-2354.98767838	-2355.028831963	-2354.98767838
6	-2347.93633446	-2347.89251390	-2347.88455866	-2347.89251390	-2347.89251390	-2351.0441864	-2351.02175944	-2351.012175944	-2354.98947596	-2354.98745806	-2354.98947596	-2354.98745806	-2354.98947596	-2354.98745806	-2354.98947596
7	-2347.93632521	-2347.89250447	-2347.89179225	-2347.89179225	-2347.89179225	-2351.04411086	-2351.02172642	-2351.01217642	-2354.98946263	-2354.98946263	-2354.98946263	-2354.98946263	-2354.98946263	-2354.98946263	-2354.98946263
8	-2347.93510870	-2347.88702557	-2347.88899594	-2347.88899594	-2347.88899594	-2351.04900482	-2351.02078383	-2351.012078383	-2354.98658930	-2354.98658930	-2354.98658930	-2354.98658930	-2354.98658930	-2354.98658930	-2354.98658930
9	-2347.93339467	-2347.88702557	-2347.88899594	-2347.88899594	-2347.88899594	-2351.03701743	-2351.02377100	-2351.012377100	-2354.98386752	-2354.98386752	-2354.98386752	-2354.98386752	-2354.98386752	-2354.98386752	-2354.98386752
10	-2347.936146151	-2347.88792303	-2347.888792303	-2347.888792303	-2347.888792303	-2351.03701743	-2351.02377100	-2351.012377100	-2354.98655152	-2354.98655152	-2354.98655152	-2354.98655152	-2354.98655152	-2354.98655152	-2354.98655152
11	-2347.936145208	-2347.888567151	-2347.888567151	-2347.888567151	-2347.888567151	-2351.03701208	-2351.0121749978	-2351.0121749978	-2354.98652604	-2354.98652604	-2354.98652604	-2354.98652604	-2354.98652604	-2354.98652604	-2354.98652604
12	-2347.92030149	-2347.88455856	-2347.88455856	-2347.88455856	-2347.88455856	-2351.03994208	-2351.00993965	-2351.00993965	-2354.97645554	-2354.97645554	-2354.97645554	-2354.97645554	-2354.97645554	-2354.97645554	-2354.97645554
13	-2347.91542282	-2347.88434600	-2347.88434600	-2347.88434600	-2347.88434600	-2351.02853084	-2351.00991208	-2351.00991208	-2354.99211142	-2354.99211142	-2354.99211142	-2354.99211142	-2354.99211142	-2354.99211142	-2354.99211142
14	-2347.91515828	-2347.887184153	-2347.887184153	-2347.887184153	-2347.887184153	-2351.03540627	-2350.99216089	-2350.99216089	-2354.99474572	-2354.99474572	-2354.99474572	-2354.99474572	-2354.99474572	-2354.99474572	-2354.99474572
15	-2347.91323292	-2347.86948623	-2347.86948623	-2347.86948623	-2347.86948623	-2351.02192382	-2350.99557636	-2350.99557636	-2354.95478657	-2354.95478657	-2354.95478657	-2354.95478657	-2354.95478657	-2354.95478657	-2354.95478657
16	-2347.91323292	-2347.86927681	-2347.86927681	-2347.86927681	-2347.86927681	-2351.02190462	-2350.98944121	-2350.98944121	-2354.95442461	-2354.95442461	-2354.95442461	-2354.95442461	-2354.95442461	-2354.95442461	-2354.95442461
17	-2347.91189357	-2347.86926434	-2347.86926434	-2347.86926434	-2347.86926434	-2351.02184118	-2350.98931230	-2350.98931230	-2354.95442461	-2354.95442461	-2354.95442461	-2354.95442461	-2354.95442461	-2354.95442461	-2354.95442461
18	-2347.909303055	-2347.867748009	-2347.867748009	-2347.867748009	-2347.867748009	-2351.01704861	-2350.99544090	-2350.99544090	-2354.95573800	-2354.95573800	-2354.95573800	-2354.95573800	-2354.95573800	-2354.95573800	-2354.95573800
19	-2347.90929232	-2347.85621308	-2347.85621308	-2347.85621308	-2347.85621308	-2351.01702928	-2350.99176986	-2350.99176986	-2354.94171515	-2354.94171515	-2354.94171515	-2354.94171515	-2354.94171515	-2354.94171515	-2354.94171515
20	-2347.90842660	-2347.85454604	-2347.85454604	-2347.85454604	-2347.85454604	-2351.02850467	-2350.98726327	-2350.98726327	-2354.94258848	-2354.94258848	-2354.94258848	-2354.94258848	-2354.94258848	-2354.94258848	-2354.94258848
21	-2347.90682568	-2347.85367811	-2347.85367811	-2347.85367811	-2347.85367811	-2351.02890667	-2350.99235852	-2350.99235852	-2354.97564844	-2354.97564844	-2354.97564844	-2354.97564844	-2354.97564844	-2354.97564844	-2354.97564844
22	-2347.9019592	-2347.84903277	-2347.84903277	-2347.84903277	-2347.84903277	-2351.01250042	-2350.96262933	-2350.96262933	-2354.96227091	-2354.96227091	-2354.96227091	-2354.96227091	-2354.96227091	-2354.96227091	-2354.96227091
23	-2347.90032911	-2347.84902945	-2347.84902945	-2347.84902945	-2347.84902945	-2351.01241198	-2350.96262409	-2350.96262409	-2354.963632	-2354.963632	-2354.963632	-2354.963632	-2354.963632	-2354.963632	-2354.963632
24	-2347.90032516	-2347.84772966	-2347.84772966	-2347.84772966	-2347.84772966	-2351.01241198	-2350.95571189	-2350.95571189	-2354.93713841	-2354.93713841	-2354.93713841	-2354.93713841	-2354.93713841	-2354.93713841	-2354.93713841
25	-2347.88811829	-2347.82719098	-2347.82719098	-2347.82719098	-2347.82719098	-2350.9894377	-2350.96145315	-2350.96145315	-2354.93714724	-2354.93714724	-2354.93714724	-2354.93714724	-2354.93714724	-2354.93714724	-2354.93714724
26	-2347.88811829	-2347.82564935	-2347.82564935	-2347.82564935	-2347.82564935	-2350.9894377	-2350.96145315	-2350.96145315	-2354.93714724	-2354.93714724	-2354.93714724	-2354.93714724	-2354.93714724	-2354.93714724	-2354.93714724
27	-2347.88722173	-2347.82554500	-2347.82554500	-2347.82554500	-2347.82554500	-2350.99716929	-2350.95709381	-2350.95709381	-2354.95175022	-2354.95175022	-2354.95175022	-2354.95175022	-2354.95175022	-2354.95175022	-2354.95175022
28	-2347.88719086	-2347.82544294	-2347.82544294	-2347.82544294	-2347.82544294	-2350.99716929	-2350.95709381	-2350.95709381	-2354.95185163	-2354.95185163	-2354.95185163	-2354.95185163	-2354.95185163	-2354.95185163	-2354.95185163
29	-2347.88719086	-2347.82544294	-2347.82544294	-2347.82544294	-2347.82544294	-2350.99716929	-2350.95709381	-2350.95709381	-2354.93720214	-2354.93720214	-2354.93720214	-2354.93720214	-2354.93720214	-2354.93720214	-2354.93720214
30	-2347.88716334	-2347.81216389	-2347.81216389	-2347.81216389	-2347.81216389	-2350.98477155	-2350.95179448	-2350.95179448	-2354.93737472	-2354.93737472	-2354.93737472	-2354.93737472	-2354.93737472	-2354.93737472	-2354.93737472
31	-2347.88709185	-2347.81215644	-2347.81215644	-2347.81215644	-2347.81215644	-2351.00476664	-2350.98766631	-2350.98766631	-2354.93745725	-2354.93745725	-2354.93745725	-2354.93745725	-2354.93745725	-2354.93745725	-2354.93745725
32	-2347.87494119	-2347.80890757	-2347.80890757	-2347.80890757	-2347.80890757	-2351.00476664	-2350.98766631	-2350.98766631	-2354.93745725	-2354.93745725	-2354.93745725	-2354.93745725	-2354.93745725	-2354.93745725	-2354.93745725
33	-2347.86783003	-2347.80832631	-2347.80832631	-2347.80832631	-2347.80832631	-2350.99545006	-2350.94889763	-2350.94889763	-2354.93811749	-2354.93811749	-2354.93811749	-2354.93811749	-2354.93811749	-2354.93811749	-2354.93811749
34	-2347.86724768	-2347.80831623	-2347.80831623	-2347.80831623	-2347.80831623	-2350.99373334	-2350.94888715	-2350.94888715	-2354.93637501	-2354.93637501	-2354.93637501	-2354.93637501	-2354.93637501	-2354.93637501	-2354.93637501
35	-2347.86724664	-2347.80812841	-2347.80812841	-2347.80812841	-2347.80812841	-2350.99372917	-2350.94772455	-2350.94772455	-2354.93637534	-2354.93637534	-2354.93637534	-2354.93637534	-2354.93637534	-2354.93637534	-2354.93637534
36	-2347.7506879	-2347.7506879	-2347.7506879	-2347.7506879	-2347.7506879	-2350.91357829	-2350.90897638	-2350.90897638	-2354.94406755	-2354.94406755	-2354.94406755	-2354.94406755	-2354.94406755	-2354.94406755	-2354.94406755
37	-2347.7506879	-2347.7506879	-2347.7506879	-2347.7506879	-2347.7506879	-2350.90897638	-2350.90897638	-2350.90897638	-2354.9456174	-2354.9456174	-2354.9456174	-2354.9456174	-2354.9456174	-2354.9456174	-2354.9456174
38	-2347.7506879	-2347.7506879	-2347.7506879	-2347.7506879	-2347.7506879	-2350.90897638	-2350.90897638	-2350.90897638	-2354.945						

Table S60: Computed absolute energies with the TPBE0 method for the $\text{Fe}(o\text{-tol})_4^{2-}$ complex when using the (6,5) active space.

No.	tPBE0		
	Quintet	Triplet	Singlet
1	-2353.29898916	-2353.25140304	-2353.22038063
2	-2353.29882984	-2353.25138536	-2353.22115825
3	-2353.27694887	-2353.22093344	
4	-2353.27391092	-2353.22830594	-2353.21815290
5	-2353.27389514	-2353.22800363	-2353.21235162
6	-2353.22619039	-2353.19872202	
7	-2353.22617828	-2353.19870900	
8	-2353.22371915	-2353.19815609	
9	-2353.22124931	-2353.19974381	
10	-2353.22277152	-2353.19832331	
11	-2353.22275755	-2353.19150743	
12	-2353.21241703	-2353.19048336	
13	-2353.20103927	-2353.19046930	
14	-2353.21829500	-2353.17855292	
15	-2353.19439816	-2353.17529773	
16	-2353.19437710	-2353.17344618	
17	-2353.19379185	-2353.17343164	
18	-2353.19412889	-2353.17159449	
19	-2353.19412128	-2353.17033963	
20	-2353.20985673	-2353.17057787	
21	-2353.20844275	-2353.17577599	
22	-2353.19719216	-2353.15329819	
23	-2353.19278452	-2353.15329492	
24	-2353.19277394	-2353.15731169	
25	-2353.17488338	-2353.16505746	
26	-2353.17488938	-2353.13869841	
27	-2353.18062539	-2353.15734779	
28	-2353.18611188	-2353.15731158	
29	-2353.18571027	-2353.16187251	
30	-2353.17541194	-2353.15333716	
31	-2353.19847512	-2353.15334218	
32	-2353.18095488	-2353.15746095	
33	-2353.180954	-2353.15212380	
34	-2353.18962450	-2353.15211413	
35	-2353.18962578	-2353.15893586	
36		-2353.14681786	
37		-2353.14753932	
38		-2353.14624530	
39		-2353.14623648	
40		-2353.13970015	
41		-2353.13813577	
42		-2353.11932903	
43		-2353.11932855	
44		-2353.11806942	
45		-2353.10754224	

Table S61: Computed absolute energies with the SA-CASSCF, CASPT2, tPBE methods for the $\text{Fe}(\text{o-tol})_4^{2-}$ complex when using the (6,10) active space.

No.	SA-CASSCF			CASPT2			tPBE		
	Quintet	Triplet	Singlet	Quintet	Triplet	Singlet	Quintet	Triplet	Singlet
1	-2348.10912766	-2347.10262266	-2347.10435641	-2351.10478922	-2351.0102748922	-2351.02748922	-2354.96612698	-2354.96612698	-2354.96612698
2	-2348.10825581	-2348.03569149	-2348.0339409	-2351.04079355	-2351.00575541	-2351.02655347	-2354.99020049	-2354.99020049	-2354.99020049
3	-2348.08806310	-2348.03318459	-2348.038858868	-2351.07990060	-2351.03853959	-2351.00567862	-2355.00476724	-2354.98516656	-2354.98280474
4	-2348.08548914	-2348.076955120	-2348.07693095	-2351.07693095	-2351.02357990	-2351.00681547	-2355.00132518	-2354.95767957	-2354.95767957
5	-2348.08547534	-2348.01684165	-2348.01684112	-2351.07691458	-2351.02364021	-2351.00437299	-2355.00130966	-2354.95835714	-2354.95249795
6	-2348.01628045	-2347.67380100	-2347.67380100	-2351.02047457	-2350.99118000	-2350.96336168	-2354.93459065	-2354.93459065	-2354.93459065
7	-2348.01267719	-2347.9737179	-2347.9737179	-2350.99116388	-2350.99116388	-2350.99116388	-2354.93341842	-2354.93341842	-2354.93341842
8	-2348.01453079	-2347.97316401	-2347.97316401	-2350.99200959	-2350.99200959	-2350.99200959	-2354.95726933	-2354.95726933	-2354.95726933
9	-2348.01310690	-2347.97092348	-2347.97092348	-2350.991215041	-2350.98772167	-2350.98772167	-2354.95625248	-2354.95625248	-2354.95625248
10	-2348.01059569	-2347.97016206	-2347.97016206	-2350.9911531008	-2350.99143915	-2350.99143915	-2354.9604298	-2354.9604298	-2354.9604298
11	-2348.01058557	-2347.96676151	-2347.96676151	-2351.01355787	-2350.98532172	-2350.98532172	-2354.96038656	-2354.96038656	-2354.96038656
12	-2348.00028557	-2347.96533139	-2347.96533139	-2351.01216119	-2350.97985979	-2350.97985979	-2354.94721429	-2354.94721429	-2354.94721429
13	-2347.96531852	-2347.96531852	-2347.96531852	-2350.9824854	-2350.9824854	-2350.9824854	-2354.95940489	-2354.95940489	-2354.95940489
14	-2347.99405815	-2347.99405815	-2347.99405815	-2350.9975224	-2350.9975224	-2350.9975224	-2354.91527202	-2354.91527202	-2354.91527202
15	-2347.99170618	-2347.94999771	-2347.94999771	-2350.991517400	-2350.96576171	-2350.96576171	-2354.92842045	-2354.92842045	-2354.92842045
16	-2347.99169123	-2347.94908232	-2347.94908232	-2350.99150883	-2350.95854562	-2350.95854562	-2354.92839717	-2354.92839717	-2354.92839717
17	-2347.99087232	-2347.94906933	-2347.94906933	-2350.992676702	-2350.995852194	-2350.995852194	-2354.92710469	-2354.92710469	-2354.92710469
18	-2347.98853439	-2347.94780573	-2347.94780573	-2350.9947974	-2350.96644736	-2350.96644736	-2354.94868347	-2354.94868347	-2354.94868347
19	-2347.98804414	-2347.93849830	-2347.93849830	-2350.9824854	-2350.96059384	-2350.96059384	-2354.93744191	-2354.93744191	-2354.93744191
20	-2347.98803156	-2347.93648256	-2347.93648256	-2350.99080021	-2350.96096632	-2350.96096632	-2354.910202339	-2354.910202339	-2354.910202339
21	-2347.98674134	-2347.935566093	-2347.935566093	-2350.99797539	-2350.95408708	-2350.95408708	-2354.94816881	-2354.94816881	-2354.94816881
22	-2347.985162518	-2347.9285162518	-2347.9285162518	-2350.98682218	-2350.9532964	-2350.9532964	-2354.93532964	-2354.93532964	-2354.93532964
23	-2347.97957972	-2347.92852200	-2347.92852200	-2350.9862177	-2350.95023996	-2350.95023996	-2354.92987929	-2354.92987929	-2354.92987929
24	-2347.97957904	-2347.92646258	-2347.92646258	-2350.9861059	-2350.93091488	-2350.93091488	-2354.92986921	-2354.92986921	-2354.92986921
25	-2347.96663750	-2347.90973250	-2347.90973250	-2350.978767	-2350.93136717	-2350.93136717	-2354.90754310	-2354.90754310	-2354.90754310
26	-2347.96662854	-2347.90776491	-2347.90776491	-2350.97083241	-2350.92831851	-2350.92831851	-2354.92387873	-2354.92387873	-2354.92387873
27	-2347.96652806	-2347.90776109	-2347.90776109	-2350.97266380	-2350.92830222	-2350.92830222	-2354.92842932	-2354.92842932	-2354.92842932
28	-2347.90575206	-2347.90575206	-2347.90575206	-2350.96487178	-2350.947094	-2350.947094	-2354.91434383	-2354.91434383	-2354.91434383
29	-2347.9847.96612468	-2347.89749395	-2347.89749395	-2350.96487570	-2350.95536004	-2350.95536004	-2354.91440771	-2354.91440771	-2354.91440771
30	-2347.96510661	-2347.89635189	-2347.89635189	-2350.96196441	-2350.92317934	-2350.92317934	-2354.91215392	-2354.91215392	-2354.91215392
31	-2347.98834452	-2347.89634452	-2347.89634452	-2350.97943745	-2350.93217338	-2350.93217338	-2354.94278205	-2354.94278205	-2354.94278205
32	-2347.95797164	-2347.89277526	-2347.89277526	-2350.97610005	-2350.92017353	-2350.92017353	-2354.93872448	-2354.93872448	-2354.93872448
33	-2347.95109467	-2347.89255856	-2347.89255856	-2350.97069493	-2350.91910928	-2350.91910928	-2354.93532939	-2354.93532939	-2354.93532939
34	-2347.95044180	-2347.89254844	-2347.89254844	-2350.96227595	-2350.91996962	-2350.91996962	-2354.93430813	-2354.93430813	-2354.93430813
35	-2347.95044076	-2347.89229839	-2347.89229839	-2350.96927713	-2350.91963291	-2350.91963291	-2354.93430499	-2354.93430499	-2354.93430499
36	-2347.84682344	-2347.84260666	-2347.84260666	-2350.8817106	-2350.8817106	-2350.8817106	-2354.9009807	-2354.9009807	-2354.9009807
37	-2347.84181619	-2347.84181619	-2347.84181619	-2350.87984994	-2350.87984994	-2350.87984994	-2354.89828341	-2354.89828341	-2354.89828341
38	-2347.84181207	-2347.84181207	-2347.84181207	-2350.87984233	-2350.87984233	-2350.87984233	-2354.89826349	-2354.89826349	-2354.89826349
39	-2347.83621904	-2347.83451052	-2347.83451052	-2350.87114798	-2350.86952442	-2350.86952442	-2354.89360758	-2354.89360758	-2354.89360758
40	-2347.83451052	-2347.83451052	-2347.83451052	-2350.87114798	-2350.86952442	-2350.86952442	-2354.8926272	-2354.8926272	-2354.8926272
41	-2347.81364258	-2347.81364258	-2347.81364258	-2350.84285764	-2350.84285764	-2350.84285764	-2354.87240088	-2354.87240088	-2354.87240088
42	-2347.81363975	-2347.81298960	-2347.81298960	-2350.84285764	-2350.84285764	-2350.84285764	-2354.87240723	-2354.87240723	-2354.87240723
43	-2347.81298960	-2347.81298960	-2347.81298960	-2350.84285764	-2350.84285764	-2350.84285764	-2354.872447	-2354.872447	-2354.872447
44	-2347.74814740	-2347.74814740	-2347.74814740	-2350.80345469	-2350.80345469	-2350.80345469	-2354.87741740	-2354.87741740	-2354.87741740
45	-2347.74814740	-2347.74814740	-2347.74814740	-2350.80345469	-2350.80345469	-2350.80345469	-2354.87741740	-2354.87741740	-2354.87741740

Table S62: Computed absolute energies with the tPBE0 methods for the $\text{Fe}(o\text{-tol})_4^{2-}$ complex when using the (6,10) active space.

No.		Quintet	Singlet
	tPBE0	Triplet	
1	-2353.29797383	-2353.25159205	-2353.21830305
2	-2353.29697965	-2353.25157324	-2353.21947717
3	-2353.27559121	-2353.24717107	-2353.21925073
4	-2353.27236617	-2353.2286931	-2353.21541098
5	-2353.27235108	-2353.2287827	-2353.21100874
6	-2353.22659137	-2353.19439324	
7	-2353.22657929	-2353.19438300	
8	-2353.22158470	-2353.19336055	
9	-2353.22046609	-2353.19300001	
10	-2353.22295116	-2353.19407771	
11	-2353.22293631	-2353.18538938	
12	-2353.21048211	-2353.18640754	
13	-2353.21846484	-2353.18639505	
14	-2353.19878980	-2353.17443577	
15	-2353.19241488	-2353.17149826	
16	-2353.19422069	-2353.16847144	
17	-2353.19304660	-2353.16845446	
18	-2353.20864620	-2353.16671997	
19	-2353.19259179	-2353.16228119	
20	-2353.19258302	-2353.16725100	
21	-2353.20781194	-2353.16048278	
22	-2353.19691960	-2353.15207428	
23	-2353.19230440	-2353.15207177	
24	-2353.19229567	-2353.15396795	
25	-2353.18463458	-2353.15816545	
26	-2353.18456618	-2353.15221674	
27	-2353.18795401	-2353.15218589	
28	-2353.17729033	-2353.13881954	
29	-2353.17733695	-2353.15404186	
30	-2353.17539209	-2353.14585270	
31	-2353.19718173	-2353.14588716	
32	-2353.19352227	-2353.15218312	
33	-2353.18939071	-2353.14535668	
34	-2353.18834155	-2353.14531809	
35	-2353.18833893	-2353.15240487	
36		-2353.13046727	
37		-2353.13639272	
38		-2353.13416661	
39		-2353.13415439	
40		-2353.12926045	
41		-2353.12821976	
42		-2353.10906581	
43		-2353.10779075	
44		-2353.09509993	
45		-2353.09509993	

Table S63: Computed absolute energies with the SA-CASSCF, CASPT2, and tPBE methods for the $\text{Fe}(o\text{-tol})_4^{2-}$ complex when using the (12,8) active space.

No.	SA-CASSCF			CASPT2			tPBE		
	Quintet	Triplet	Singlet	Quintet	Triplet	Singlet	Quintet	Triplet	Singlet
1	-2348.02442758	-2347.94876515	-2347.90093870	-2351.01253360	-2351.01253326	-2355.04772168	-2354.960349233	-2354.960349135	
2	-2348.02426197	-2347.94858554	-2347.89933763	-2351.02456882	-2351.0539729	-2355.04711770	-2355.00038841	-2354.96128486	
3	-2348.00296218	-2347.94636401	-2347.89932728	-2351.10164171	-2351.04979523	-2355.02444172	-2354.99589671	-2354.96127222	
4	-2348.00058236	-2347.92904796	-2347.89856045	-2351.09894091	-2351.03741932	-2355.02162474	-2354.96970944	-2354.95916998	
5	-2348.00056662	-2347.92902634	-2347.89734986	-2351.09892238	-2351.03769871	-2355.02160823	-2354.96976223	-2354.95306336	
6		-2347.92761688		-2351.03451365		-2354.97477209			
7		-2347.92747146		-2351.03457091		-2354.97464972			
8		-2347.92643472		-2351.04042378		-2354.971641982			
9		-2347.92413877		-2351.03735526		-2354.96855532			
10		-2347.92255383		-2351.02752704		-2354.97111159			
11		-2347.92242771		-2351.02756182		-2354.97105278			
12		-2347.91092403		-2351.0280149		-2354.95957560			
13		-2347.90678182		-2351.02411400		-2354.97317674			
14		-2347.90443081		-2351.01344634		-2354.944560842			
15		-2347.90240683		-2351.01180324		-2354.9402169			

Table S64: Computed absolute energies with the tPBE0 method for the $\text{Fe}(o\text{-tol})_4^{2-}$ complex when using the (12,8) active space.

No.	tPBE0		
	Quintet	Triplet	Singlet
1	-2353.291189816	-2353.23756054	-2353.19552819
2	-2353.29140377	-2353.23743769	-2353.19579805
3	-2353.28407184	-2353.23351354	-2353.19578599
4	-2353.296636415	-2353.20954407	-2353.19401760
5	-2353.266634783	-2353.20857826	-2353.18913724
6		-2353.21298329	
7		-2353.21285516	
8		-2353.21034605	
9		-2353.20745118	
10		-2353.20897365	
11		-2353.20889651	
12		-2353.19741271	
13		-2353.20657801	
14		-2353.18448902	
15		-2353.18061873	

S77

6.3.7 $\text{Co}(o\text{-tol})_4^{2-}$ Complex

Table S65: Computed absolute energies with the SA-CASSCF, CASPT2, tPBE, and tPBE0 methods for the $\text{Co}(o\text{-tol})_4^{2-}$ complex when using the (7,5) active space.

No.	SA-CASSCF			CASPT2			tPBE			tPBE0	
	Quartet	Doublet	Quartet	Doublet	Quartet	Doublet	Quartet	Doublet	Quartet	Doublet	Doublet
1	-2468.56262326	-2468.47402236	-2471.71360371	-2471.64566201	-2475.69079818	-2475.63457075	-2473.90875445	-2473.84443365			
2	-2468.54051859	-2468.47391427	-2471.68537461	-2471.64554629	-2475.66471168	-2475.63502711	-2473.88366341	-2473.84474890			
3	-2468.53831308	-2468.47391324	-2471.68196849	-2471.64554537	-2475.66134710	-2475.63502464	-2473.88058860	-2473.84474679			
4	-2468.53831084	-2468.47255084	-2471.68188675	-2471.64438306	-2475.66134472	-2475.63670986	-2473.88058625	-2473.84567011			
5	-2468.52213244	-2468.47210560	-2471.66530975	-2471.64338936	-2475.63798240	-2475.63691679	-2473.85901991	-2473.84571399			
6	-2468.52213081	-2468.46551725	-2471.66530831	-2471.63297171	-2475.63798158	-2475.61281212	-2473.85901889	-2473.82598840			
7	-2468.52126247	-2468.45584247	-2471.66759212	-2471.62406941	-2475.63387378	-2475.60852255	-2473.85572095	-2473.82035253			
8	-2468.45789988	-2468.45466767	-2471.62509357	-2471.62256626	-2475.63375250	-2475.60656015	-2473.83978935	-2473.81858703			
9	-2468.45690696	-2468.45466612	-2471.62138339	-2471.62256461	-2475.62425467	-2475.60655734	-2473.83241774	-2473.81858454			
10	-2468.45690516	-2468.44325697	-2471.62138346	-2471.61803320	-2475.62425145	-2475.61085572	-2473.83241488	-2473.81895603			
11	-2468.44235150		-2471.61067311		-2475.60932289		-2473.81758004				
12	-2468.44233008		-2471.61507640		-2475.60651116		-2473.81546589				
13	-2468.44232844		-2471.61505966		-2475.60647800		-2473.81544061				
14	-2468.44013677		-2471.60840495		-2475.59958172		-2473.80972048				
15	-2468.44013486		-2471.60840141		-2475.59958274		-2473.80972077				
16	-2468.43698920		-2471.60817984		-2475.60372684		-2473.81204243				
17	-2468.43393888		-2471.60364523		-2475.59961667		-2473.80819722				
18	-2468.42425883		-2471.59301711		-2475.59093651		-2473.79926709				
19	-2468.42384258		-2471.58968376		-2475.59022024		-2473.79862583				
20	-2468.42384133		-2471.58968317		-2475.59021861		-2473.79862429				
21	-2468.41907902		-2471.57951989		-2475.57723816		-2473.78769838				
22	-2468.41907715		-2471.57951527		-2475.57723451		-2473.78769517				
23	-2468.41684565		-2471.57425556		-2475.57555052		-2473.78587430				
24	-2468.41047107		-2471.56968634		-2475.57156605		-2473.78129231				
25	-2468.41046906		-2471.56968071		-2475.57156395		-2473.78129023				
26	-2468.41001993		-2471.56661388		-2475.56949177		-2473.77962381				
27	-2468.39725966		-2471.54285412		-2475.55794871		-2473.76777645				
28	-2468.39657587		-2471.54310758		-2475.55889804		-2473.76831750				
29	-2468.36584018		-2471.55584611		-2475.60621304		-2473.79611983				
30	-2468.35892149		-2471.54898571		-2475.60073910		-2473.79028470				

Table S66: Computed absolute energies with the SA-CASSCF, CASPT2, tPBE, and tPBE0 methods for the Co(*o*-tol)₄²⁻ complex when using the (7,10) active space.

No.	SA-CASSCF			CASPT2			tPBE			tPBE0		
	Quartet	Doublet	Quartet	Doublet	Quartet	Doublet	Quartet	Doublet	Quartet	Doublet	Quartet	Doublet
1	-2468.66666100	-2468.58054343	-2471.67482143	-2471.60307962	-2475.65166696	-2475.59269212	-2473.90541547	-2473.83965495	-2473.83958767	-2473.83958561	-2473.87742666	-2473.83958767
2	-2468.64408672	-2468.58045498	-2471.64798802	-2471.60331247	-2475.62626140	-2475.59263190	-2473.88071773	-2473.83958767	-2473.83958767	-2473.83958767	-2473.87742436	-2473.84001133
3	-2468.64143606	-2468.58045381	-2471.64503546	-2471.60331097	-2475.62275686	-2475.59262954	-2473.87742666	-2473.83958561	-2473.83958767	-2473.83958767	-2475.59337120	-2473.83966511
4	-2468.64143417	-2468.577896513	-2471.64503298	-2471.60065227	-2475.62275442	-2475.59369340	-2473.87742436	-2473.84001133	-2473.83958767	-2473.83958767	-2475.60104922	-2473.83966511
5	-2468.62519345	-2468.577854685	-2471.62739605	-2471.60000115	-2475.60104922	-2475.59337120	-2473.85708528	-2473.83966511	-2473.83958767	-2473.83958767	-2475.60104840	-2473.85708425
6	-2468.62519181	-2468.57013092	-2471.62739408	-2471.60104840	-2475.60892551	-2475.58892551	-2473.85708425	-2473.81829844	-2473.81829844	-2473.81829844	-2475.56768761	-2473.81829844
7	-2468.62432154	-2468.56119514	-2471.62843988	-2471.58118456	-2475.59674594	-2475.56484023	-2473.85363984	-2473.81392896	-2473.81392896	-2473.81392896	-2475.59507098	-2473.83855588
8	-2468.56901058	-2468.55990717	-2471.58767475	-2471.58011779	-2475.56371263	-2475.56371263	-2473.81276127	-2473.81276127	-2473.81276127	-2473.81276127	-2471.58612922	-2473.56370979
9	-2468.56830710	-2468.55990542	-2471.58612922	-2471.58011519	-2475.58587080	-2475.56370979	-2473.83147988	-2473.81275870	-2473.81275870	-2473.81275870	-2471.57354731	-2473.83147718
10	-2468.56830528	-2468.55122311	-2471.58612759	-2471.57354731	-2475.58586781	-2475.56392571	-2473.81075006	-2473.81075006	-2473.81075006	-2473.81075006	-2471.57145681	-2473.80853279
11												
12												
13												
14												
15												
16												
17												
18												
19												
20												
21												
22												
23												
24												
25												
26												
27												
28												
29												
30												

Table S67: Computed absolute energies with the SA-CASSCF, CASPT2, tPBE, and tPBE0 methods for the Co(*o*-tol)₄²⁻ complex when using the (13,8) active space.

No.	SA-CASSCF			CASPT2			tPBE			tPBE0		
	Quartet	Doublet	Quartet	Doublet	Quartet	Doublet	Quartet	Doublet	Quartet	Doublet	Quartet	Doublet
1	-2468.55751725	-2468.46904796	-2471.70967325	-2471.63697336	-2475.68566875	-2475.62592414	-2473.90363088	-2473.83670510	-2473.83728803	-2473.83728384	-2473.83728384	-2473.83728384
2	-2468.53425377	-2468.46892791	-2471.68247826	-2471.63671599	-2475.65890224	-2475.62674140	-2473.87774012	-2473.83728803	-2473.83728384	-2473.83728384	-2473.83728384	-2473.83728384
3	-2468.53210897	-2468.46892675	-2471.67944689	-2471.63671478	-2475.65551879	-2475.62673620	-2473.87466634	-2473.83728384	-2473.83728384	-2473.83728384	-2473.83728384	-2473.83728384
4	-2468.53210650	-2468.46760597	-2471.67944659	-2471.63376746	-2475.65551651	-2475.62568806	-2473.87466401	-2473.83616754	-2473.83616754	-2473.83616754	-2473.83616754	-2473.83616754
5	-2468.51502581	-2468.46735842	-2471.66369790	-2471.63292470	-2475.63147229	-2475.62601854	-2473.85236067	-2473.83635351	-2473.83635351	-2473.83635351	-2473.83635351	-2473.83635351
6	-2468.51502421	-2468.45969136	-2471.66369850	-2471.62589300	-2475.63147222	-2475.60460290	-2473.85236022	-2473.81837502	-2473.81837502	-2473.81837502	-2473.81837502	-2473.81837502
7	-2468.51426418	-2468.44987086	-2471.66552148	-2471.6148436	-2475.62775157	-2475.59709347	-2473.84937972	-2473.81028782	-2473.81028782	-2473.81028782	-2473.81028782	-2473.81028782
8	-2468.45193387	-2468.44880409	-2471.62592674	-2471.61313638	-2475.63168217	-2475.59576490	-2473.83674510	-2473.80902470	-2473.80902470	-2473.80902470	-2473.80902470	-2473.80902470
9	-2468.45099604	-2468.44880247	-2471.62278751	-2471.61313516	-2475.62234631	-2475.59576329	-2473.82950874	-2473.80902309	-2473.80902309	-2473.80902309	-2473.80902309	-2473.80902309
10	-2468.45099393	-2468.43804573	-2471.62278457	-2471.61010739	-2475.62234225	-2475.60139490	-2473.82950517	-2473.81055761	-2473.81055761	-2473.81055761	-2473.81055761	-2473.81055761
11	-2468.43711647	-2471.60800710	-2471.60800710	-2471.60800710	-2475.59876979	-2475.59876979	-2473.80835646	-2473.80835646	-2473.80835646	-2473.80835646	-2473.80835646	-2473.80835646
12	-2468.43711505	-2471.60800472	-2471.60800472	-2471.60800472	-2475.59876843	-2475.60040197	-2473.80939766	-2473.80939766	-2473.80939766	-2473.80939766	-2473.80939766	-2473.80939766
13	-2468.43638473	-2471.60314528	-2471.60314528	-2471.60314528	-2475.59429889	-2475.59429889	-2473.80434516	-2473.80434516	-2473.80434516	-2473.80434516	-2473.80434516	-2473.80434516
14	-2468.43448395	-2471.60119257	-2471.60119257	-2471.60119257	-2475.59429780	-2475.59429780	-2473.80434379	-2473.80434379	-2473.80434379	-2473.80434379	-2473.80434379	-2473.80434379
15	-2468.43448175	-2471.60118954	-2471.60118954	-2471.60118954	-2475.59743668	-2475.59743668	-2473.80584319	-2473.80584319	-2473.80584319	-2473.80584319	-2473.80584319	-2473.80584319
16	-2468.43106273	-2471.60357261	-2471.60357261	-2471.60357261	-2475.59419373	-2475.59419373	-2473.80276241	-2473.80276241	-2473.80276241	-2473.80276241	-2473.80276241	-2473.80276241
17	-2468.42846846	-2471.59981639	-2471.59981639	-2471.59981639	-2475.58056321	-2475.58056321	-2473.78977936	-2473.78977936	-2473.78977936	-2473.78977936	-2473.78977936	-2473.78977936
18	-2468.41742781	-2471.58483145	-2471.58483145	-2471.58483145	-2475.58077024	-2475.58077024	-2473.78986170	-2473.78986170	-2473.78986170	-2473.78986170	-2473.78986170	-2473.78986170
19	-2468.41713607	-2471.58264495	-2471.58264495	-2471.58264495	-2475.58076837	-2475.58076837	-2473.78986002	-2473.78986002	-2473.78986002	-2473.78986002	-2473.78986002	-2473.78986002
20	-2468.41713495	-2471.58264581	-2471.58264581	-2471.58264581	-2475.56710242	-2475.56710242	-2473.77831899	-2473.77831899	-2473.77831899	-2473.77831899	-2473.77831899	-2473.77831899
21	-2468.41196871	-2471.57270279	-2471.57270279	-2471.57270279	-2475.5670938	-2475.5670938	-2473.77731623	-2473.77731623	-2473.77731623	-2473.77731623	-2473.77731623	-2473.77731623
22	-2468.41196677	-2471.57269894	-2471.57269894	-2471.57269894	-2475.56729911	-2475.56729911	-2473.777801149	-2473.777801149	-2473.777801149	-2473.777801149	-2473.777801149	-2473.777801149
23	-2468.41014861	-2471.56904745	-2471.56904745	-2471.56904745	-2475.55941569	-2475.55941569	-2473.77043138	-2473.77043138	-2473.77043138	-2473.77043138	-2473.77043138	-2473.77043138
24	-2468.40347844	-2471.56058924	-2471.56058924	-2471.56058924	-2475.55941359	-2475.55941359	-2473.77492926	-2473.77492926	-2473.77492926	-2473.77492926	-2473.77492926	-2473.77492926
25	-2468.40347626	-2471.56058591	-2471.56058591	-2471.56058591	-2475.55714718	-2475.55714718	-2473.76855635	-2473.76855635	-2473.76855635	-2473.76855635	-2473.76855635	-2473.76855635
26	-2468.40278385	-2471.55793327	-2471.55793327	-2471.55793327	-2475.54677209	-2475.54677209	-2473.75738510	-2473.75738510	-2473.75738510	-2473.75738510	-2473.75738510	-2473.75738510
27	-2468.38922413	-2471.53597819	-2471.53597819	-2471.53597819	-2475.53607844	-2475.53607844	-2473.75819687	-2473.75819687	-2473.75819687	-2473.75819687	-2473.75819687	-2473.75819687
28	-2468.388887906	-2471.53607844	-2471.53607844	-2471.53607844	-2475.60440307	-2475.60440307	-2473.79345453	-2473.79345453	-2473.79345453	-2473.79345453	-2473.79345453	-2473.79345453
29	-2468.36060890	-2471.55638561	-2471.55638561	-2471.55638561	-2475.59583673	-2475.59583673	-2473.78509818	-2473.78509818	-2473.78509818	-2473.78509818	-2473.78509818	-2473.78509818
30	-2468.35288251	-2471.54680562	-2471.54680562	-2471.54680562	-2475.59583673	-2475.59583673	-2473.78509818	-2473.78509818	-2473.78509818	-2473.78509818	-2473.78509818	-2473.78509818

6.3.8 Ni(*o*-tol)₄²⁻ Complex

Table S68: Computed absolute energies with the SA-CASSCF, CASPT2, tPBE, and tPBE0 methods for the Ni(*o*-tol)₄²⁻ complex when using the (8,5) active space.

No.	SA-CASSCF			CASPT2			tPBE			tPBE0		
	Triplet	Singlet	Triplet	Singlet	Triplet	Singlet	Triplet	Singlet	Triplet	Singlet	Triplet	Singlet
1	-2595.76033140	-2595.68877214	-2599.02367277	-2598.98059564	-2602.97978466	-2602.95733332	-2601.17492135	-2601.14019303				
2	-2595.74316715	-2595.68263265	-2599.00160181	-2598.97629425	-2602.95234049	-2602.95776257	-2601.15004716	-2601.13898009				
3	-2595.74134021	-2595.66965270	-2598.99866603	-2598.95455724	-2602.95040052	-2602.93256768	-2601.14813544	-2601.11683894				
4	-2595.73826874	-2595.66814464	-2598.99096893	-2598.95077512	-2602.95159208	-2602.92744486	-2601.14826125	-2601.11261981				
5	-2595.72745154	-2595.66509729	-2598.98112618	-2598.94731638	-2602.92983432	-2602.92279259	-2601.12923863	-2601.10836877				
6	-2595.72197656	-2595.63916711	-2598.97056683	-2598.93358443	-2602.92508859	-2602.93584797	-2601.12431058	-2601.11167776				
7	-2595.71098145	-2595.63793053	-2598.95337036	-2598.91921761	-2602.91681911	-2602.89762385	-2601.11535970	-2601.08270052				
8	-2595.65752537	-2595.63565910	-2598.93337581	-2598.92116352	-2602.91888009	-2602.92232451	-2601.10354141	-2601.10065816				
9	-2595.65067430	-2595.62654440	-2598.92305910	-2598.90782497	-2602.90665654	-2602.90419862	-2601.09266098	-2601.08478507				
10	-2595.64482478	-2595.62242957	-2598.91616210	-2598.89787957	-2602.90054617	-2602.89327944	-2601.08661582	-2601.07556697				
11		-2595.62005718		-2598.89403905		-2602.89945692		-2601.07960699				
12		-2595.61347417		-2598.88293123		-2602.87159096		-2601.05706176				
13		-2595.61230244		-2598.87565359		-2602.88181098		-2601.06443385				
14		-2595.60972021		-2598.87477715		-2602.87352644		-2601.05757488				
15		-2595.46862630		-2598.78038437		-2602.89691993		-2601.03984652				

Table S69: Computed absolute energies with the SA-CASSCF, CASPT2, tPBE, and tPBE0 methods for the Mo(*o*-tol)₄ complex when using the (8,10) active space.

No.	SA-CASSCF			CASPT2			tPBE			tPBE0		
	Triplet	Singlet	Triplet	Singlet	Triplet	Singlet	Triplet	Singlet	Triplet	Singlet	Singlet	
1	-2595.89600988	-2595.82652930	-2598.97049546	-2598.91884518	-2602.92631720	-2602.89538458	-2601.16874037	-2601.12817076				
2	-2595.87808818	-2595.82003747	-2598.94883375	-2598.91218972	-2602.89995966	-2602.89491720	-2601.14449179	-2601.12619727				
3	-2595.87606487	-2595.80586844	-2598.94621507	-2598.89289727	-2602.89800858	-2602.87091669	-2601.14252265	-2601.10465463				
4	-2595.87287003	-2595.80357821	-2598.94095768	-2598.88948982	-2602.90000451	-2602.86590428	-2601.14322089	-2601.10032276				
5	-2595.86181906	-2595.80068879	-2598.92947920	-2598.88686996	-2602.87977230	-2602.85924907	-2601.12528399	-2601.09460900				
6	-2595.85578315	-2595.77767406	-2598.92094163	-2598.86990430	-2602.87498223	-2602.87076644	-2601.12018246	-2601.09749335				
7	-2595.84455842	-2595.77542530	-2598.90681786	-2598.86193106	-2602.86775656	-2602.83629191	-2601.11195703	-2601.07107526				
8	-2595.79724932	-2595.77304318	-2598.88042606	-2598.8599933	-2602.86597769	-2602.85699639	-2601.09879560	-2601.08600809				
9	-2595.79027629	-2595.76380882	-2598.87225017	-2598.84832467	-2602.85420564	-2602.83522017	-2601.08822330	-2601.06736733				
10	-2595.78465972	-2595.75919626	-2598.86623155	-2598.84071251	-2602.84865862	-2602.83273622	-2601.08265890	-2601.06435123				
11		-2595.75697219	-2598.83885518	-2598.83951938	-2602.83951938	-2601.06888258	-2601.06888258	-2601.06888258				
12		-2595.75031989	-2598.82958110	-2598.82958110	-2602.81234214	-2601.04683658	-2601.04683658	-2601.04683658				
13		-2595.74828482	-2598.82381850	-2598.82381850	-2602.82305169	-2601.05435997	-2601.05435997	-2601.05435997				
14		-2595.74617420	-2598.82301541	-2598.82301541	-2602.81668776	-2601.04905937	-2601.04905937	-2601.04905937				
15		-2595.61389358	-2598.71824169	-2598.71824169	-2602.81086450	-2601.01162177	-2601.01162177	-2601.01162177				

Table S70: Computed absolute energies with the SA-CASSCF, CASPT2, tPBE, and tPBE0 methods for the $\text{Ni}(o\text{-tol})_4^{2-}$ complex when using the (14,8) active space.

No.	SA-CASSCF			CASPT2			tPBE			tPBE0		
	Triplet	Singlet	Triplet	Singlet	Triplet	Singlet	Triplet	Singlet	Triplet	Singlet	Triplet	Singlet
1	-2595.75780754	-2595.68861858	-2599.01920810	-2598.96896509	-2602.97578376	-2602.94835579	-2601.17128971	-2601.13342149				
2	-2595.73944556	-2595.68289068	-2598.99778005	-2598.96165820	-2602.94866124	-2602.94707790	-2601.14635732	-2601.13103110				
3	-2595.73766442	-2595.66897606	-2598.99491082	-2598.94324578	-2602.94691353	-2602.92322494	-2601.14460125	-2601.10966272				
4	-2595.73436303	-2595.66737109	-2598.98738698	-2598.94019848	-2602.94709689	-2602.91875718	-2601.14391343	-2601.10591066				
5	-2595.72318636	-2595.66423019	-2598.97853411	-2598.93907274	-2602.92489803	-2602.91552543	-2601.12447011	-2601.10270162				
6	-2595.71740434	-2595.63850817	-2598.96819010	-2598.92492907	-2602.91989709	-2602.92919940	-2601.11927390	-2601.10652659				
7	-2595.70610832	-2595.63667373	-2598.95102674	-2598.91394955	-2602.91217855	-2602.89180493	-2601.11066099	-2601.07802113				
8	-2595.65409733	-2595.63449181	-2598.93554905	-2598.91360200	-2602.91904054	-2602.91554587	-2601.10280474	-2601.09528236				
9	-2595.64708899	-2595.62531173	-2598.92449798	-2598.90088971	-2602.90598667	-2602.89740306	-2601.09126225	-2601.07938023				
10	-2595.64128670	-2595.62109493	-2598.91804869	-2598.89244066	-2602.90024710	-2602.88758565	-2601.08550700	-2601.07096297				
11		-2595.61871086	-2598.88805118	-2598.88805118	-2602.89337370	-2602.89337370	-2601.07470799	-2601.07470799				
12		-2595.61205859	-2598.87785730	-2598.87785730	-2602.86641422	-2602.86641422	-2601.05282531	-2601.05282531				
13		-2595.61100275	-2598.87022817	-2598.87022817	-2602.87554146	-2602.87554146	-2601.05940678	-2601.05940678				
14		-2595.60838224	-2598.86925015	-2598.86925015	-2602.86790315	-2602.86790315	-2601.05302292	-2601.05302292				
15		-2595.47219768	-2598.80075314	-2598.80075314	-2602.90004484	-2602.90004484	-2601.04308305	-2601.04308305				

7 Geometrical Distortions Following Lower Energetic Vibrational Modes

Using the geometry optimized structures with DFT, we selected two vibrational modes of $\text{Ti}(o\text{-tol})_4^{2-}$, $\text{V}(o\text{-tol})_4^-$, and $\text{Cr}(o\text{-tol})_4$ complexes related to the symmetric stretching of the metal-aryl bonds, and the aryl-metal-aryl scissoring modes (See Figure S23). Following the normal modes, we selected eight structures for which we computed the triplet ground state T_0 , the first singlet and triplet excited states S_1 and T_1 , and associated energy gaps: $\Delta E_{T_0-S_1}$, $\Delta E_{T_0-T_1}$, and $\Delta E_{S_1-T_1}$. The energy differences are reported in Tables S71-S76. Additionally, the relative energies for the lowest-lying triplet and singlet excited states and the triplet ground state are shown in Figures S24-S29.

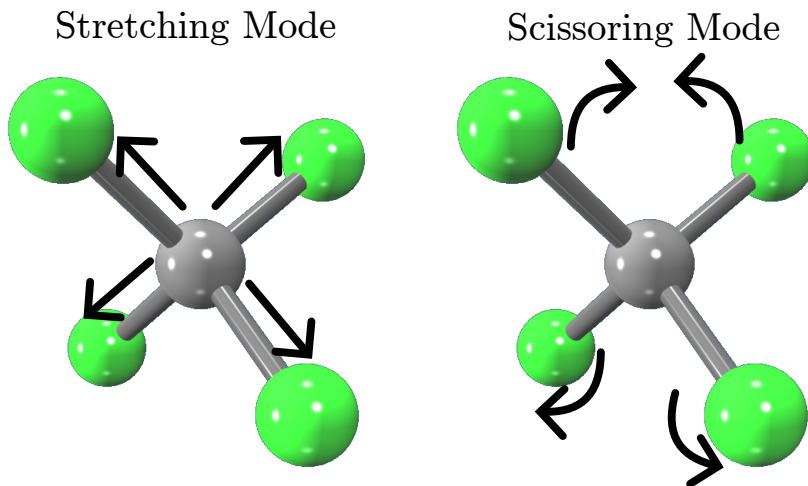


Figure S23: Schemes for the stretching and scissoring modes between the metal center and the *o*-tolyl ligands considered for the geometrical distortions of $\text{Cr}(o\text{-tol})_4$, $\text{V}(o\text{-tol})_4^-$, $\text{Ti}(o\text{-tol})_4^{2-}$ complexes.

Table S71: Energy differences in eV between ground state T_0 and first excited state S_1 , between the two triplet excited states T_0-T_1 , and between the singlet and triplet excited states S_1-T_1 of $\text{Cr}(o\text{-tol})_4$ complex for the Cr–C symmetric stretching. The equilibrium bond distance is $d = 1.98 \text{ \AA}$.

$\Delta d (\text{\AA})$	$\Delta E_{T_0-S_1}$		$\Delta E_{T_0-T_1}$		$\Delta E_{S_1-T_1}$	
	CASPT2	tPBE0	CASPT2	tPBE0	CASPT2	tPBE0
0.077	1.52	1.29	2.00	2.06	0.48	0.76
0.058	1.50	1.28	2.03	2.08	0.52	0.80
0.039	1.49	1.27	2.06	2.11	0.57	0.85
0.019	1.47	1.25	2.09	2.14	0.62	0.89
0.000	1.46	1.24	2.13	2.17	0.67	0.93
-0.019	1.44	1.22	2.16	2.20	0.72	0.97
-0.039	1.43	1.21	2.19	2.23	0.77	1.02
-0.058	1.41	1.20	2.23	2.26	0.82	1.06
-0.077	1.39	1.18	2.26	2.29	0.87	1.11

Table S72: Energy differences in eV between ground state T_0 and first excited state S_1 , between the two triplet excited states T_0-T_1 , and between the singlet and triplet excited states S_1-T_1 of $\text{Cr}(o\text{-tol})_4$ complex for the C–Cr–C scissoring mode. The equilibrium bond angle is $\theta = 104.9^\circ$.

$\Delta\theta (\text{ }^\circ)$	$\Delta E_{T_0-S_1}$		$\Delta E_{T_0-T_1}$		$\Delta E_{S_1-T_1}$	
	CASPT2	tPBE0	CASPT2	tPBE0	CASPT2	tPBE0
-6.569	1.44	1.24	2.06	2.19	0.62	0.95
-4.922	1.45	1.24	2.13	2.18	0.69	0.94
-3.277	1.45	1.24	2.13	2.17	0.68	0.94
-1.636	1.45	1.24	2.13	2.17	0.67	0.93
0.000	1.46	1.24	2.13	2.17	0.67	0.93
1.634	1.45	1.24	2.13	2.17	0.67	0.93
3.261	1.45	1.24	2.13	2.17	0.68	0.94
4.882	1.45	1.24	2.13	2.18	0.69	0.94
6.497	1.44	1.24	2.06	2.19	0.62	0.95

Table S73: Energy differences in eV between ground state T_0 and first excited state S_1 , between the two triplet excited states T_0-T_1 , and between the singlet and triplet excited states S_1-T_1 of $V(o\text{-tol})_4^-$ complex for the V–C symmetric stretching. The equilibrium bond distance is $d = 2.07 \text{ \AA}$.

$\Delta d (\text{\AA})$	$\Delta E_{T_0-S_1}$		$\Delta E_{T_0-T_1}$		$\Delta E_{S_1-T_1}$	
	CASPT2	tPBE0	CASPT2	tPBE0	CASPT2	tPBE0
-0.098	1.09	0.78	1.49	1.45	0.40	0.67
-0.074	1.11	0.80	1.44	1.40	0.32	0.60
-0.049	1.14	0.82	1.39	1.35	0.25	0.53
-0.025	1.16	0.84	1.34	1.30	0.18	0.46
0.000	1.17	0.85	1.29	1.25	0.11	0.40
0.025	1.19	0.87	1.24	1.21	0.05	0.34
0.049	1.21	0.88	1.20	1.17	-0.01	0.28
0.074	1.22	0.90	1.16	1.13	-0.07	0.23
0.099	1.24	0.91	1.12	1.09	-0.12	0.17

Table S74: Energy differences in eV between ground state T_0 and first excited state S_1 , between the two triplet excited states T_0-T_1 , and between the singlet and triplet excited states S_1-T_1 of $V(o\text{-tol})_4^-$ complex for the C–V–C scissoring mode. The equilibrium bond angle is $\theta = 105.2^\circ$.

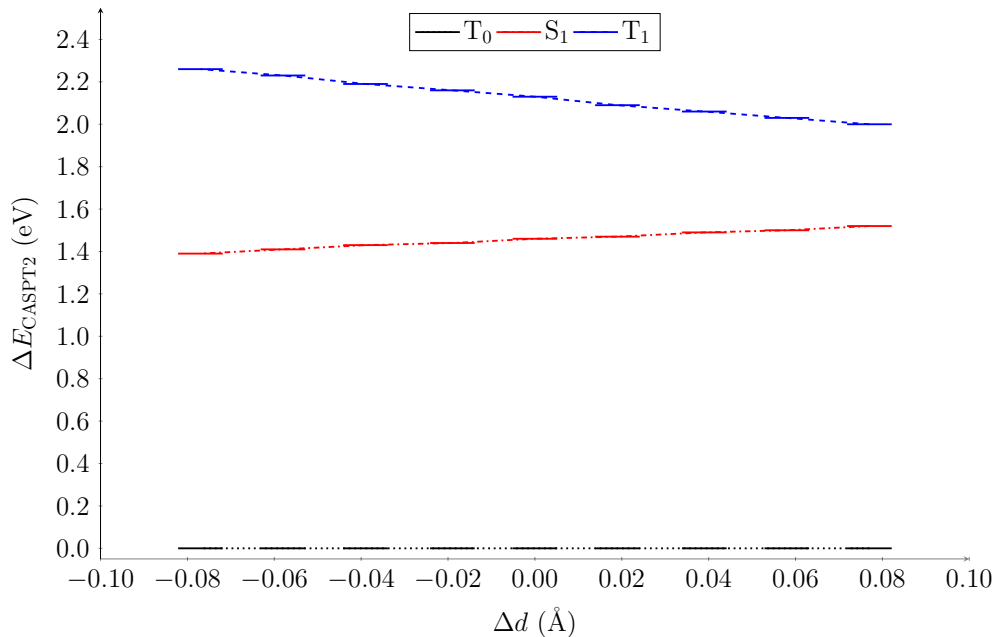
$\Delta\theta (\text{ }^\circ)$	$\Delta E_{T_0-S_1}$		$\Delta E_{T_0-T_1}$		$\Delta E_{S_1-T_1}$	
	CASPT2	tPBE0	CASPT2	tPBE0	CASPT2	tPBE0
6.022	1.22	0.87	1.24	1.22	0.02	0.35
4.523	1.21	0.86	1.29	1.27	0.09	0.41
3.019	1.20	0.86	1.34	1.32	0.15	0.46
1.512	1.19	0.86	1.36	1.32	0.18	0.46
0.000	1.18	0.85	1.29	1.25	0.11	0.40
-1.512	1.19	0.86	1.36	1.32	0.18	0.46
-3.019	1.20	0.86	1.34	1.32	0.15	0.46
-4.523	1.21	0.86	1.29	1.27	0.09	0.41
-6.022	1.22	0.87	1.24	1.22	0.02	0.35

Table S75: Energy differences in eV between ground state T_0 and first excited state S_1 , between the two triplet excited states T_0-T_1 , and between the singlet and triplet excited states S_1-T_1 of $\text{Ti}(o\text{-tol})_4^{2-}$ complex for the Ti–C symmetric stretching. The equilibrium bond distance is $d = 2.16 \text{ \AA}$.

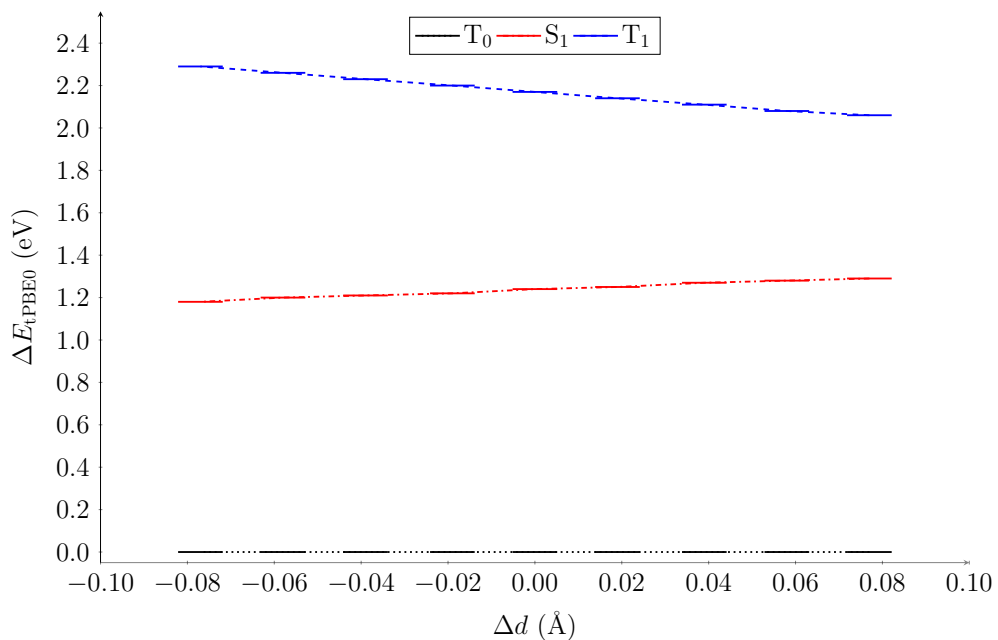
$\Delta d (\text{\AA})$	$\Delta E_{T_0-S_1}$		$\Delta E_{T_0-T_1}$		$\Delta E_{S_1-T_1}$	
	CASPT2	tPBE0	CASPT2	tPBE0	CASPT2	tPBE0
0.077	0.74	0.65	0.64	0.64	-0.10	-0.01
0.058	0.70	0.62	0.63	0.63	-0.07	0.01
0.039	0.65	0.60	0.62	0.63	-0.03	0.03
0.019	0.61	0.57	0.62	0.64	0.01	0.06
0.000	0.56	0.55	0.61	0.64	0.05	0.09
-0.019	0.52	0.52	0.61	0.65	0.09	0.13
-0.039	0.47	0.50	0.62	0.66	0.14	0.16
-0.058	0.43	0.47	0.63	0.68	0.20	0.21
-0.077	0.39	0.45	0.65	0.70	0.26	0.26

Table S76: Energy differences in eV between ground state T_0 and first excited state S_1 , between the two triplet excited states T_0-T_1 , and between the singlet and triplet excited states S_1-T_1 of $\text{Ti}(o\text{-tol})_4^{2-}$ complex for the C–Ti–C scissoring mode. The equilibrium bond angle is $\theta = 106.0^\circ$.

$\Delta\theta (\text{ }^\circ)$	$\Delta E_{T_0-S_1}$		$\Delta E_{T_0-T_1}$		$\Delta E_{S_1-T_1}$	
	CASPT2	tPBE0	CASPT2	tPBE0	CASPT2	tPBE0
7.000	0.56	0.55	0.61	0.63	0.05	0.09
5.000	0.56	0.55	0.61	0.64	0.05	0.09
2.277	0.56	0.55	0.61	0.64	0.05	0.09
1.708	0.56	0.55	0.61	0.64	0.05	0.09
1.139	0.56	0.55	0.61	0.64	0.05	0.09
0.570	0.56	0.55	0.61	0.64	0.05	0.09
0.000	0.56	0.55	0.61	0.64	0.05	0.09
-0.569	0.56	0.55	0.61	0.64	0.05	0.09
-1.140	0.56	0.55	0.61	0.64	0.05	0.09
-1.710	0.56	0.55	0.61	0.64	0.05	0.09
-2.281	0.56	0.55	0.61	0.64	0.05	0.09
-5.000	0.56	0.55	0.61	0.64	0.05	0.09
-7.000	0.56	0.55	0.61	0.63	0.05	0.09

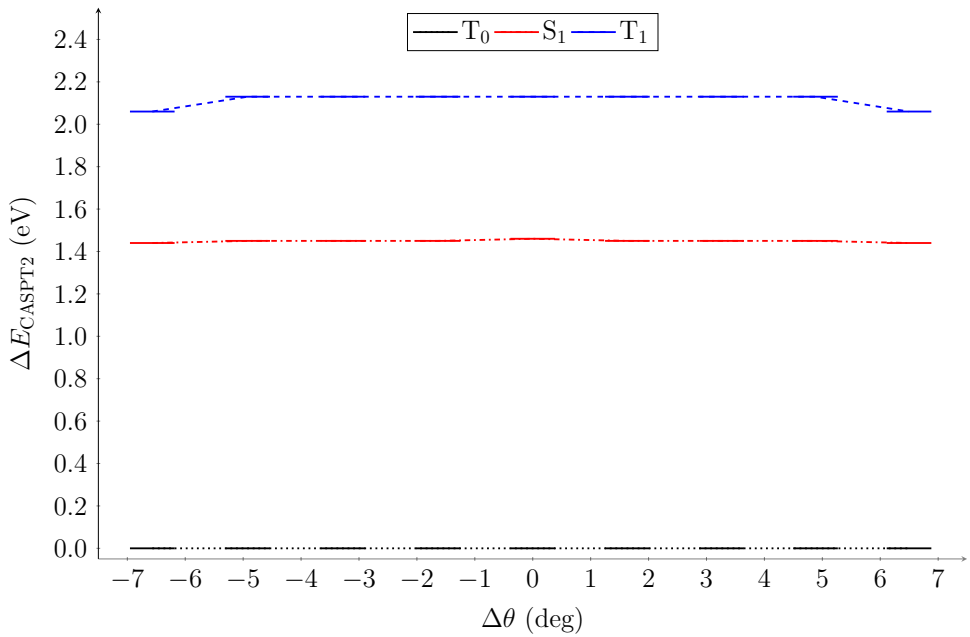


(a) CASPT2 Relative energies

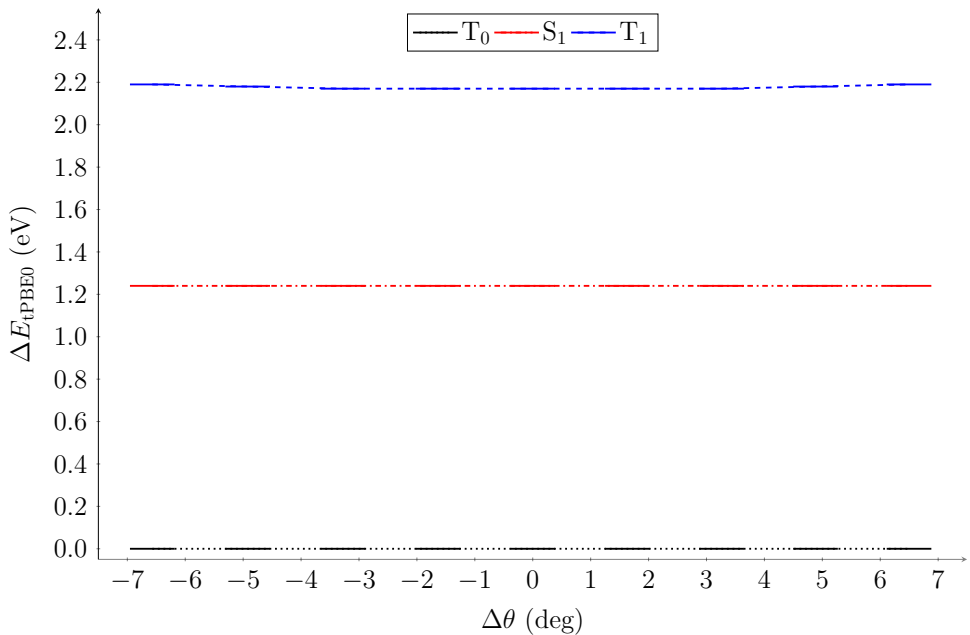


(b) tPBE0 Relative energies

Figure S24: (a) CASPT2 and (b) tPBE0 Relative energies for the lowest-lying three states of Cr(*o*-tol)₄ complex for the Cr–C symmetric stretching normal mode. The equilibrium bond distance is $d = 1.98$ Å.

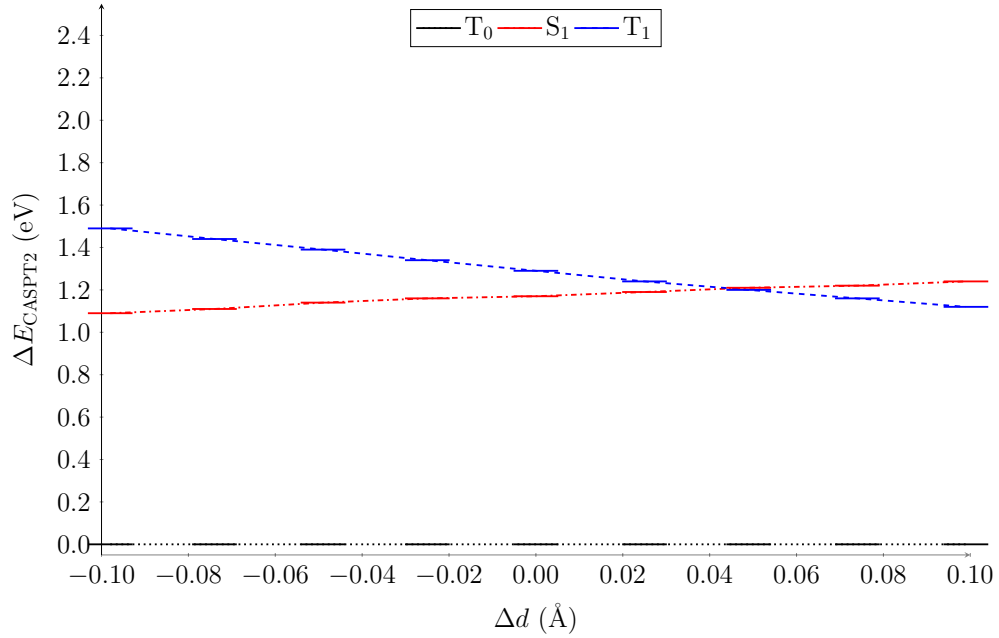


(a) CASPT2 Relative energies

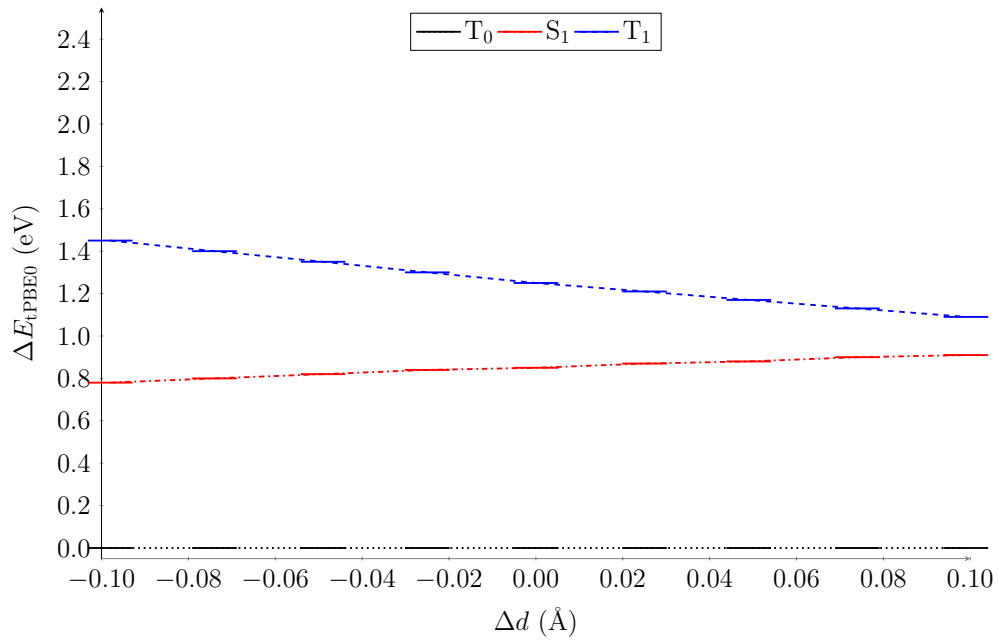


(b) tPBE0 Relative energies

Figure S25: (a) CASPT2 and (b) tPBE0 Relative energies for the lowest-lying three states of Cr(*o*-tol)₄ complex for the C–Cr–C scissoring normal mode. The equilibrium angle is $\theta = 104.9^\circ$.

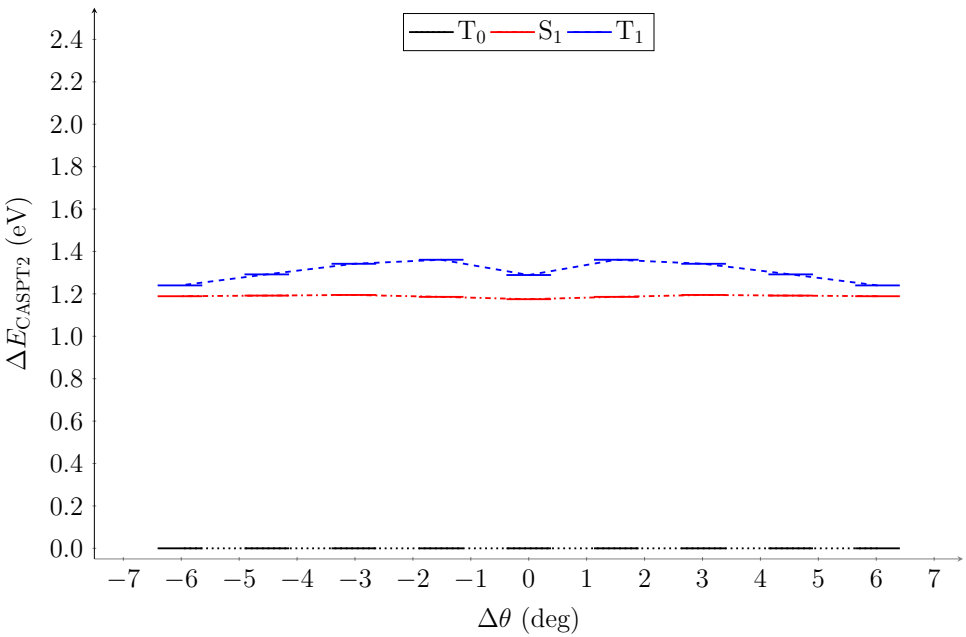


(a) CASPT2 Relative energies

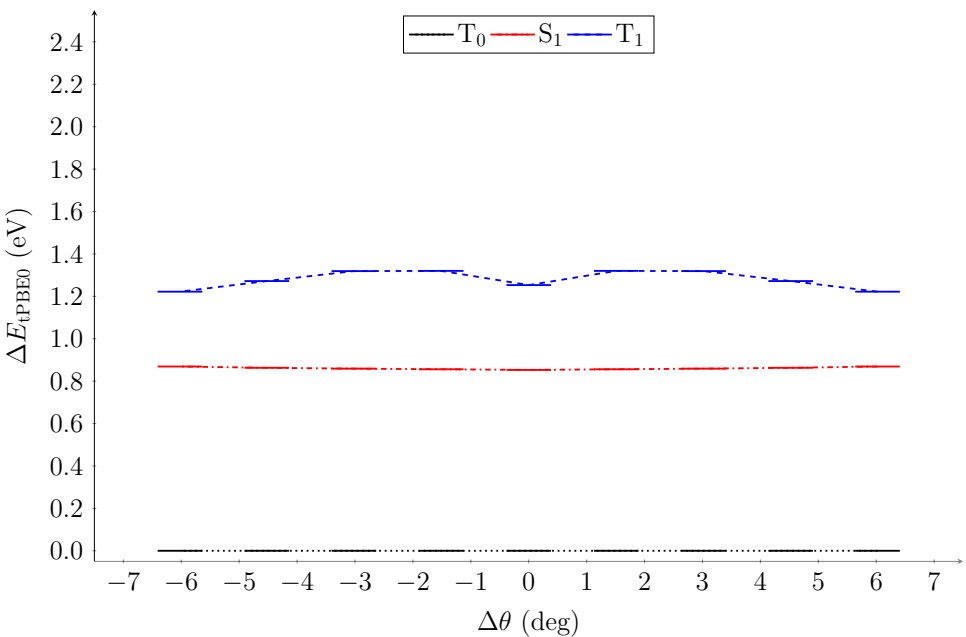


(b) tPBE0 Relative energies

Figure S26: (a) CASPT2 and (b) tPBE0 Relative energies for the lowest-lying three states of $\text{V}(o\text{-tol})_4^-$ complex for the V–C symmetric stretching normal mode. The equilibrium bond distance is $d = 2.07 \text{ \AA}$.

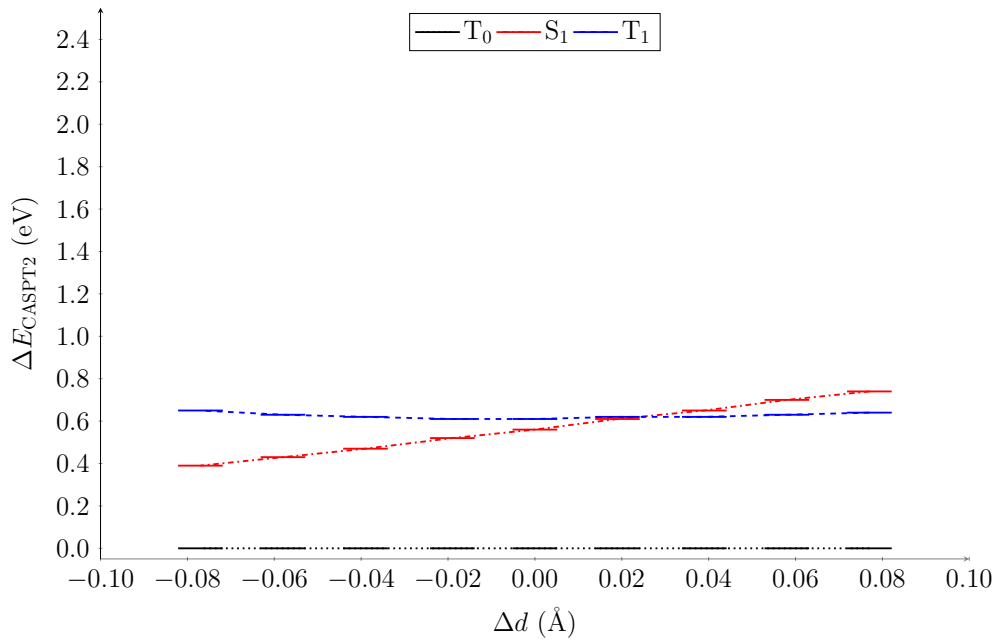


(a) CASPT2 Relative energies

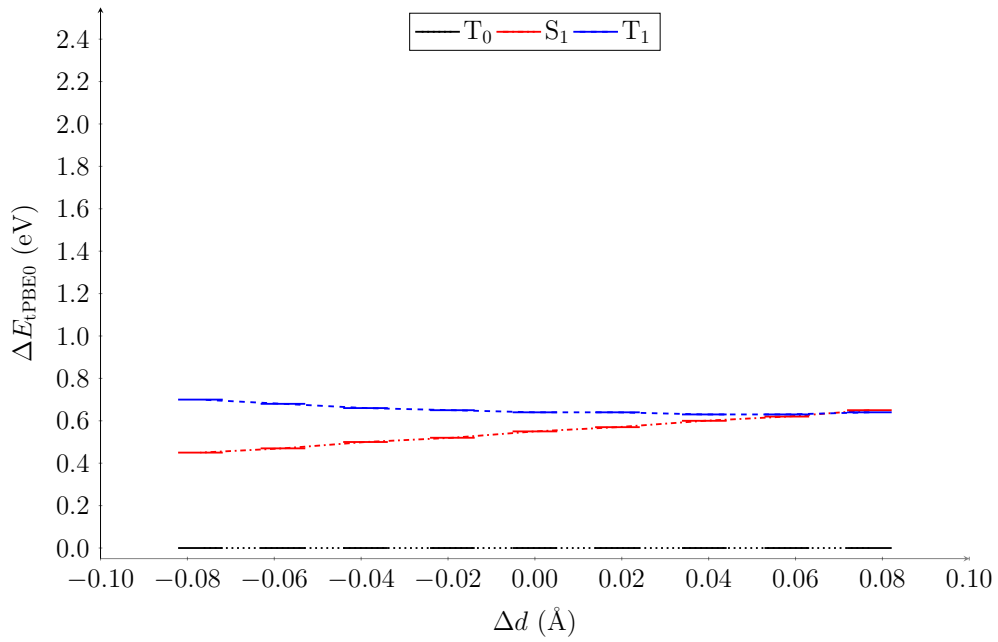


(b) tPBE0 Relative energies

Figure S27: (a) CASPT2 and (b) tPBE0 Relative energies for the lowest-lying three states of $\text{V}(o\text{-tol})_4^-$ complex for the C–V–C scissoring normal mode. The equilibrium angle is $\theta = 105.2^\circ$.

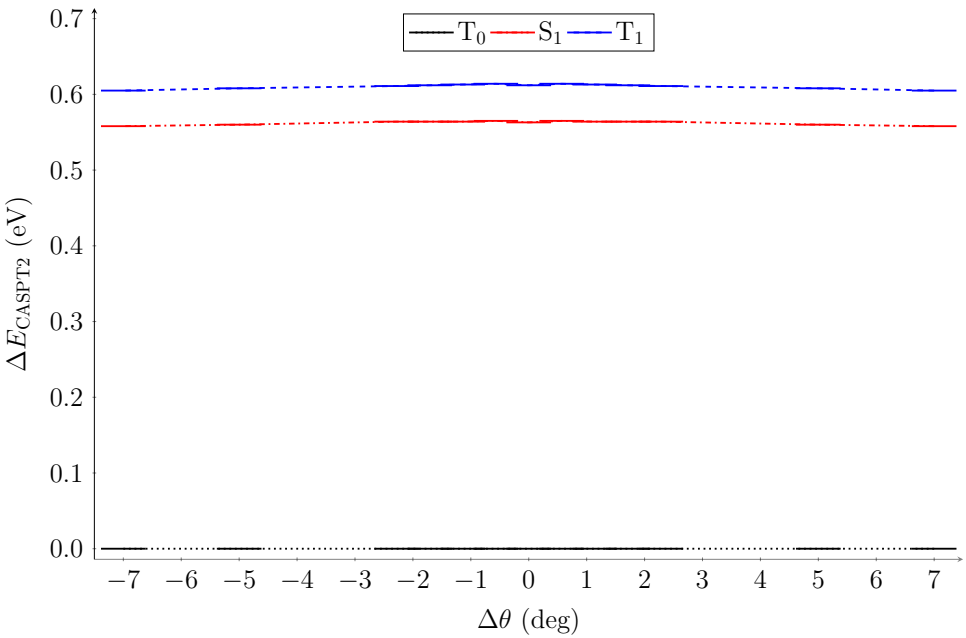


(a) CASPT2 Relative energies

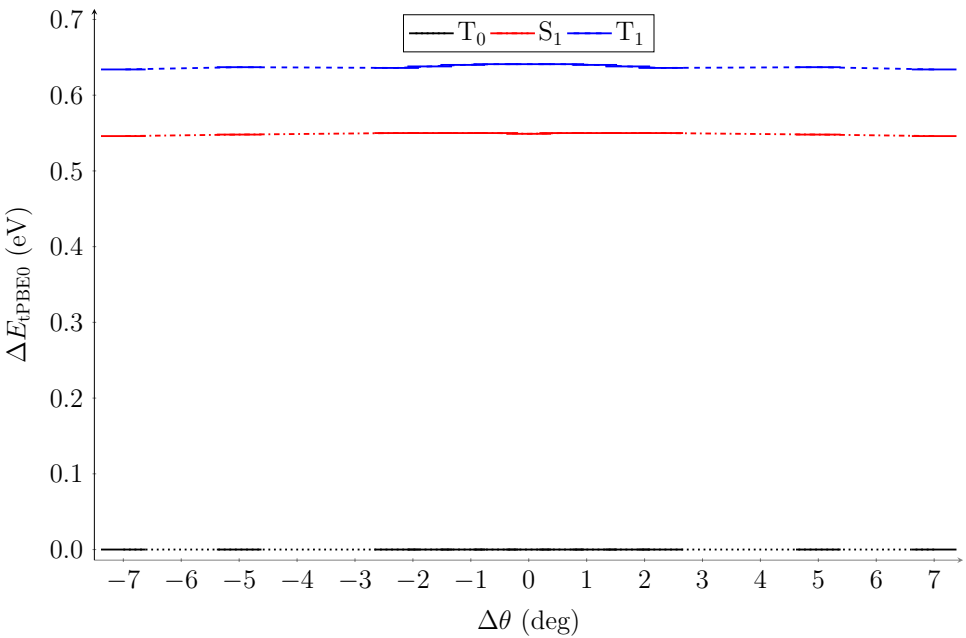


(b) tPBE0 Relative energies

Figure S28: (a) CASPT2 and (b) tPBE0 Relative energies for the lowest-lying three states of $\text{Ti}(o\text{-tol})_4^{2-}$ complex for the Ti–C symmetric stretching normal mode. The equilibrium bond distance is $d = 2.16 \text{ \AA}$.



(a) CASPT2 Relative energies

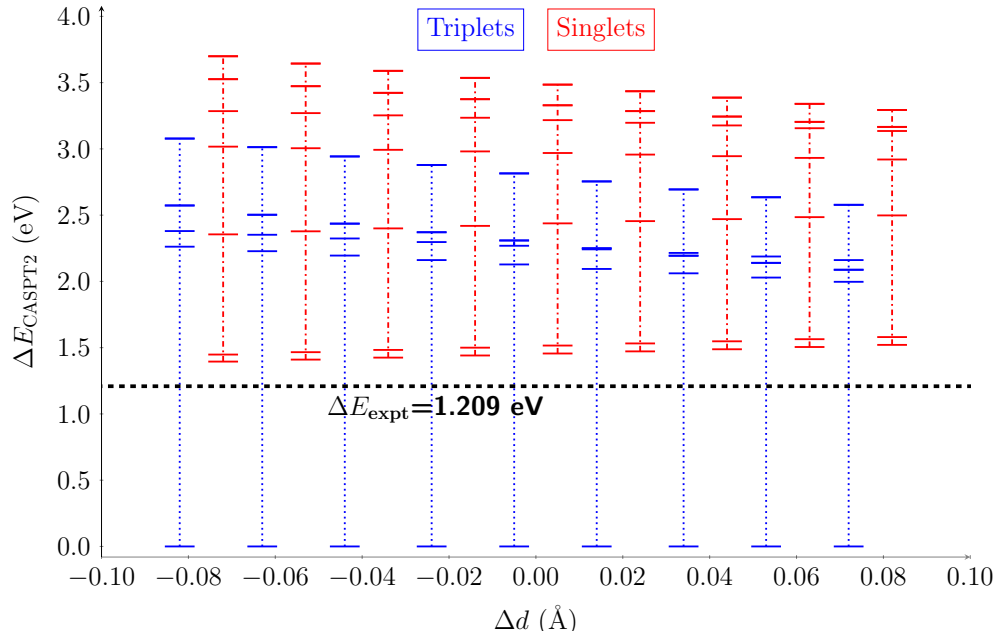


(b) tPBE0 Relative energies

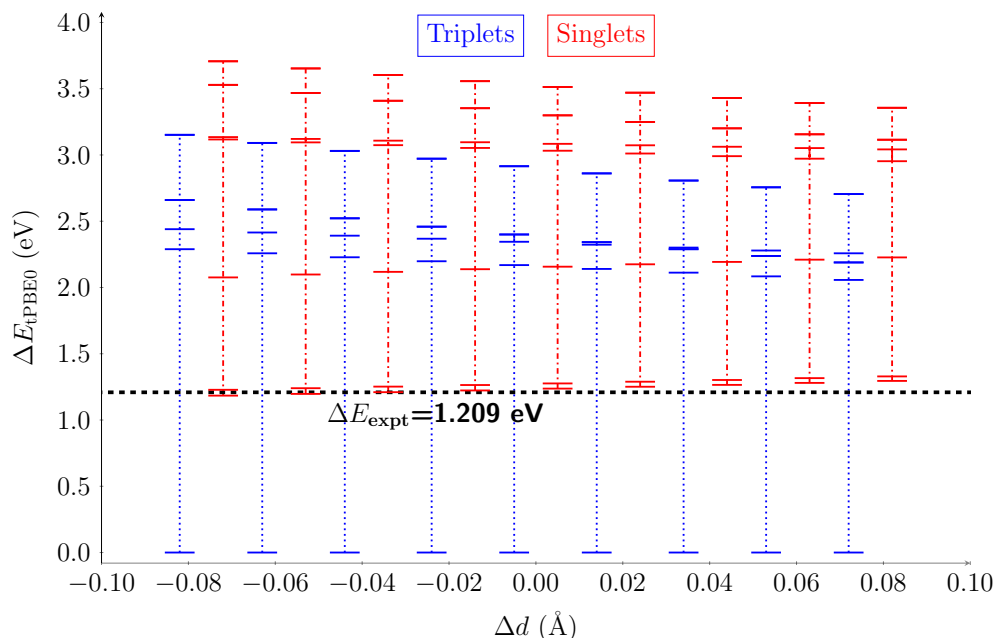
Figure S29: (a) CASPT2 and (b) tPBE0 Relative energies for the lowest-lying three states of $\text{Ti}(o\text{-tol})_4^{2-}$ complex for the C–Ti–C scissoring normal mode. The equilibrium angle is $\theta = 106.0^\circ$.

In the subsequent plots, we followed the triplet and singlet manifolds through the scan

coordinate.

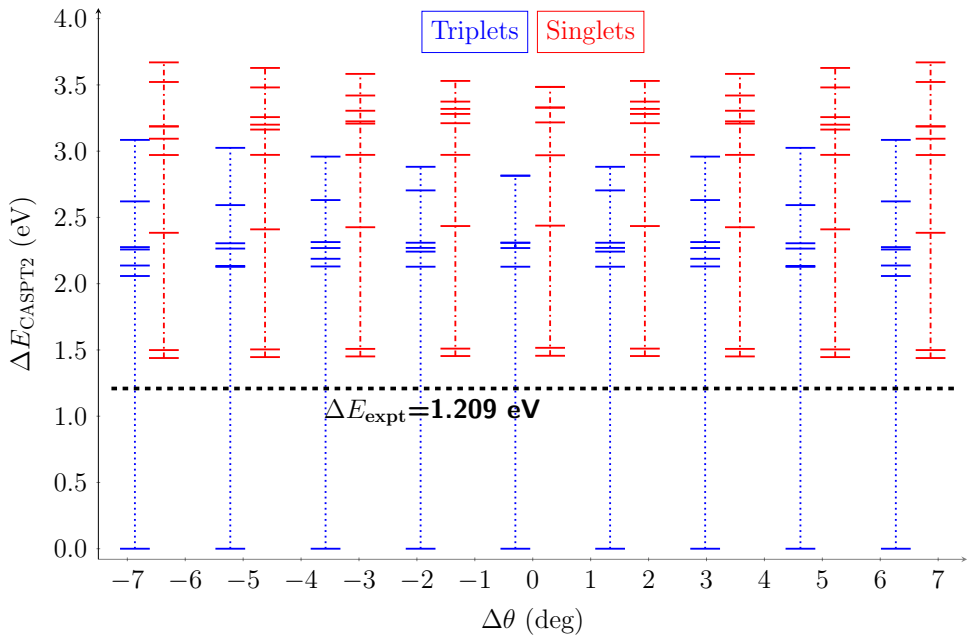


(a) CASPT2 Relative energies

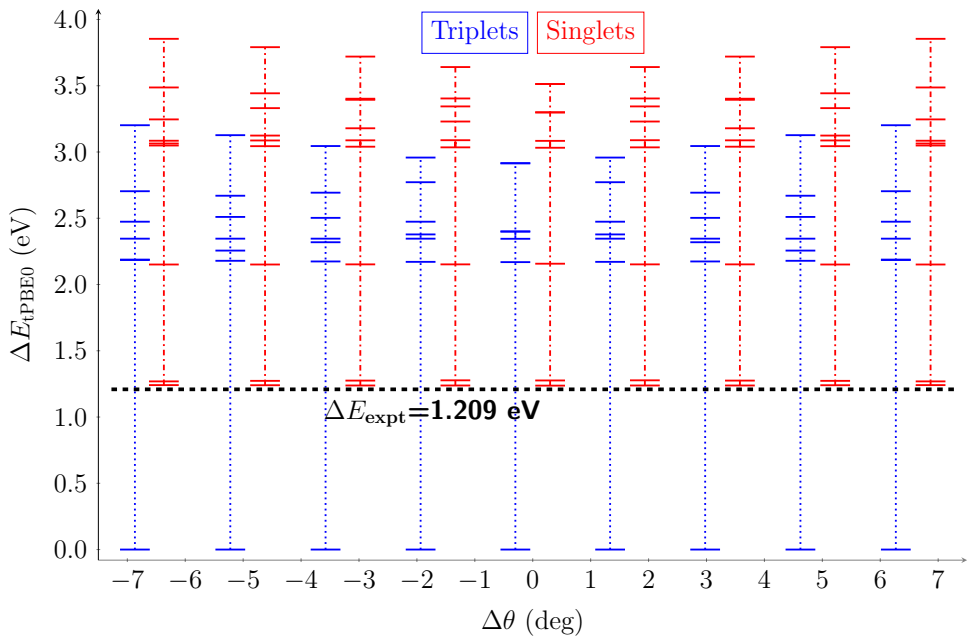


(b) tPBE0 Relative energies

Figure S30: (a) CASPT2 and (b) tPBE0 Relative energies for the lowest-lying 7 triplet and 9 singlet states of Cr(*o*-tol)₄ complex for the Cr-C symmetric stretching normal mode. The equilibrium bond distance is $d = 1.98 \text{ \AA}$.

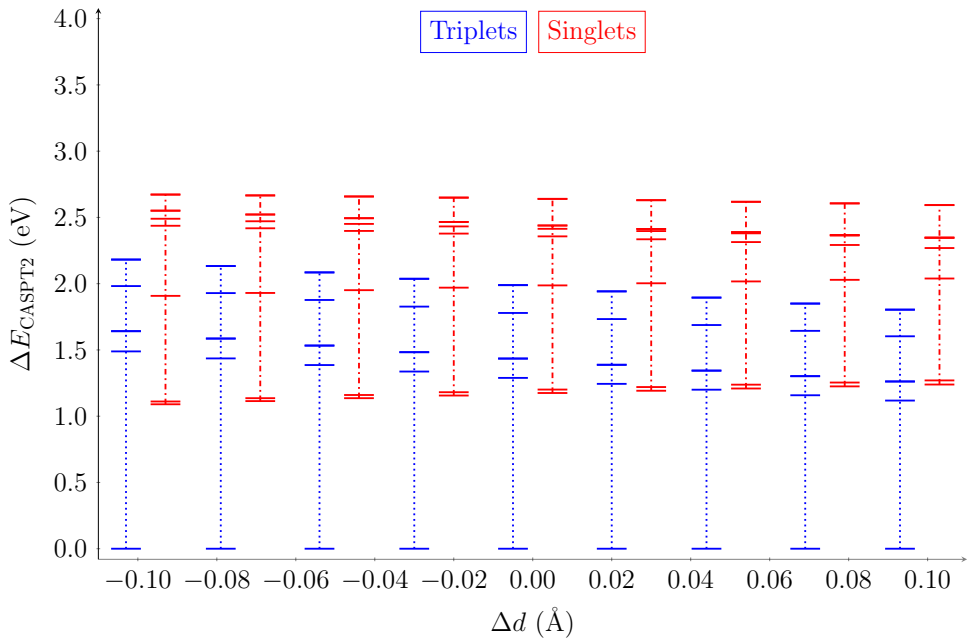


(a) CASPT2 Relative energies

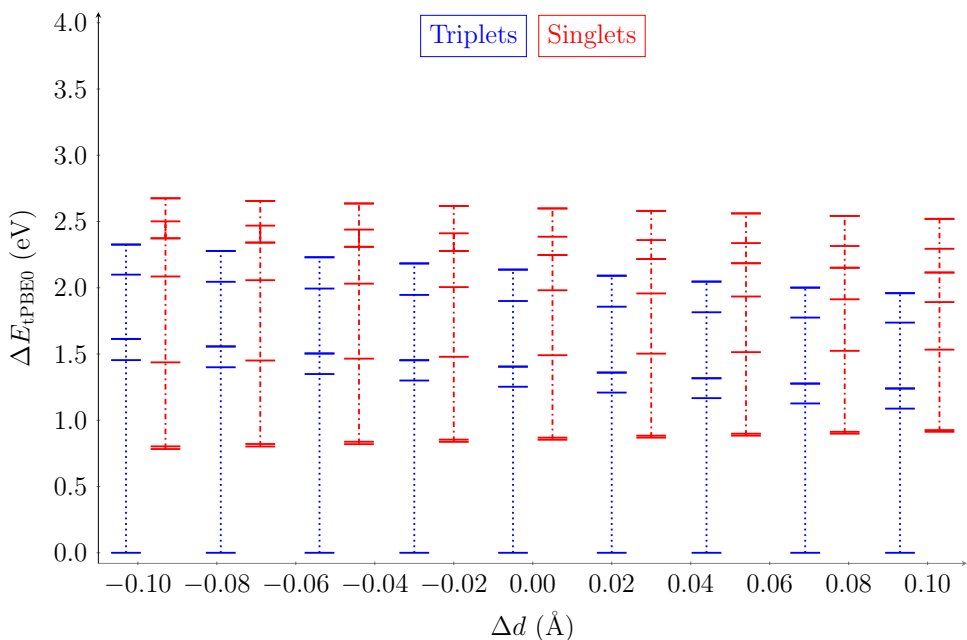


(b) tPBE0 Relative energies

Figure S31: (a) CASPT2 and (b) tPBE0 Relative energies for the lowest-lying 7 triplet and 9 singlet states of $\text{Cr}(o\text{-tol})_4$ complex for the C–Cr–C scissoring normal mode. The equilibrium angle is $\theta = 104.9^\circ$.

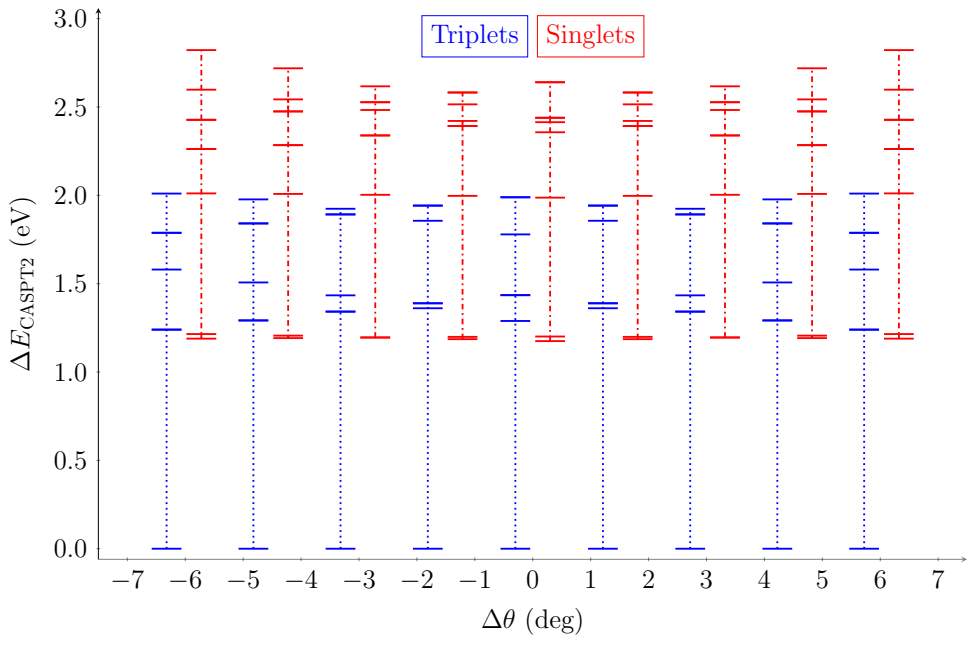


(a) CASPT2 Relative energies

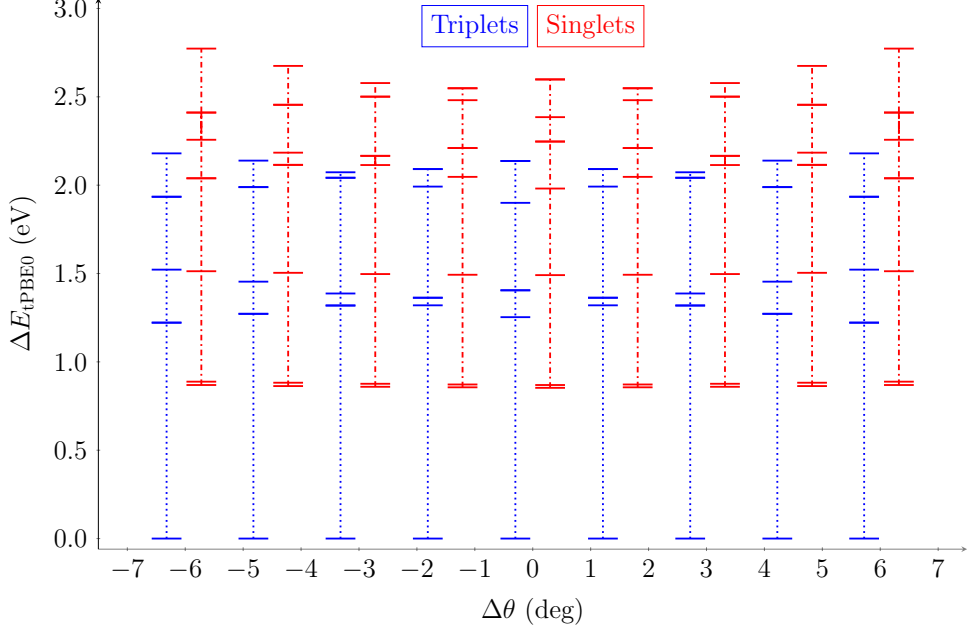


(b) tPBE0 Relative energies

Figure S32: (a) CASPT2 and (b) tPBE0 Relative energies for the lowest-lying 7 triplet and 9 singlet states of $\text{V}(o\text{-tol})_4^-$ complex for the V–C symmetric stretching normal mode. The equilibrium bond distance is $d = 2.07 \text{ \AA}$.

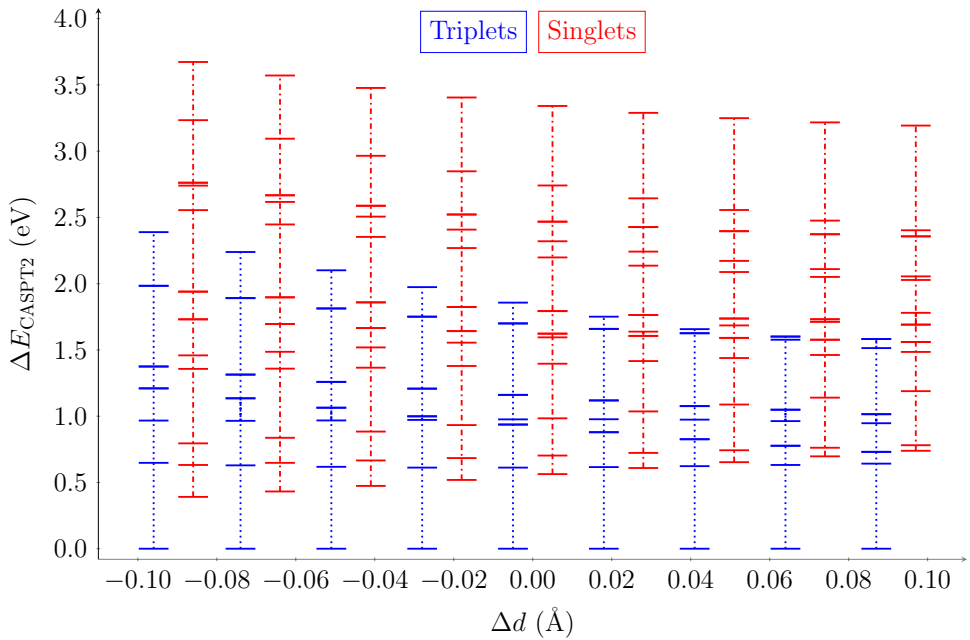


(a) CASPT2 Relative energies

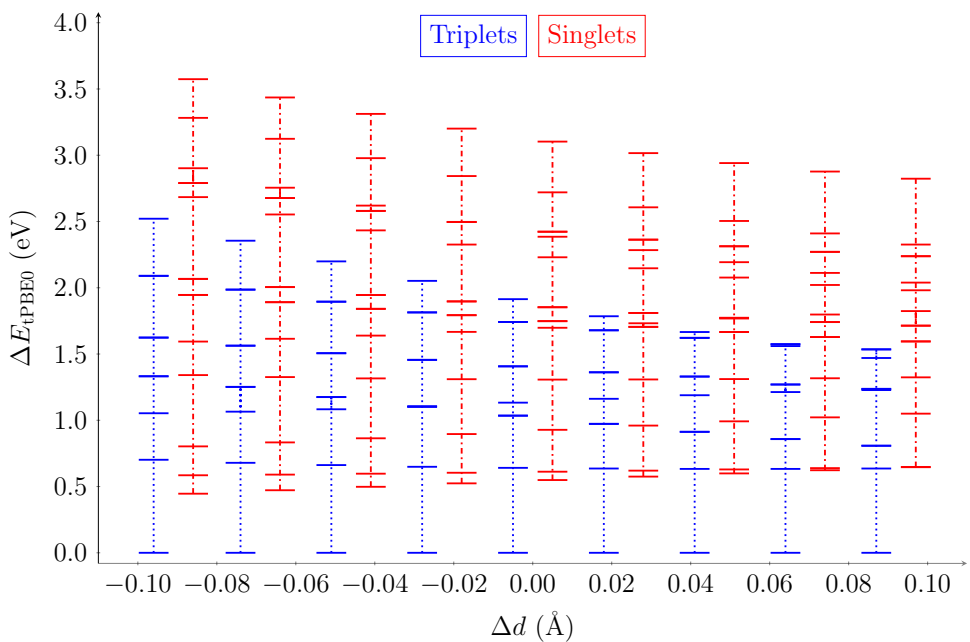


(b) tPBE0 Relative energies

Figure S33: (a) CASPT2 and (b) tPBE0 Relative energies for the lowest-lying 7 triplet and 9 singlet states of $\text{V}(o\text{-tol})_4^-$ complex for the C–V–C scissoring normal mode. The equilibrium angle is $\theta = 105.2^\circ$.

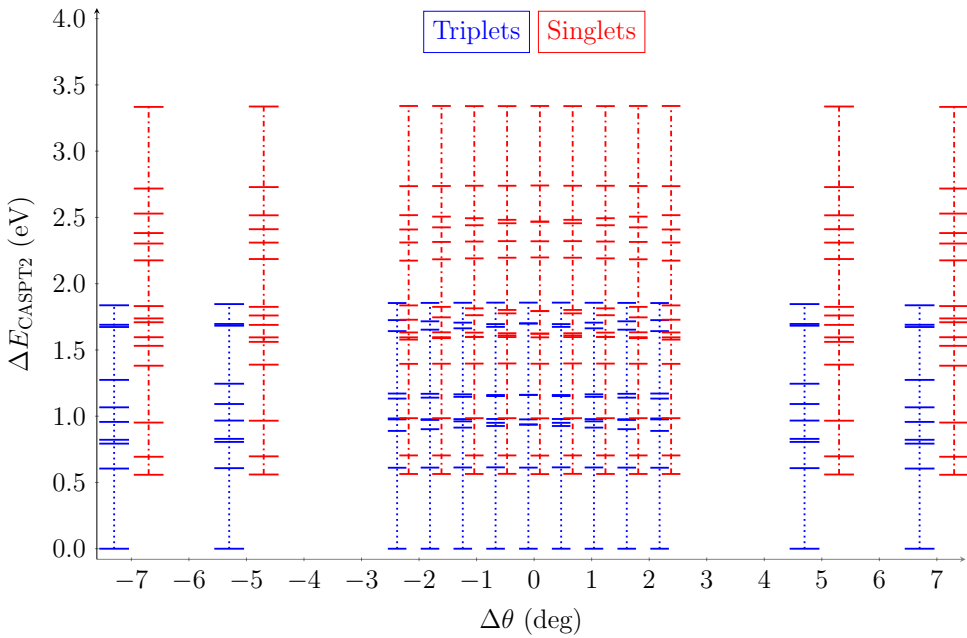


(a) CASPT2 Relative energies

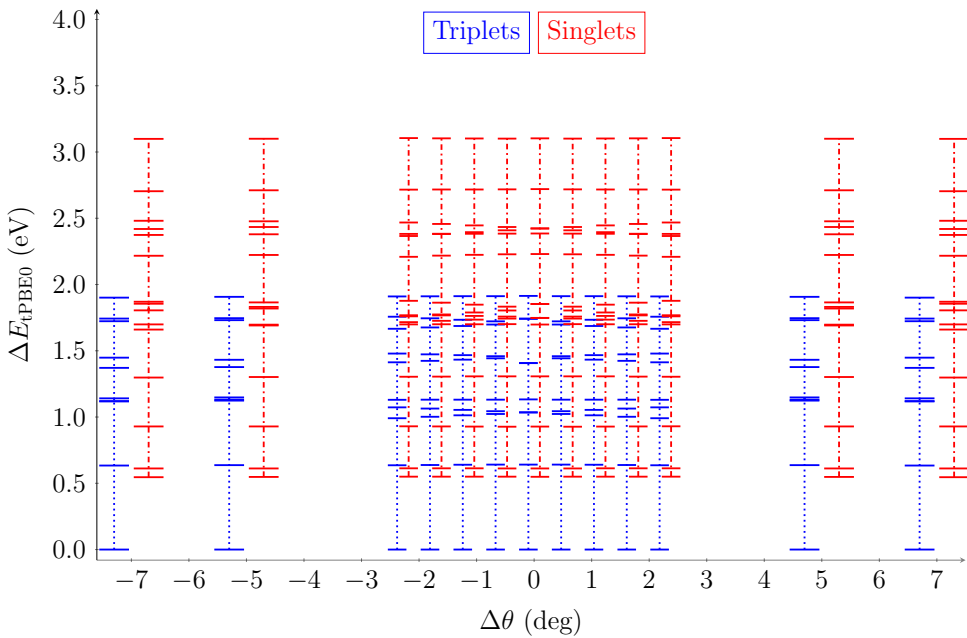


(b) tPBE0 Relative energies

Figure S34: (a) CASPT2 and (b) tPBE0 Relative energies for the lowest-lying 10 triplet and 15 singlet states of $\text{Ti}(o\text{-tol})_4^{2-}$ complex for the Ti-C symmetric stretching normal mode. The equilibrium bond distance is $d = 2.16 \text{ \AA}$.



(a) CASPT2 Relative energies



(b) tPBE0 Relative energies

Figure S35: (a) CASPT2 and (b) tPBE0 Relative energies for the lowest-lying 10 triplet and 15 singlet states of $\text{Ti}(o\text{-tol})_4^{2-}$ complex for the C–Ti–C scissoring normal mode. The equilibrium angle is $\theta = 106.0^\circ$.

The ZFS axial parameter $|D|$ was computed using the distorted structures obtained along

the normal modes for $\text{Cr}(o\text{-tol})_4$, $\text{V}(o\text{-tol})_4^-$, and $\text{Ti}(o\text{-tol})_4^{2-}$ complexes. In Figures S36-S41 are displayed the $|D|$ values computed with CASPT2 and tPBE0.

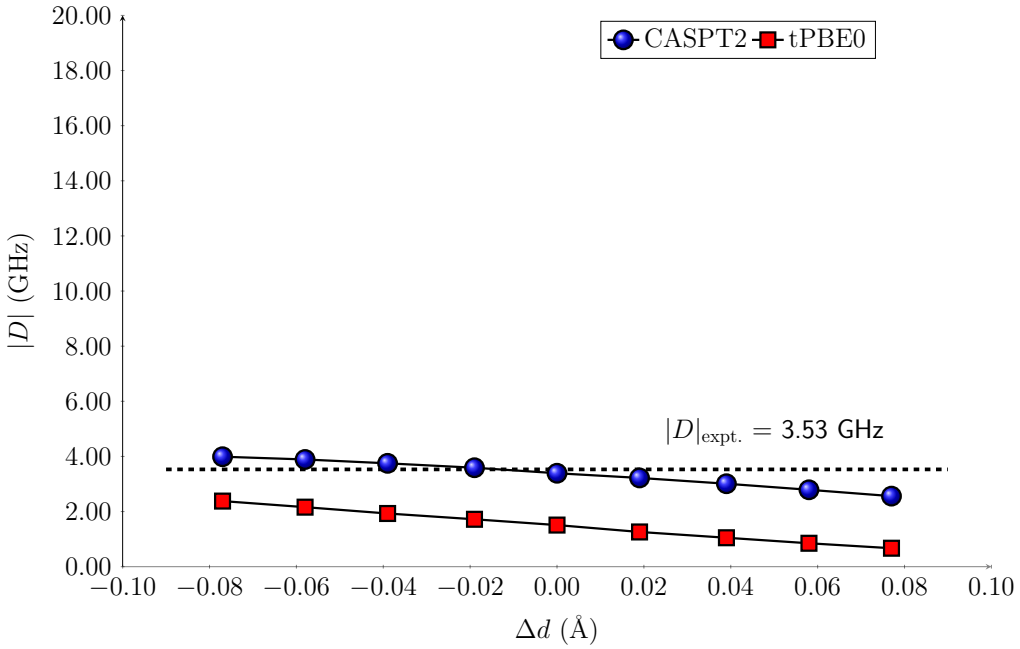


Figure S36: CASPT2 and tPBE0 axial parameter ($|D|$) of $\text{Cr}(o\text{-tol})_4$ complex for the Cr–C symmetric stretching normal mode. The equilibrium bond distance is $d = 1.98 \text{ \AA}$.

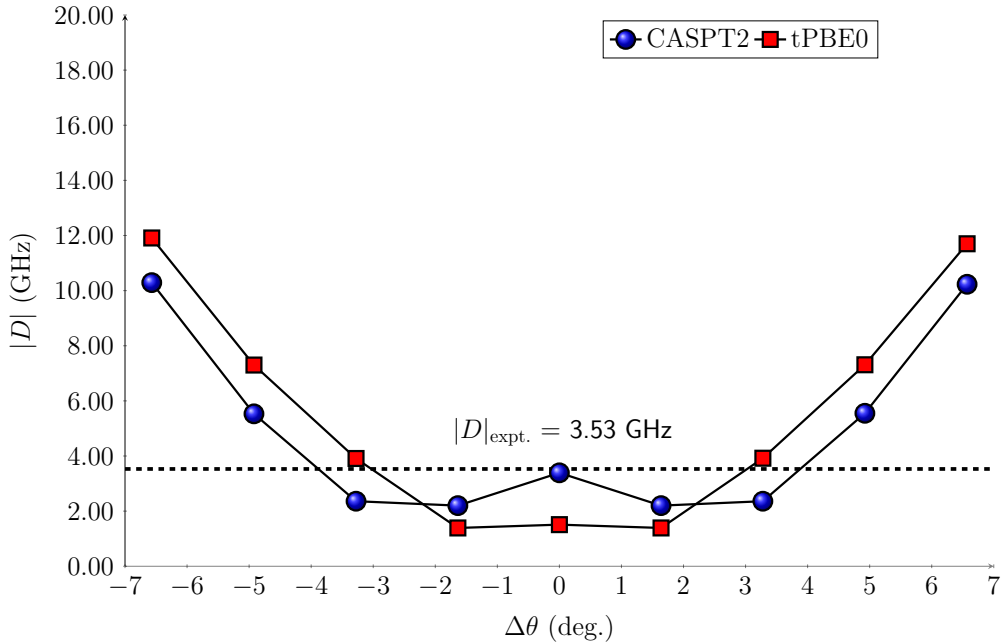


Figure S37: CASPT2 and tPBE0 axial parameter ($|D|$) of $\text{Cr}(o\text{-tol})_4$ complex for the C–Cr–C scissoring normal mode. The equilibrium bond angle is $\theta = 104.9^\circ$.

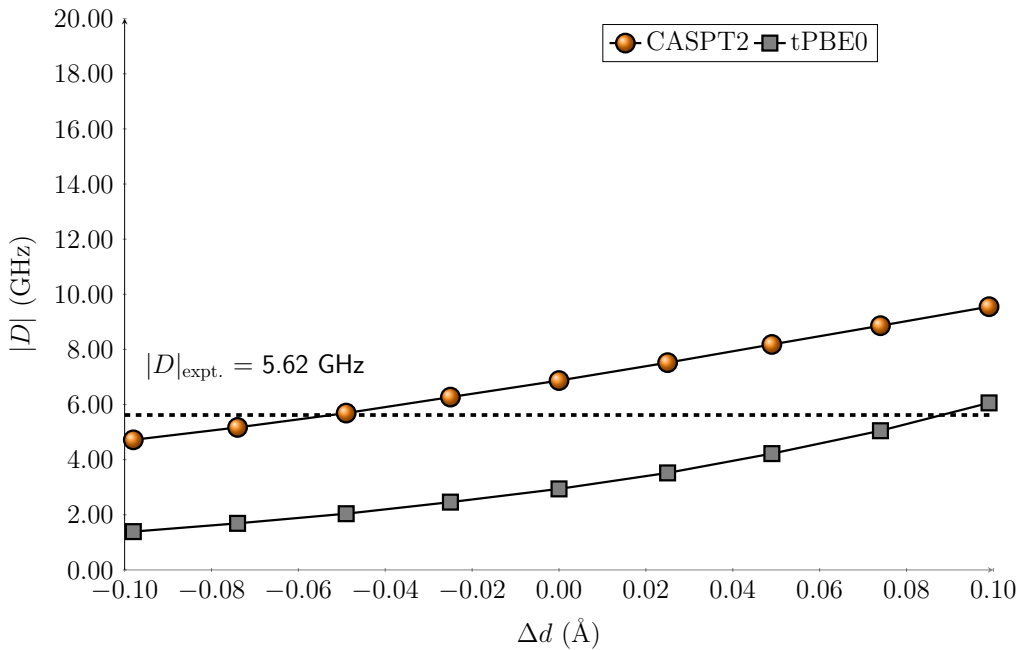


Figure S38: CASPT2 and tPBE0 axial parameter ($|D|$) of $V(o\text{-tol})_4^-$ complex for the V–C symmetric stretching normal mode. The equilibrium bond distance is $d = 2.07 \text{ \AA}$.

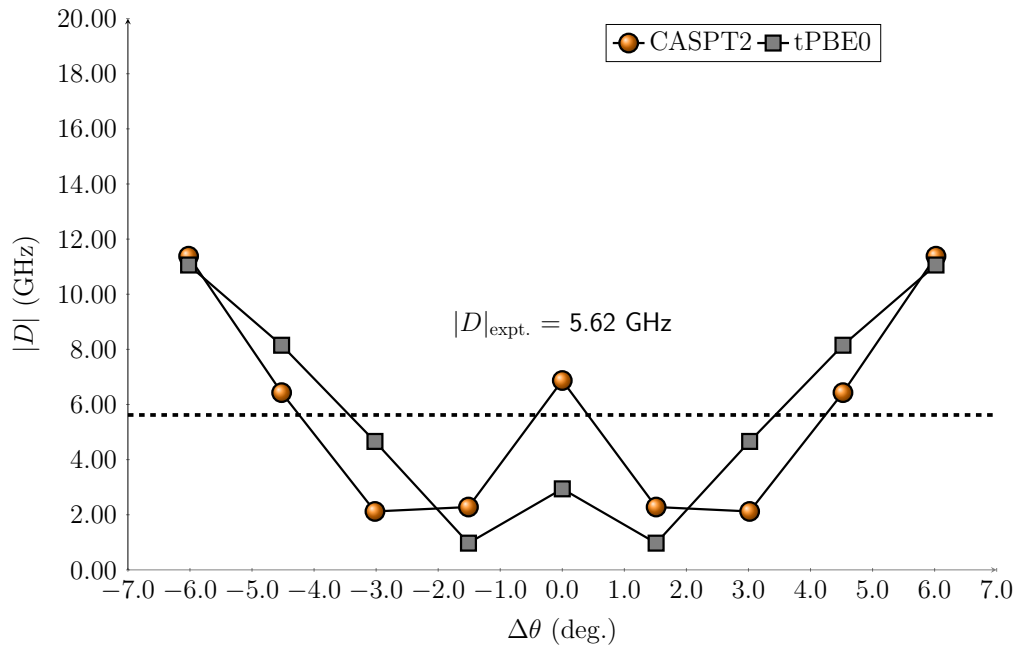


Figure S39: Zero-field splitting parameters computed with CASPT2 and tPBE0 methods for the $V(o\text{-tol})_4^-$ complex considering the C–V–C scissoring normal mode. The equilibrium bond angle is $\theta = 105.2^\circ$.

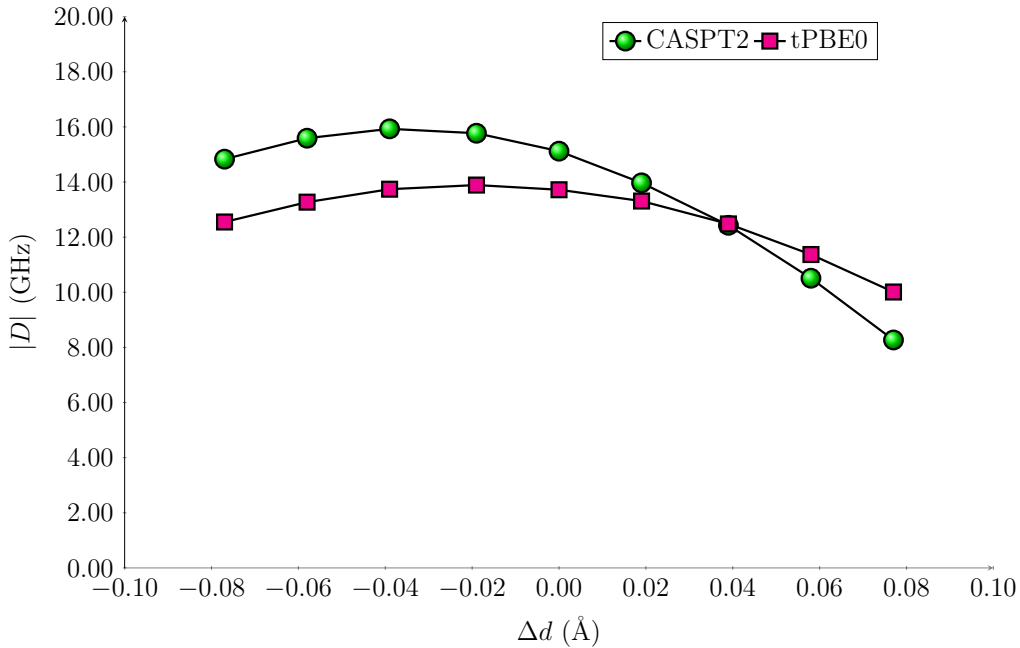


Figure S40: CASPT2 and tPBE0 axial parameter ($|D|$) of $\text{Ti}(o\text{-tol})_4^{2-}$ complex for the Ti–C symmetric stretching normal mode. The equilibrium bond distance is $d = 2.16 \text{ \AA}$.

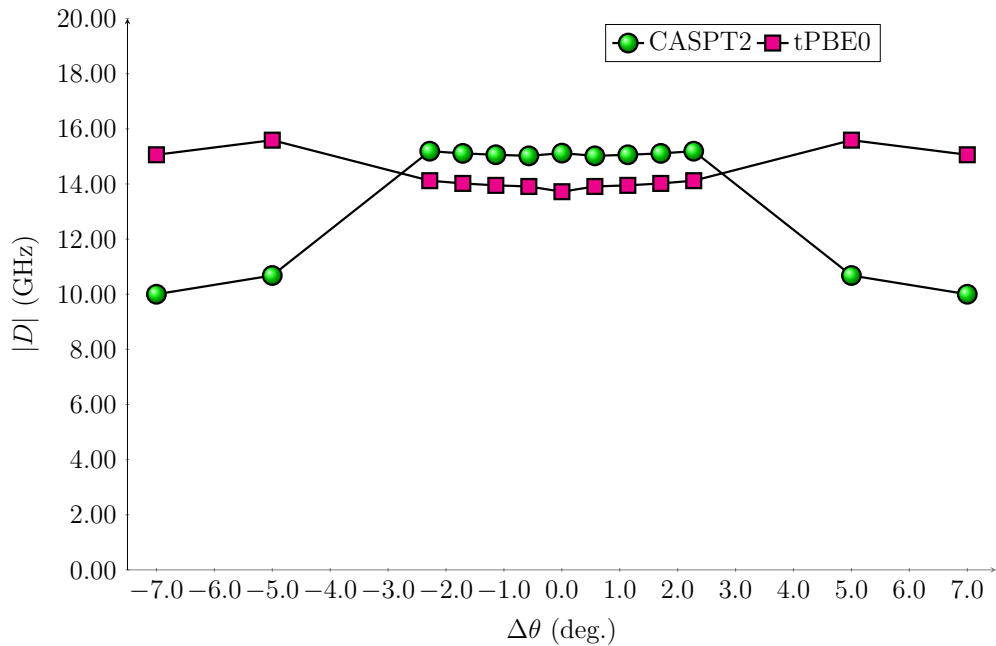


Figure S41: CASPT2 and tPBE0 axial parameter ($|D|$) of $\text{Ti}(o\text{-tol})_4^{2-}$ complex for the C–Ti–C scissoring normal mode. The equilibrium bond angle is $\theta = 106.0^\circ$.

Table S77: Zero-field splitting parameter $|D|$ in GHz computed with CASSCF, CASPT2, tPBE, and tPBE0 methods for the $\text{Cr}(o\text{-tol})_4$ complex considering the Cr–C stretching mode. The equilibrium bond distance is $d = 1.98 \text{ \AA}$.

Δd (\AA)	CASSCF	CASPT2	tPBE	tPBE0
0.077	3.22	2.56	0.67	0.67
0.058	3.44	2.79	0.51	0.85
0.039	3.67	3.01	0.33	1.05
0.019	3.89	3.22	0.12	1.26
0.000	4.09	3.39	0.15	1.51
-0.019	4.28	3.59	0.37	1.72
-0.039	4.45	3.75	0.60	1.93
-0.058	4.59	3.89	0.88	2.16
-0.077	4.71	3.99	1.15	2.38

Table S78: Zero-field splitting parameter $|D|$ in GHz computed with CASSCF, CASPT2, tPBE, and tPBE0 methods for the $\text{Cr}(o\text{-tol})_4$ complex considering the C–Cr–C scissoring mode. The equilibrium angle is $\theta = 104.9^\circ$.

$\Delta\theta$ ($^\circ$)	CASSCF	CASPT2	tPBE	tPBE0
6.495	8.20	10.29	0.00	11.91
4.881	4.74	5.53	8.60	7.30
3.259	1.84	2.36	4.98	3.91
1.632	3.39	2.20	1.76	1.39
0.001	4.09	3.39	0.15	1.51
-1.638	3.39	2.20	1.76	1.39
-3.279	1.86	2.36	4.98	3.92
-4.923	4.75	5.55	8.60	7.31
-6.570	8.20	10.23	14.23	11.70

Table S79: Zero-field splitting parameter $|D|$ in GHz computed with CASSCF, CASPT2, tPBE, and tPBE0 methods for the $\text{V}(o\text{-tol})_4^-$ complex considering the V–C stretching mode. The equilibrium bond distance is $d = 2.07 \text{ \AA}$.

Δd (\AA)	CASSCF	CASPT2	tPBE	tPBE0
-0.098	4.52	4.72	0.73	1.39
-0.074	5.05	5.17	0.56	1.69
-0.049	5.63	5.69	0.34	2.04
-0.025	6.27	6.27	0.06	2.46
0.000	6.96	6.87	0.31	2.94
0.025	7.71	7.52	0.79	3.52
0.049	8.52	8.18	1.43	4.22
0.074	9.40	8.86	2.25	5.05
0.099	10.34	9.55	3.31	6.06

Table S80: Zero-field splitting parameter $|D|$ in GHz computed with CASSCF, CASPT2, tPBE, and tPBE0 methods for the $\text{V}(o\text{-tol})_4^-$ complex considering the C–V–C scissoring mode. The equilibrium angle is $\theta = 105.2^\circ$.

$\Delta\theta$ (°)	CASSCF	CASPT2	tPBE	tPBE0
6.022	13.31	11.38	10.01	11.06
4.523	8.32	6.43	8.33	8.15
3.019	3.30	2.12	5.73	4.66
1.512	1.77	2.28	2.84	0.97
0.000	6.96	6.87	0.31	2.94
-1.512	1.77	2.28	2.84	0.97
-3.019	3.30	2.12	5.73	4.66
-4.523	8.32	6.43	8.33	8.15
-6.022	13.31	11.38	10.01	11.06

Table S81: Zero-field splitting parameter $|D|$ in GHz computed with CASSCF, CASPT2, tPBE, and tPBE0 methods for the $\text{Ti}(o\text{-tol})_4^{2-}$ complex considering the Ti–C stretching mode. The equilibrium bond distance is $d = 2.16 \text{ \AA}$.

Δd (\text{\AA})	CASSCF	CASPT2	tPBE	tPBE0
0.077	15.66	8.27	7.42	10.01
0.058	16.28	10.51	9.09	11.37
0.039	16.78	12.43	10.46	12.48
0.019	17.11	13.97	11.51	13.31
0.000	17.21	15.12	12.06	13.72
-0.019	17.07	15.77	12.38	13.89
-0.039	16.66	15.93	12.37	13.74
-0.058	16.01	15.59	12.00	13.27
-0.077	15.12	14.83	11.38	12.55

Table S82: Zero-field splitting parameter $|D|$ in GHz computed with CASSCF, CASPT2, tPBE, and tPBE0 methods for the $\text{Ti}(o\text{-tol})_4^{2-}$ complex considering the C–Ti–C scissoring mode. The equilibrium angle is $\theta = 106.0^\circ$.

$\Delta\theta$ (°)	CASSCF	CASPT2	tPBE	tPBE0
7.000	16.49	10.00	13.93	15.06
5.000	16.85	10.68	14.60	15.59
-2.281	17.44	15.19	12.58	14.12
-1.710	17.34	15.11	12.48	14.02
-1.140	17.27	15.06	12.41	13.95
-0.570	17.23	15.02	12.37	13.91
0.001	17.21	15.12	12.06	13.72
0.570	17.23	15.02	12.37	13.91
1.139	17.27	15.06	12.41	13.95
1.708	17.34	15.11	12.48	14.02
2.277	17.44	15.19	12.57	14.12
5.000	16.85	10.68	14.60	15.59
7.000	16.49	10.00	13.93	15.06

References

- (1) Bayliss, S. L.; Laorenza, D. W.; Mintum, P. J.; Kovos, B. D.; Freedman, D. E.; Awschalom, D. D. Optically addressable molecular spins for quantum information processing. *Science* **2020**, 370, 1309–1312.
- (2) Laorenza, D. W.; Mullin, K. R.; Weiss, L. R.; Bayliss, S. L.; Deb, P.; Awschalom, D. D.; Rondinelli, J. M.; Freedman, D. E. Coherent spin-control of $S = 1$ vanadium and molybdenum complexes. *Chem. Sci.* **2024**, 15, 14016–14026.
- (3) Gattesch, D.; Sessoli, R.; Villain, J. *Molecular Nanomagnets: Mesoscopic Physics and Nanotechnology*; Oxford University Press, 2006.
- (4) Pederson, M. R.; Khanna, S. N. Magnetic anisotropy barrier for spin tunneling in $\text{Mn}_{12}\text{O}_{12}$ molecules. *Phys. Rev. B* **1999**, 60, 9566–9572.
- (5) Reviakine, R.; Arbuznikov, A. V.; Tremblay, J.-C.; Remenyi, C.; Malkina, O. L.; Malkin, V. G.; Kaupp, M. Calculation of zero-field splitting parameters: Comparison

- of a two-component noncolinear spin-density-functional method and a one-component perturbational approach. *The Journal of Chemical Physics* **2006**, 125, 054110.
- (6) Chibotaru, L.; Ungur, L.; Soncini, A. The Origin of Nonmagnetic Kramers Doublets in the Ground State of Dysprosium Triangles: Evidence for a Toroidal Magnetic Moment. *Angew. Chem. Int. Ed.* **2008**, 47, 4126–4129.
- (7) Chibotaru, L. F.; Ungur, L.; Aronica, C.; Elmoll, H.; Pilet, G.; Luneau, D. Structure, Magnetism, and Theoretical Study of a Mixed-Valence $\text{CoII}_3\text{CoIII}_4$ Heptanuclear Wheel: Lack of SMM Behavior despite Negative Magnetic Anisotropy. *J. Am. Chem. Soc* **2008**, 130, 12445–12455.
- (8) Chibotaru, L. F.; Ungur, L. Ab initio calculation of anisotropic magnetic properties of complexes. I. Unique definition of pseudospin Hamiltonians and their derivation. *J. Chem. Phys.* **2012**, 137, 064112.
- (9) Sauza-de la Vega, A.; Pandharkar, R.; Stroscio, G.; Sarkar, A.; Truhlar, D.; Gagliardi, L. Multiconfiguration Pair-Density Functional Theory for Chromium(IV) Molecular Qubits. *JACS Au* **2022**, 2, 2029–2037.
- (10) Roos, B. O. The complete active space self-consistent field method and its applications in electronic structure calculations. *Adv. Chem. Phys.* **1987**, 69, 399–445.
- (11) Andersson, K.; Malmqvist, P.; Roos, B. O. Second-order Perturbation Theory with a Complete Active Space Self-consistent Field Reference Function. *J. Chem. Phys.* **1992**, 96, 1218–1226.
- (12) Pulay, P. A perspective on the CASPT2 method. *Int. J. Quantum Chem.* **2011**, 111, 3273–3279.
- (13) Li Manni, G.; Carlson, R. K.; Luo, S.; Ma, D.; Olsen, J.; Truhlar, D. G.; Gagliardi, L.

Multiconfiguration Pair-Density Functional Theory. *J. Chem. Theory Comput.* **2014**, 10, 3669–3680.

- (14) Pandharkar, R.; Hermes, M. R.; Truhlar, D. G.; Gagliardi, L. A New Mixing of Nonlocal Exchange and Nonlocal Correlation with Multiconfiguration Pair-Density Functional Theory. *J. Phys. Chem. Lett.* **2020**, 11, 10158–10163.
- (15) Zhou, C.; Wu, D.; Gagliardi, L.; Truhlar, D. G. Calculation of the Zeeman Effect for Transition-Metal Complexes by Multiconfiguration Pair-Density Functional Theory. *J. Chem. Theory Comput.* **2021**, 17, 5050 –5063.
- (16) Wu, D.; Zhou, C.; Bao, J. J.; Gagliardi, L.; Truhlar, D. G. Zero-Field Splitting Calculations by Multiconfiguration Pair-Density Functional Theory. *J. Chem. Theory Comput.* **2022**, 18, 2199–2207.
- (17) Goh, T.; Pandharkar, R.; Gagliardi, L. Multireference Study of Optically Addressable Vanadium-Based Molecular Qubit Candidates. *J. Phys. Chem. A* **2022**, 126, 6329–6335.
- (18) Hertler, P. R.; Sauza-de la Vega, A.; Darù, A.; Sarkar, A.; Lewis, R. A.; Wu, G.; Gagliardi, L.; Hayton, T. W. A homoleptic Fe(IV) ketimide complex with a low-lying excited state. *Chem. Sci.* **2024**, 15, 16559–16566.
- (19) Andrews, D. L.; Scholes, G. D.; Wiederrecht, G. P. *Comprehensive Nanoscience And Technology*; Elsevier, 2011.
- (20) Koseki, S.; Matsunaga, N.; Asada, T.; Schmidt, M. W.; Gordon, M. S. Spin–Orbit Coupling Constants in Atoms and Ions of Transition Elements: Comparison of Effective Core Potentials, Model Core Potentials, and All-Electron Methods. *J. Phys. Chem. A* **2019**, 123, 2325–2339.